STRUCTURE AND STRATIGRAPHY OF THE SOUTHERN LITTLE HARQUAHALA MOUNTAINS LA PAZ COUNTY, ARIZONA

by

Stephen Miller Richard

A Thesis Submitted to the Faculty of the

DEPARTMENT OF GEOSCIENCES

In Partial Fulfillment of the Requirements
For the Degree of

Master of Science

In the Graduate College

THE UNIVERSITY OF ARIZONA

1 9 8 3

STATEMENT BY AUTHOR

This thesis has been submitted in partial fulfillment of requirements for an advanced degree at the University of Arizona and is deposited at the University Library to be made available to borrowers under rules of the Library.

Brief quotations from this thesis are allowable without special permission, provided that accurate acknowledgment of source is made. Requests for permission for extended quotation from or reproduction of this manuscript in whole or in part may be granted by the head of the major department or the Dean of the Graduate College when in his judgment the proposed use of the material is in the interests of scholarship. In all other instances, however, permission must be obtained from the author.

SIGNED: Stephen M. Richard

APPROVAL BY THESIS DIRECTOR

This thesis has been approved on the date shown below:

PETER J. CONEY
Professor of Geosciences

3/30/1983
Date

ACKNOWLEDGEMENTS

I am indebted to a host of friends and asociates who have assisted me in this endeavor. S. J. Reynolds introduced me to the area and has been a continuing source of information and assistance. Professors P. J. Coney and W. R. Dickinson provided guidance throughout the project. Time spent at the Blythe Field Station was enjoyable due to the companionship of L. E. Harding and R. A. Leveque. The ideas and interpretations contained here have been cultivated in discussions with G. J. Axen, G. H. Davis, L. D. Ditullio, Stanley B. Keith, L. E. Harding, H. W. Peirce, J. E. Spencer, and R. M. Tosdal. Field assistance was provided by Dawn Harvey, K. F. Inman, W. S. Jefferson and N. Riggs. The manuscript was reviewed by H. M. Richard and typed by JoAnn Overs and J. L. Lowry. N. Riggs and R. F. Brokaw Jr. assisted with the drafting. Financial support was provided by GSA grant # 27088, NSF grant #8018500 awarded to P. J. Coney and L. E. Harding, a research assistantship from the Arizona Bureau of Geology and Mineral Technology, and grants from Tri-Con Mining Ltd. and Gulf Minerals Co.

TABLE OF CONTENTS

	Page
LIST OF ILLUSTRATIONS	vi
LIST OF TABLES	x
ABSTRACT	xi
INTRODUCTION	1
Location, Physiography, Access	1
Previous Work	1
Present Study	6
REGIONAL GEOLOGIC SETTING	8
GENERAL GEOLOGY OF THE LITTLE HARQUAHALA MOUNTAINS	12
STRATIGRAPHY	
Introduction	14
Precambrian Rocks	15
Paleozoic Rocks	16
Bolsa Quartzite	17
Abrigo Formation	19
Martin Formation	20
Redwall Limestone	21
Supai Formation	23
Coconino Sandstone	25
Kaibab Limestone	27
Paleozoic(?) Breccia-Conglomerate	29
Mesozoic Rocks	33
Mesozoic Sandstone	33
Lower Volcanic Unit	37
Upper Volcanic Unit	40
Volcaniclastic Sediments	41
Apache Wash Formation	43
Rocks of Harquar Peak	48
Tertiary Rocks	50
Breccia	50
Conglomerate	51
Older Alluvium	52
Sore Fingers Assemblage	52
Porphyritic Monzogranite	53
Other Intrusions	54

Table of Contents continued - Page

Meta-monzogranite..... 57
Metamorphic Rocks..... 58
Dikes..... 61

STRUCTURAL GEOLOGY
Major Structures..... 83
Early Faulting 83
Refolding and Associated Structures..... 85
Foliations and Thrust Faulting..... 92
South-dipping Reverse Faults..... 102
Northwest-Dipping Normal Faults..... 103
Northeast-Dipping Low-Angle Normal Faults..... 109
High-Angle Normal Faults..... 114
Minor Structures..... 117
Joints..... 117
Veins..... 117
Northeast-trending faults in the Sore Fingers Area..... 119
South-vergent, low-angle Faults..... 119
Complex Fault Zones..... 124
Kinematics..... 124

TECTONICS 139

CONCLUSION 148

LIST OF ILLUSTRATIONS

Figures		Page
1.	Map showing location of the Little Harquahala Mountains and adjacent ranges in west-central Arizona.....	2
2.	Photograph of central Little Harquahala Mountains.....	3
3.	Physiographic features of the southern Little Harquahala Mountains.....	4
4.	Map showing access roads in the southern Little Harquahala Mountains.....	5
5.	Geologic map of the southern Little Harquahala Mountains, La Paz County, Arizona.....	In Pocket
6.	Cross sections of the southern Little Harquahala Mountains, La Paz County, Arizona.....	In Pocket
7.	Geologic map of west-central Arizona.....	In Pocket
8.	Generalized geologic map of the southern Little Harquahala Mountains.....	13
9.	Stratigraphic column of the rocks of the Southern Little Harquahala Mountains.....	In Pocket
10.	Photograph of Split Mountain.....	18
11.	Redwall Limestone and Supai Formation on west ridge of Redwall Hill.....	22
12.	Cross bedding in the Coconino Sandstone.....	26
13.	Kaibab Limestone on Hill D in the Limestone Hills.....	28
14.	Detailed stratigraphic column of the Kaibab Limestone.....	In Pocket
15.	Breccia-conglomerate on the ridge southwest of the Needle.....	31
16.	Poles to bedding in the breccia-conglomerate.....	32

List of Illustrations continued -

Figures		Page
17.	Schematic structural-stratigraphic cross section of Mesozoic rocks	In Pocket
18.	Petrology of Mesozoic clastic rocks	35
19.	Volcanic rocks of the southern Little Harquahala Mountains	38
20.	Upper member of the Apache Wash Formation	47
21.	Porphyritic monzogranite of the Sore Fingers Assemblage	55
22.	Composition of granitic rocks	56
23.	Foliations in metamorphic rocks	59
24.	Intrusive contact between porphyritic monzogranite and metamorphic rocks	60
25.	Structural domains	65
26.	Faults in the Sore Fingers Domain and Sore Fingers West Domain	66
27.	Faults in the Limestone Hills Domain	69
28.	Faults in the Martin Peak Domain	70
29.	Faults in the Golden Eagle Hill Domain	72
30.	Faults in the Mixmaster Hill Domain	74
31.	Faults in the Needle Domain	76
32.	Faults in the Elbow Hill Domain	78
33.	Faults in the Corral Hill Domain and Split Mountain Domain	80
34.	Detailed geologic map of the Limestone Hills	84
35.	Detailed geologic map of northern Martin Peak	86
36.	Aerial view of Martin Peak	87

List of Illustrations continued -

Figures		Page
37.	Detailed geologic map of Elbow Hill.....	89
38.	Axes of major folds.....	90
39.	Structures related to F_2 folding.....	91
40.	Fracture cleavage along the Sore Fingers Thrust.....	93
41.	Contoured equal area plot of poles to cleavage along the Sore Fingers Thrust.....	95
42.	Contoured equal area plot of poles to cleavage in Mesozoic clastic rocks.....	95
43.	Contoured equal area plot of poles to foliation in the Limestone Hills domain.....	96
44.	Contoured equal area plot of poles to foliation in Paleozoic rocks of the main outcrop belt.....	96
45.	Sore Fingers Thrust and normal faults.....	99
46.	Faults related to the foliation-forming event.....	101
47.	Northwest-dipping normal fault system in Paleozoic rocks.....	104
48.	Distribution of dips of bedding on Corral Hill.....	105
49.	Simplified geologic map of the Mixmaster Hill-Golden Eagle Hill allochthon.....	108
50.	Detailed geologic map of Mixmaster Hill.....	In Pocket
51.	Northeast-dipping normal faults.....	110
52.	Fault zone along East Sore Fingers normal fault.....	112
53.	Needle Fault set.....	115
54.	Contoured equal area plot of poles to joint surfaces in the Sore Fingers Domain.....	118

List of Illustrations continued -

Figures		Page
55.	Northeast-trending faults in the Sore Fingers area	120
56.	South-dipping reverse faults and minor structures in the main Paleozoic outcrop belt	121
57.	Contoured equal area plot of minor fold axes	126
58.	Selected minor fold axes	127
59.	Models for F_2 development	129
60.	Evolution of F_2 structures	131
61.	Paleogeologic map, after Sore Fingers thrusting	135
62.	Paleogeologic map, after northeast-dipping normal faulting	136
63.	Strike lines of minor normal faults in Paleozoic rocks	137

LIST OF TABLES

Table		Page
1.	Dike lithologies	62
2.	Structural characteristics of dikes	63
3.	Faults in Sore Fingers Domain	67
4.	Faults in Limestone Hills Domain and Sore Fingers West Domain	68
5.	Faults in Martin Peak Domain	71
6.	Faults in the Golden Eagle Hill Domain	73
7.	Faults in the Mixmaster Hill Domain	75
8.	Faults in the Elbow Hill Domain	79
9.	Faults in the Needle Domain	77
10.	Faults in Corral Hill Domain	81
11.	Faults in Split Mountain Domain	82
12.	Chronology of faults	122
13.	Characteristics of fault sets	123

ABSTRACT

In the southern Little Harquahala Mountains deformed Paleozoic and Mesozoic strata and underlying Precambrian crystalline rocks are in thrust contact above Mesozoic volcanic and sedimentary rocks on the north and Precambrian and Mesozoic (?) granitic and metamorphic rocks on the south. Upper plate rocks include Precambrian monzogranite overlain by 1000 m of Paleozoic strata, up to 900 m of Jurassic(?) volcanic and volcaniclastic rocks and a minimum of 750 m of lithofeldspathic clastic rocks. Prior to thrusting, these rocks were folded into a northeast-trending, southeast-vergent recumbent syncline and refolded about steep northerly-plunging axes. The relationship between thrust faults bounding the upper plate on the north and south is uncertain. Data from outside the map area indicate that the faults are pre-late cretaceous in age. Other structures include post-thrusting (?) northwest-dipping normal faults, post-thrusting northeast-dipping, low-angle normal faults and northerly-trending, high-angle normal faults.

INTRODUCTION

Location, Physiography and Access

The Little Harquahala Mountains are located in eastern La Paz County, Arizona, within the Basin and Range Province of Arizona (Figure 1). This study describes the geology of the southeastern half of the range. The principal physiographic features of the study area are a northeast-trending ridge which intersects a northwest-trending series of hills in the central part of the study area (Figure 2). Elevations range from 455 to 840 meters (1500 to 2760 feet). The only named physiographic features in the area are Martin Peak, the Needle and Sore Fingers. In order to facilitate discussion of the geology, a number of other hills have been given informal names as indicated in Figure 3. Access to the area is excellent by the all weather Hovatter and Buckeye-Salome Roads that connect with Interstate 10 and U.S. 60. Unimproved dirt roads and jeep trails provide access to other parts of the range (Figure 4).

Previous Work

Little detailed mapping has been done in western Arizona (see discussion in Reynolds, 1980). The first published geologic maps of the area were by Lee (1908) and Darton, et. al. (1924). A more detailed and accurate map of the region was published by Wilson (1960). Miller (1966, 1970) and Jemmett (1966) studied the Plomosa Mountains. Ciancanelli (1965) mapped a portion of the Granite Wash Mountains, and Varga (1977) mapped the Socorro Peak area in the

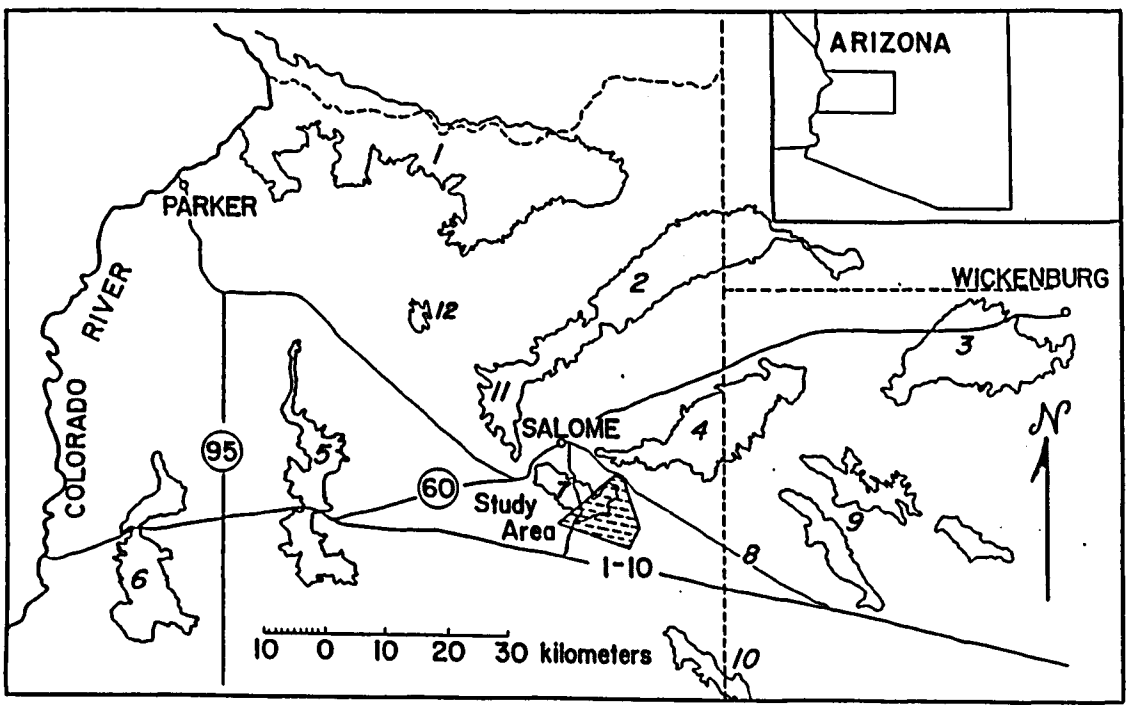

Figure 1. Map showing location of the Little Harquahala Mountains and adjacent ranges in west-central Arizona.

Outline of ranges follows topographic contour at the base of the mountains, from U.S.G.S. 1:500000 topographic map of Arizona.

Key to numbers: 1 - Buckskin Mountains; 2 - Harcuvar Mountains; 3 - Vulture Mountains; 4 - Harquahala Mountains; 5 - Plomosa Mountains; 6 - Dome Rock Mountains; 7 - Little Harquahala Mountains; 8 - Buckeye-Salome Road; 9 - Big Horn Mountains; 10 - Eagletail Mountains; 11 - Granite Wash Mountains; 12 - Bouse Hills.

Figure 2. Photograph of Central Little Harquahala Mountains

View is towards the northeast from Martin Peak, at the intersection of the northeast-trending ridges of the main Paleozoic outcrop belt and the northwest-trending central axis. The prominent peaks are from right to left, the Needle, Redwall Hill and Elbow Hill. Mixmaster Hill lies in the foreground to the right of the Needle. Paleozoic rocks of the western Harquahala Mountains (Varga, 1977) are just visible to the left of Redwall Hill below the prominent arch of the central Harquahala Mountains which dominates the far skyline.

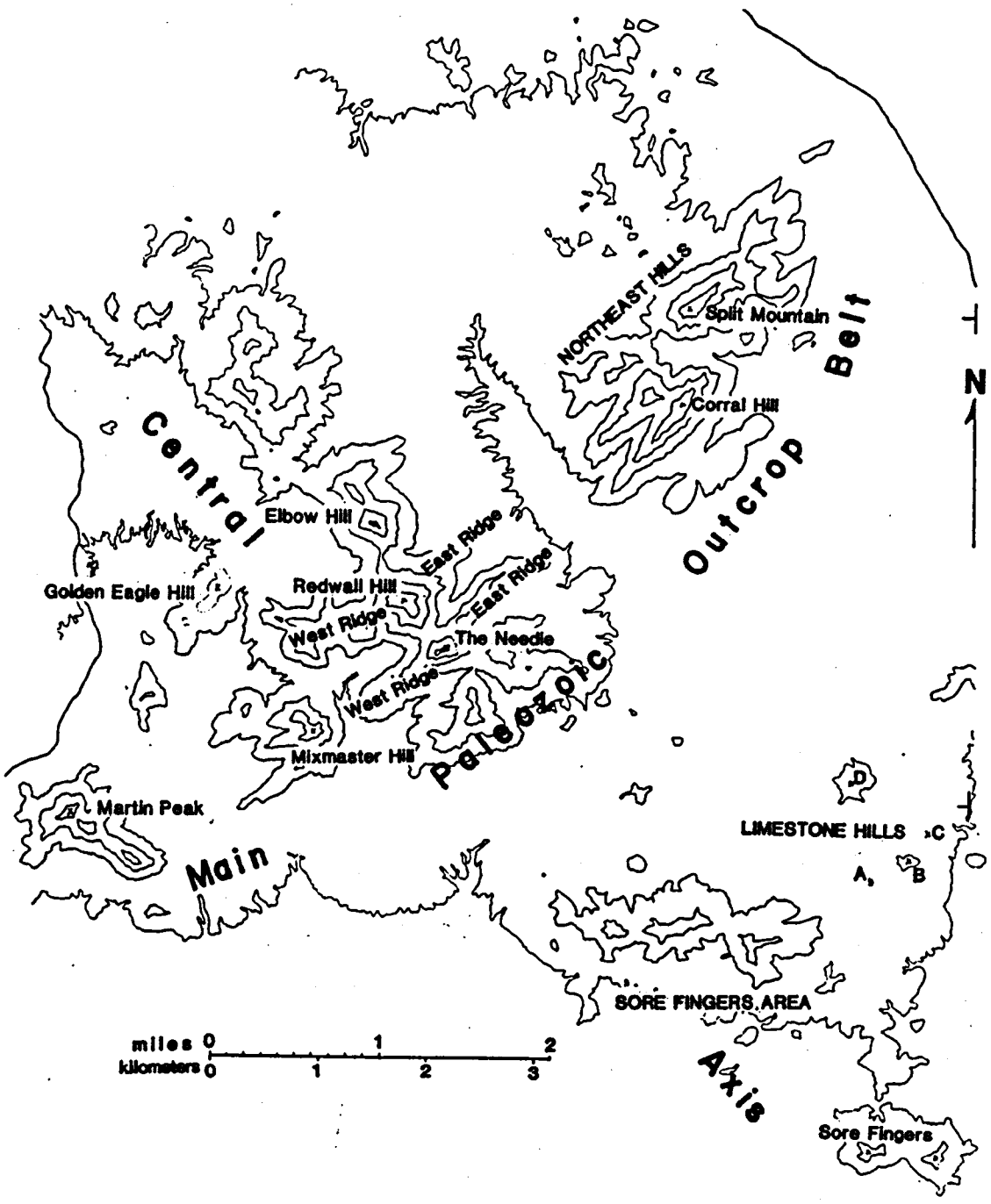

Figure 3. Physiographic features of the southern Little Harquahala Mountains.

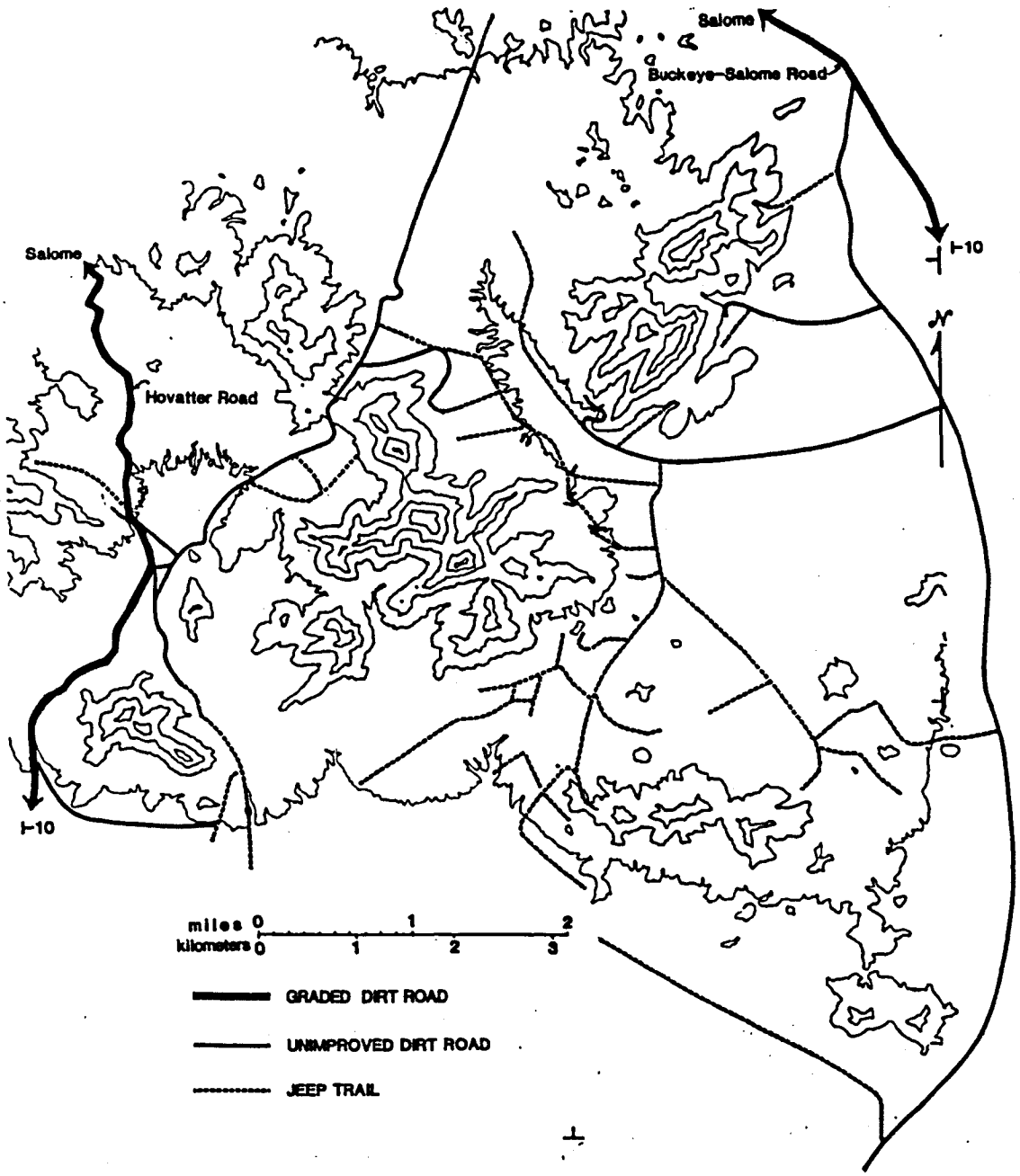

Figure 4. Map showing access roads in the Southern Little Harquahala Mountains.

western Harquahala Mountains. A map of the White Marble Mine area adjacent to Socorro Peak on the northeast was published by Keith and others (1981). Reconnaissance maps of the Harquahala Mountains have been presented in Reynolds, Keith and Coney (1980), Rehrig and Reynolds (1980) and Reynolds (1982). McKee (1954) measured the Paleozoic section in the Little Harquahala Mountains. Marshak (1978) briefly described the Mesozoic section in the northern Little Harquahala Mountains, along with several other sections in west-central Arizona. Harding (1980, 1982) has measured and described in detail Mesozoic clastic sections in the Livingston Hills, southern Plomosa Mountains and Dome Rock Mountains.

Present Study

The author was first acquainted with the geology of the region on a reconnaissance trip to the western Harquahala Mountains with Steve Reynolds and Ed DeWitt in the fall of 1979. The complexity and apparent magnitude of structures found at that time far exceeded that indicated by previous mapping by Wilson (1960) or Varga (1977). Further reconnaissance mapping in the region revealed a series of stacked thrust plates involving Mesozoic, Paleozoic and Precambrian rocks (Reynolds, Keith and Coney, 1980). Because structural complexity and metamorphism make interpretation of relations in the western Harquahala Mountains area difficult, mapping in the southern Little Harquahala Mountains was undertaken to provide additional data on the geometry and kinematics of deformation in the region. Sixty-

seven field days were spent mapping 23 square miles in the southern Little Harquahala Mountains during the spring and fall of 1981. The base map used was a 1:12000 enlargement of part of the Hope, Arizona 15' series U.S.G.S. quadrangle (Figure 5).

REGIONAL GEOLOGIC SETTING

A short summary of the geology of west-central Arizona is included here to provide a context for the present study. The oldest rocks in west-central Arizona are 1.4 to 1.7 billion year-old metamorphic and granitic rocks that constitute the crystalline basement of the region. Paleozoic rocks were deposited on the craton east of the Cordilleran miogeocline. Disconformities in the Paleozoic section represent periods of uplift and erosion or non-deposition. Mesozoic rocks accumulated and were deformed in intra-arc and back-arc settings dominated by compressional and probable strike-slip tectonics. Jurassic volcanic and intrusive rocks and Jurassic or Cretaceous clastic rocks, locally associated with Paleozoic rocks occur in a west-trending belt extending from the Little Harquahala and Granite Wash Mountains to the Dome Rock Mountains (Figure 7), and from there to the Coxcomb Mountains in southeast California. Two clastic sequences have been recognized in this assemblage: the McCoy Mountains Formation (Pelka, 1973; Miller, 1970; Harding, 1982) and the Apache Wash Formation (Harding, 1982). Both sequences were deposited on Jurassic hypabyssal or volcanic rocks, and are similar in gross petrography and depositional setting, but they have different stratigraphy and detailed petrography. The Apache Wash Formation was deposited on Jurassic arc rocks which overlie Paleozoic and Precambrian rocks that can be correlated with other rocks in

Arizona. Paleozoic strata are nowhere exposed in strstigraphic continuity below Jurassic rocks underlying the McCoy Mountains Formation. The clastic sequences were deposited in deep structural basins interpreted to be related to Jurassic or early Cretaceous high-angle and strike-slip faulting (Harding, 1982). The Apache Wash Formation is interpreted by Harding (1982) to be absent west of the Plomosa Mountains.

A complex zone of thrust faults bounds McCoy Mountains Formation outcrops on the north in southeast California and in the Dome Rock Mountains of Arizona. Folded and metamorphosed Precambrian, Paleozoic and Mesozoic rocks are interleaved along this north-dipping fault zone. In the southern Plomosa Mountains and western Harquahala Mountain region, subhorizontal faults juxtapose the McCoy Mountains and Apache Wash Formations, and other faults place sheets of Precambrian crystalline rocks on the sedimentary rocks (Miller and McKee, 1971; Reynolds, Keith and Coney, 1980). Late Cretaceous and early Tertiary plutons cut these low angle faults (Reynolds, 1982). Paleozoic rocks between thrusts in the western Harquahala Mountains are folded into a large-scale southeast-vergent recumbent fold which is the oldest structure in the area (Varga, 1977; Keith and others, 1981).

Mid-Tertiary sedimentary and volcanic rocks were deposited in local continental basins (Eberly and Stanley, 1978). Extensional deformation, characterized by low-angle normal or detachment faults, accompanied or occured soon after deposition of these rocks (Rehrig

and Reynolds, 1980; Davis and others, 1980). Major detachment zones are present along the Colorado River (Frost and Martin, 1982) and along the northeast margin of the Harquahala, Harcuvar, and Buckskin Mountains (Rehrig and Reynolds, 1980). Mylonitic gneisses with gently dipping foliation and northeast-trending lineation in the northeastern Harquahala and Harcuvar Mountains were derived from Precambrian, Mesozoic and Tertiary intrusive and metamorphic rocks. These gneisses yield a K-Ar biotite age of 25.3 m.y. (Rehrig and Reynolds, 1980), indicating mid-Tertiary cooling of the gneiss. Southwest-dipping Tertiary volcanic and sedimentary rocks and Precambrian gneisses overlie a major, gently dipping detachment fault that cuts the mylonitic gneiss. Volcanic rocks above the fault have been dated at 15.8 m.y. (K-Ar whole rock age, Scarborough and Wilt, 1979). The southwest dip of Tertiary strata above this fault, in the western Bighorn Mountains, and in the Plomosa Mountains indicates rotation on a northwest-trending axis due to extension in a northeast direction. Change in strike of bedding in Tertiary rocks above the detachment fault in the northeast Harcuvar Mountains (Reynolds, 1982) indicates that the northeast-trending arches dominating the present physiography formed during or after detachment faulting. Northwest-trending, right-reverse faults marked by prominent physiographic breaks appear to offset all other structures in the Harquahala Mountains. The Hidden Treasure Fault of Varga (1977) and an inferred fault along Centennial Wash (Varga, 1977) are interpreted to be part of this set of faults. Northeast-trending ranges in west-central Arizona are

truncated on the southwest along a prominent northwest-trending linear zone. Right separation of Paleozoic rocks between the southern Plomosa Mountains and the Little Harquahala Mountains suggests strike-slip movement along this zone.

GENERAL GEOLOGY OF THE LITTLE HARQUAHALA MOUNTAINS

Precambrian porphyritic monzogranite in the central part of the Little Harquahala Mountains is overlain by a highly faulted, northeast-trending, cratonic Paleozoic section (Figure 8). The Paleozoic rocks are depositionally overlain by Mesozoic volcanic and volcaniclastic rocks and Mesozoic lithofeldspathic sandstones. On the south the sedimentary rocks overlie altered igneous and metamorphic rocks of the Sore Fingers Assemblage along the Sore Fingers thrust and low-angle normal faults. On the north, the Hercules thrust places the Precambrian monzogranite on Mesozoic clastic, volcaniclastic, and volcanic rocks informally known as the rocks of Harquar Peak. Lower-plate Mesozoic rocks are lithologically and stratigraphically different from Mesozoic rocks in the upper plate. The rocks of Harquar Peak are intruded in the northern part of the range by the Granite Wash granodiorite (Reynolds, 1980). Along the western edge of the range, southwest-dipping volcanic rocks of probable Miocene age overlie monzogranite and clastic rocks in the upper and lower plates of the Hercules thrust. The Little Harquahala Mountains are structurally bounded on the northeast by an inferred northwest-trending, oblique-slip fault in the vicinity of Centennial Wash (Varga, 1977).

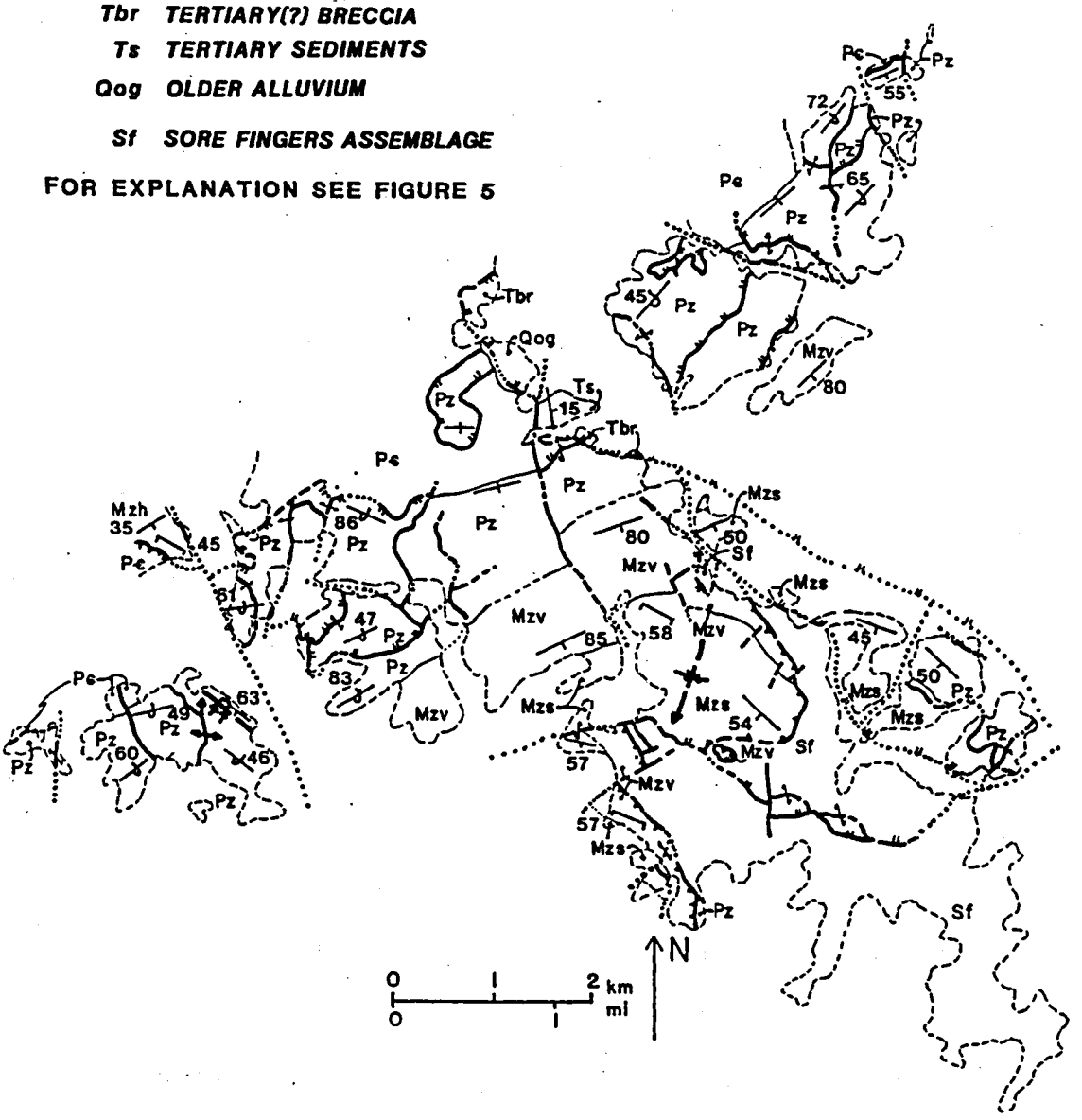

Figure 8. Generalized geologic map of the southern Little Harquahala Mountains.

STRATIGRAPHY

Introduction

Rocks ranging in age from Precambrian to Tertiary crop out in the southern Little Harquahala Mountains. Pre-Cenozoic rocks in the Southern Little Harquahala Mountains (Figure 9) include approximately 1000 meters of Paleozoic strata, a highly variable thickness of Mesozoic volcanic and volcaniclastic rocks up to 900 meters thick, and a minimum of 750 meters of Mesozoic lithofeldspathic sandstone, siltstone and conglomerate correlated with the Apache Wash Formation of the southern Plomosa Mountains (Harding, 1982). Precambrian igneous and metamorphic rocks underlie the Paleozoic strata. An unknown thickness of Mesozoic clastic and volcanic rocks is present below the Hercules thrust in the northern part of the area. Igneous and metamorphic rocks of uncertain age present in the southern part of the map area are included in the Sore Fingers Assemblage. Finally, a variety of dikes are recognized. Due to the structural complexity and to internal disruption, thicknesses of the stratified units have been determined by averaging measurements from the map in areas where the stratigraphy is least disrupted. Phaneritic igneous rock classification follows I.U.G.S. recommendations (Streckeisen, 1973). The rock units are divided into five major groups reflecting the

geologic development of the area: 1) Precambrian rocks; 2) Paleozoic strata; 3) Mesozoic continental deposits; 4) Cenozoic deposits and 5) the Sore Fingers Assemblage.

Precambrian Rocks

Precambrian monzogranite crops out in the northwestern part of the area between the Paleozoic rocks and the Hercules thrust. Amphibolite gneiss occurs in a small area adjacent to the thrust and is intruded by the monzogranite (Figure 5).

The monzogranite is in depositional and fault contact with Paleozoic rocks, Tertiary breccia, and Tertiary(?) older alluvium. The monzogranite is assigned a Precambrian age because it is unconformably overlain by the Cambrian Bolsa Quartzite. The monzogranite consists of about 43% quartz, 29% plagioclase, 18% potassium feldspar, 5% secondary muscovite, and 5% altered mafic minerals, based on one point count of a relatively unaltered sample. Primary biotite is altered to aggregates of muscovite and magnetite. Masses of hematite, chlorite, opaque minerals, and sericite are interpreted to be altered mafic minerals. Low relief of plagioclases and irregular staining of potassium feldspars suggests albitization of feldspars. The monzogranite is non-resistant and is exposed in washes and on slopes below the Paleozoic rocks. It is ubiquitously altered in the vicinity of the unconformity with the Bolsa Quartzite to an assemblage of light green, argillized or epidotized feldspar set in a reddish, argillic groundmass with abundant relict quartz. In less

intensely altered zones further from the unconformity, the monzogranite consists of a medium-grained quartz, plagioclase, and minor biotite groundmass with 1-3 cm long potassium feldspar phenocrysts. Some of the alteration at the unconformity may be due to pre-Bolsa weathering, but the presence of similar alteration in the Bolsa Quartzite requires later chemical changes as well.

Amphibolite gneiss consisting of medium-grained hornblende and plagioclase crystals occurs in a small area above the Hercules thrust, at the northwest edge of the map area. Near-vertical, northeast-trending foliation in the gneiss is characteristic of middle Proterozoic gneisses in west-central Arizona (Reynolds, 1980). The foliation is disrupted and folded within 10-15 meters of the Hercules thrust.

Paleozoic Rocks

A cratonic Paleozoic section overlies the Precambrian basement in the Little Harquahala Mountains. The stratigraphy of the Paleozoic rocks resembles the southeast Arizona Paleozoic section (Bryant, 1968) in its lower part and the Grand Canyon section (McKee, 1969) in its upper part. Miller (1970) described a similar section in the southern Plomosa Mountains and noted its resemblance to the section in the Little Harquahala Mountains. He recognized the Bolsa Quartzite, Abrigo Formation, Martin Formation, Escabrosa Limestone, Supai Formation, Coconino Sandstone, and Kaibab Limestone. Varga (1977) reported an essentially identical section in the western Harquahala

Mountains, except he stated that the Abrigo and Martin Formations are absent due to a bedding-plane fault. Varga (1977) favored correlation of the carbonate unit below the Supai Formation with the Redwall Limestone instead of the Escabrosa Limestone; this usage is followed in this report. Otherwise, the terminology used here for Paleozoic rocks is identical to that used by Miller (1970).

Bolsa Quartzite

In the Little Harquahala Mountains, the thickness of the Bolsa Quartzite ranges from 50 to 100 meters due to variation in original thickness and to post-depositional tectonic thinning or thickening. The Bolsa Quartzite lies unconformably on Precambrian monzogranite and is overlain conformably and gradationally by the Abrigo Formation. Based on the lithologic correlation with the type Bolsa Quartzite, (Ransome, 1904) a middle to upper Cambrian age is assigned to the quartzite in the map area. The unit is exposed along the northwestern edge of Paleozoic outcrops. The best exposures are on western Martin Peak, Redwall Hill, and northwest Split Mountain (Figure 10).

The Bolsa Quartzite consists of maroon, red-brown and gray-purple feldspathic-quartz grit, sand and silt. The unconformity at the base of the formation is difficult to locate exactly in areas where a thick paleo-weathered horizon caps the underlying monzogranite. In other places, a thin zone of cobble conglomerate, commonly containing angular bull-quartz clasts, occurs at the base of the Bolsa Quartzite. The basal part of the formation comprises

Figure 10. Photograph of Split Mountain.

View is looking northeast. Brown Bolsa Quartzite on the left contrasts sharply with the tan and gray beds of the Martin Formation on the right. The intervening Abrigo Formation does not form prominent outcrops.

medium-bedded, feldspathic grit with abundant planar-tabular cross bedding in sets up to 20 cm thick. Up section, the grain size decreases, beds become thinner, and cross beds are less common. In its upper part, the Bolsa Quartzite consists of thin- to medium-thin-bedded, brown sandstone with white laminations and gray or light green-grey, silty or shaly partings. The contact with the Abrigo Formation is placed at the first thick, non-resistant shaly zone.

Abrigo Formation

The thickness of the Abrigo Formation in the Little Harquahala Mountains ranges from 0 to 27 meters. The least deformed sections, which occur on Redwall Hill, the Northeast Hills, Elbow Hill, and west Martin Peak, are about 15 meters thick. The lower contact with the Bolsa Quartzite is gradational and apparently conformable. The upper contact of the Arigo Formation is placed at the base of the first thick-bedded dolomite of the Martin Formation. Paleontologic data from other parts of Arizona indicate that this contact is a disconformity (Bryant, 1968). Based on the lithologic correlation with the fossiliferous type Abrigo Formation (Ransome, 1904), an upper Cambrian age is assigned to this unit. In the Little Harquahala Mountains, the Abrigo Formation comprises interbedded thin- to medium-bedded, dark brown to red-brown sandstone, black, maroon and greenish-gray shale and siltstone, and a few medium-bedded tan carbonate beds. Sandstone beds in its lower part are up to 20 cm thick, and become thinner and less common up section. They strongly resemble

sandstones of the upper Bolsa Quartzite. They locally contain ripple cross bedding or are abundantly burrowed. Some of the shaly partings contain inarticulate fossil hash. Carbonate beds about 15-20 cm thick occur locally in the middle or upper part. Transition into the thick bedded resistant carbonates of the Martin Formation is abrupt. Due to the thin-bedded character of the Abrigo Formation, contorted folding is very common.

Martin Formation

The Martin Formation is about 100 meters thick in the Little Harquahala Mountains. It disconformably overlies the Abrigo Formation and is overlain disconformably by the Redwall Limestone. The Martin Formation is assigned an upper Devonian age based on lithologic correlation with the type Martin Formation (Ransome, 1904). The least disturbed sections are present on Elbow Hill and Corral Hill. The Martin Formation is characterized by medium gray, tan, and brown, medium-grained to porcelaneous dolomite and dolomitic limestone (Figure 10). The dolomite is well-bedded and medium- to thick-bedded; beds are internally laminated, mottled or massive. Gray beds are commonly fetid and tan and brown beds normally contain disseminated quartz-sand grains. Abundant siliceous lumps about 1 cm in diameter may be silica-replaced birds-eye structures. The basal 2 meters are chocolate brown and tan-orange or tan-grey dolomite, with a few thin sandstone interbeds. An apparently continuous sandstone bed about 15 meters above the base is approximately 30 cm thick and consists of

well-rounded to sub-rounded, poorly sorted quartz sand. Grain size ranges from .5 to 4 mm. A tan silty shale was observed about 10 meters below the Redwall Limestone on the west ridge of Redwall Hill. On the south face of Split Mountain, the upper Martin is an unusual medium-bedded, white-weathering, white or very light grey limestone or dolomitic limestone with disseminated black specks and sandy lamina. This change is probably due to alteration in the vicinity of the small intrusion and numerous dikes in the area. At the top of the Martin Formation, a laminated sandy dolomite bed about 40 cm thick is overlain by 1 to 2 meters of nondescript grey dolomite. On northeast Redwall Hill a 1-2 meter karst horizon caps the Martin Formation. Angular limestone clasts occur in a maroon-brown sandstone matrix, similar in appearance to the karst conglomerates above the Redwall Limestone. It is interpreted to represent the Devonian-Mississippian disconformity.

Redwall Limestone

In the Little Harquahala Mountains, the Redwall Limestone consists of 100 meters of limestone and dolomite. Its lower and upper contacts are both disconformable and are marked by karst horizons. The Redwall is assigned a lower Mississippian age based on its lithologic correlation with the type section (McKee and Gutschick, 1969). The best exposures are on Redwall Hill, west ridge of Redwall Hill and Split Mountain (Figure 11). The Redwall Limestone is divided into three units. The lower unit comprises in ascending order, 1) a

Figure 11. Redwall Limestone and Supai Formation on west ridge of Redwall Hill.

The section is overturned, with the top of the lower unit of the Redwall Limestone on the skyline. Below it is the cherty, cliff-forming, middle unit and the slope-forming upper unit. The underlying prominent red-brown band is the Supai Formation, with the rest of the formation forming the slope below, and the right side of the skyline.

thick bed of sandy varicolored limestone, 2) massive white limestone bed, 3) massive tan dolomite, and 4) massive white limestone. The middle unit is a variably dolomitized, cherty limestone. The upper, third unit is medium-bedded, light gray limestone. The lower two units are resistant and form prominent cliffs and bold outcrops; original depositional features are obscured by recrystallization. The upper unit is non-resistant and forms a bench, along with the basal Supai Formation, between the Redwall Limestone and the Supai Formation; it is composed of slightly to moderately recrystallized bioclastic grainstone or packstone. Crinoid columnals are the only fossils recognized. In the upper part of the Redwall Limestone, cavities filled with maroon shale or siltstone are common, and the rock grades up into local carbonate-clast conglomerate. Redwall Limestone cobbles to boulders in the conglomerate are set in a maroon, siltstone matrix lithologically identical to that forming the basal siltstone unit of the Supai Formation. The upper contact is placed at the base of the first clearly transported conglomerate, or at the base of the maroon siltstone and sandstone of the Supai Formation if there is no limestone conglomerate. Thick limestone conglomerate is exposed on the eastern part of Martin Peak, and on Redwall Hill.

The Supai Formation

In the Little Harquahala Mountains, 150 to 200 meters of interbedded shale, limestone and sandstone are correlated with the Supai Group but because individual formations within the group have

not been recognized, the Supai Group has been reduced in rank to a formation in the map area. The best section is exposed on the center spur on the southeast side of the west ridge of Redwall Hill (Figure 11). A Pennsylvanian-Permian age is assigned to the Supai Formation based on lithologic and stratigraphic correlation with the type Supai Group (McKee, 1975). As is characteristic of Pennsylvanian-Permian cyclic units, the stratigraphy of the Supai Formation is complex and highly variable. The basal unit is consistently a non-resistant maroon siltstone with interbedded sandstone and conglomerate 15 to 30 meters thick. Where best developed, this horizon overlies limestone conglomerates formed on a karst surface on top of the Redwall Limestone. In the maroon unit, chert-pebble conglomerate lenses are interbedded with laminated, maroon, fine-grained, chert- and quartz-grain sandstones. Small-scale, trough cross beds are locally present. The upper part of the maroon unit is generally fine-grained and massive. Ubiquitous shearing and cleavage development obscure the original depositional features. The rest of the Supai Formation consists of an assortment of lenticular lithosomes. Rock types include gray, medium-grained crystalline limestone; tan dolomite or dolomitic limestone; silty, brown to tan dolomite; fine- to medium-grained, white, vitreous quartzite; maroon siltstone; tan, very thin-bedded siltstone; dark gray-green, shaly siltstone; red-brown to pink, calcareous siltstone; and tan, siliceous, crystalline carbonate which weathers to form characteristic, dark brown, siliceous ribs. Beds are generally 1 to 2 meters thick. On Split Mountain a massive fine-

grained sandstone bed with abundant medium-scale, trough cross bedding is present near the top of the section. The contact with the Coconino Sandstone is placed at the base of uniform very thin-bedded white quartzite of the Coconino Sandstone.

Coconino Sandstone

The Coconino Sandstone comprises 190 meters of poorly exposed, but distinctive white quartzite in the Little Harquahala Mountains. It lies conformably on the Supai Formation, and is conformably overlain by the Kaibab Limestone. A Permian age is assigned to the Coconino Sandstone based on correlation with the type section (McKee, 1934). The Coconino Sandstone is a uniformly white to pink-brown, fine-grained vitreous quartzite. The unit is non-resistant due to intense fracturing; spotty exposures occur beneath a mantle of quartzite gravel on slopes between Supai Formation and Kaibab Limestone. The best section is located in the saddle between the Needle and Redwall Hill. The sandstone is uniformly very thin- to thin-bedded. Medium-scale trough cross beds are present but are not commonly seen (Figure 12), perhaps due to poor outcrop. Undisturbed contacts are rare. The lower contact is placed above the last brown or tan weathering impure sandstone bed of the Supai Formation. The upper contact is placed at the base of a prominent dark brown weathering dolomitic sandstone at the base of the Kaibab Limestone.

Figure 12. Cross bedding in the Coconino Sandstone.

Kaibab Limestone

In the Little Harquahala Mountains, the Kaibab Limestone consists of 210 to 400 meters of limestone, cherty limestone, dolomite and sandstone. The Kaibab conformably overlies the Coconino Sandstone. The upper contact is poorly exposed, but is interpreted to be an unconformity below the Mesozoic sandstone unit, based on regional relationships and the abrupt change in depositional environment. Dr. Karl Flessa (personal communication, 1981) identified Chaetetes (?) milleporaceus, Antiquitonia portlockiana and Cleiothyridina orbiculari among a collection from the Kaibab Limestone. These are all of Pennsylvanian-Permian age and suggest correlation with the Naco Group. Dr. Flessa favors a middle Pennsylvanian age based on these identifications. The Kaibab Limestone is normally assigned a Permian age (McKee, 1938). The stratigraphic position of the limestone in the Little Harquahala Mountains, above an obvious Coconino-Scherrer lithologic equivalent, which is uppermost Pennsylvania in age where dated, suggests that it is Post-Pennsylvanian in age. The best section through the Kaibab Limestone is located on hill D of the Limestone Hills (Figure 13). Fault blocks on east Needle Ridge and Mixmaster Mountain also contain short segments of relatively undisturbed section. The Kaibab Limestone was divided into five units for mapping (see Figure 14 for a detailed description). The lowest unit is dolomitic sandstone at its base, probably representing reworking of Coconino sand in a carbonate environment, and grades upward into cherty tan-gray dolomitic

Figure 13. Kaibab Limestone on Hill D in the Limestone Hills.

The section is upright and dips towards the left. The Coconino Sandstone is not visible at the base of the hill on the right. Other contacts are indicated on the photo.

limestone, overlain by fossiliferous gray limestone and dolomitic limestone. The unit is capped by a thin, fine-grained, tan sandstone with laminated carbonates of probable shallow water algal origin. Unit one records a transgression-regression cycle and is probably equivalent to the Toroweap Formation of the Grand Canyon. Unit two is composed of cherty, gray, bioclastic limestone. Unit three consists of uniform, medium-bedded, light to dark gray limestone. Unit four comprises medium- to thick-bedded, light gray limestone with abundant fossils and chert; it becomes sandy at the top. Unit five includes a lower tan sandstone with a few conglomerate lenses. It is overlain by cherty and fossiliferous limestone similar in character to unit four. More tan sandstone is locally present above the limestone. A disconformity may separate units four and five. Unit five is included in the Kaibab Limestone because of lithologic similarity and the close resemblance of fossils in unit five and unit four. A characteristic feature of sandstones within the Kaibab Limestone is very poor sorting or texture inversion; well rounded, medium- to coarse-sand grains occur in a matrix of very fine sand. Sandstone beds at the base and top of unit one, a thin bed within unit two, at the top of unit four, and the base of unit five all exhibit this texture.

Paleozoic(?) Breccia-Conglomerate

Massive breccia or conglomerate occurs as large intraformational masses in gradational contact with Kaibab Limestone at the west end of the ridge southwest of the Needle, on the east side

of Mixmaster Hill, and in the Redwall Limestone on Martin Peak. The unit consists of buff to red, fine-grained sandstone and pebble to boulder conglomerate (Figure 15). Fine-grained sandstones are commonly current laminated, and contain lenses of pebble conglomerate, with local graded bedding. In thin section, the sandstone consists of moderately sorted, angular quartz and chert grains in a calcite matrix. The calcite is apparently replacing a rarely preserved original phyllosilicate matrix. Most of the unit is massive cobble to boulder conglomerate. Clasts in the conglomerate are angular and range up to 3 meters in diameter. As contacts with the enclosing limestone are approached, the conglomerate becomes monolithologic and grades into broken but untransported rock. Lenses of laminated sandstone and pebble conglomerate are abundant in limestone adjacent to the breccia-conglomerate. The unit is interpreted to be a cavern filling deposit. Cave development probably occurred between deposition of the Kaibab Limestone and the Mesozoic volcanic units, based on the similarity of sandstones within the breccia-conglomerate to sandstone in unit five of the Kaibab Limestone. One puzzling aspect of the deposit is the uniform steep southwest dip of bedding measured in the deposit in all three outcrop areas (Figure 16). Large initial dips in the breccia-conglomerate are suggested to explain the present attitude of the rocks, since there is no structural evidence for the large rotation required to produce the observed orientations.

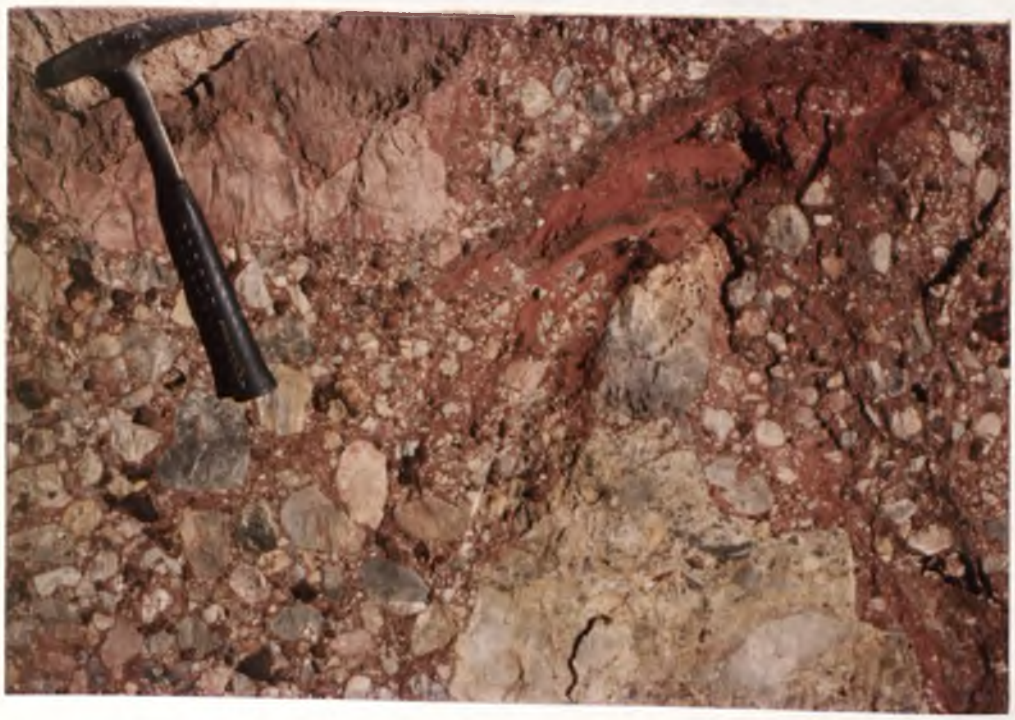

Figure 15. Breccia-Conglomerate on the ridge southwest of the Needle.

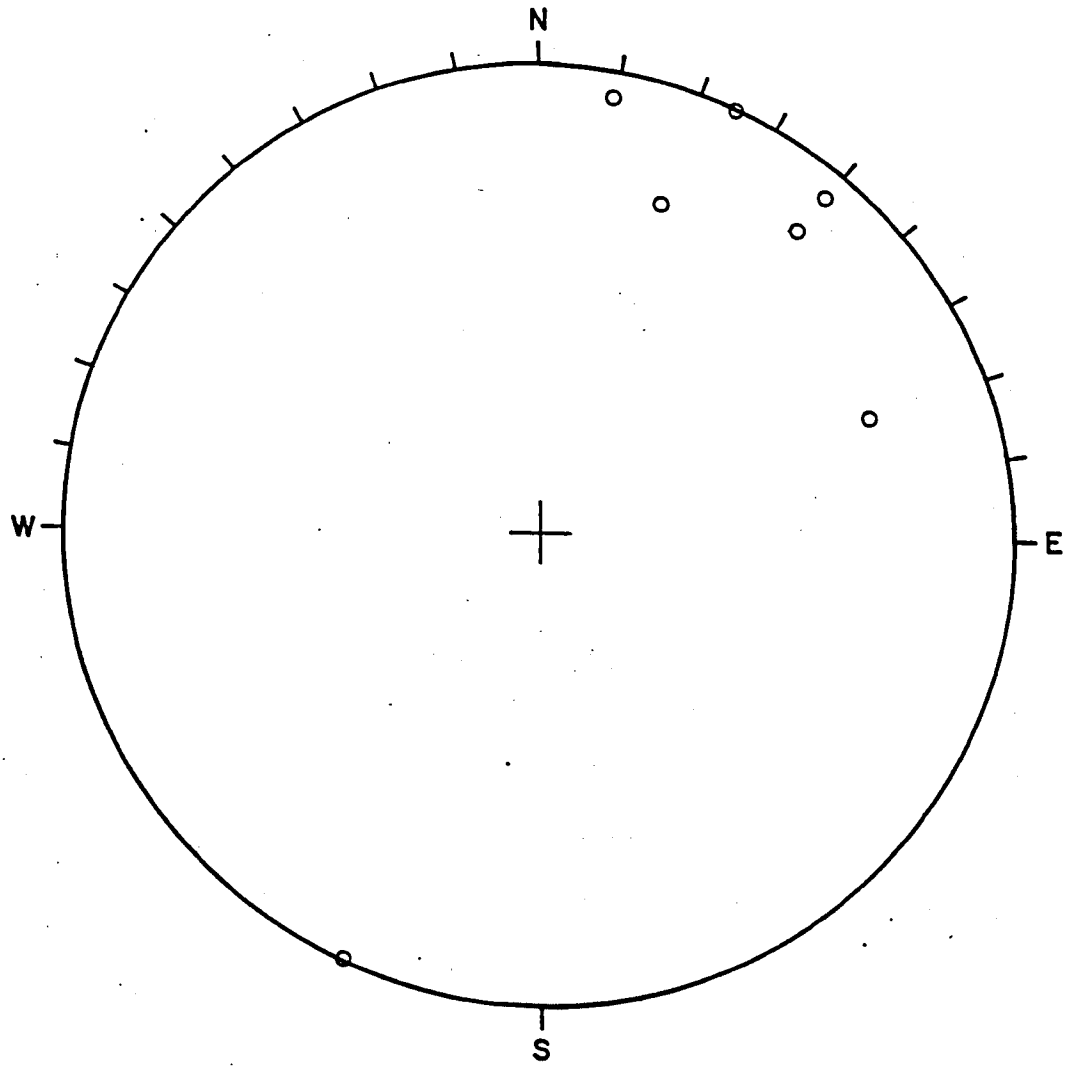

Figure 16. Poles to bedding in the breccia-conglomerate.

Mesozoic Rocks

Two different Mesozoic sequences are present in the Little Harquahala Mountains: Mesozoic rocks of Harquar Peak and Mesozoic rocks of the southern Little Harquahala Mountains. Formal nomenclature for these rocks is lacking. A Jurassic or Cretaceous age is inferred for the southern Little Harquahala Mountain section based on the presence of volcanic rocks low in the section and involvement in possible Late Cretaceous deformation. The rocks of Harquar Peak are interpreted to be of a similar age based on their gross lithologic similarity and similar involvement in the deformation. The internal stratigraphy of the rocks of Harquar Peak was not determined. Mesozoic rocks of the southern Little Harquahala Mountains were studied in greater detail. Five lithologic units were mapped: 1) Mesozoic sandstone and conglomerate; 2) lower volcanic unit; 3) upper volcanic unit; 4) volcaniclastic sediments; 5) lithofeldspathic sandstone correlated with the Apache Wash Formation (Harding, 1982).

Mesozoic Sandstone

A thin, unnamed, and previously undescribed sequence of sandstone and conglomerate overlies the Kaibab Limestone in the southern Little Harquahala Mountains. Outcrops are uncommon, and contacts are sheared. The maximum thickness of the unit is between 50 and 70 meters; the best exposures are in the valley east of the Needle. The lower contact is probably an unconformity, as suggested by the abrupt change in lithology, depositional environment and

tectonic setting. The upper contact probably does not represent a significant hiatus. The age of the sandstone is between late Permian and middle Mesozoic, because it overlies Permian carbonates, and is overlain by Jurassic volcanic rocks. The basal part of the sandstone unit consists of red, tan, and dark gray-green siltstone and fine-grained sandstone interbedded with a few white limestone beds; mafic dikes or flows are present on East Needle Ridge and southeast Corral Hill. The rest of the sandstone unit includes light gray, fine-to coarse-grained sandstone and pebble to cobble conglomerate with maroon siltstone partings (see Figure 17 for details). Clasts in the sandstone include in order of abundance: monocrystalline quartz, chert, polycrystalline quartz, limestone, potassium feldstar, magnetite, muscovite and schist. Point count data from one thin section is included in Figure 18. Conglomerate clasts include tan vitreous quartzite (Coconino?), red-brown and white coarser-grained quartzite (Bolsa?), white-weathering chert, and uncommon tan-weathering siltstone and limestone. A few lenses of limestone conglomerate occur in this unit as well. These data indicate that Paleozoic sedimentary and probable Precambrian crystalline rocks were exposed in the source area. The conglomerates are clast-supported or sand-dominated. These sediments were deposited in a fluvial environment. The similarity between maroon siltstones at the top of this unit southeast of Mixmaster Hill and those in the basal lower volcanic unit suggests an interbedded or gradational contact between

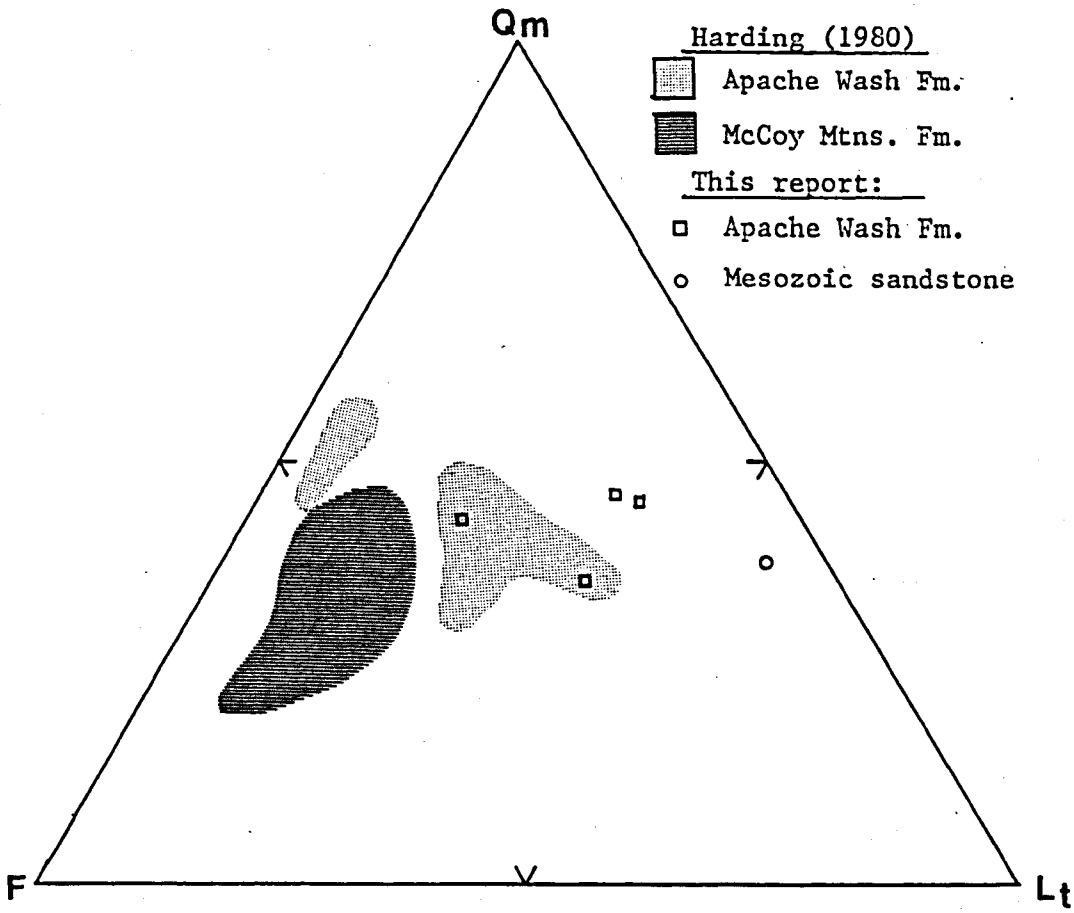

Figure 18. Petrology of Mesozoic Clastic Rocks.

Poles to triange are: Qm - monocrystalline quartz; F - Feldspars; Lt - total lithics. (Dickinson and Suczek, 1979)

the two units. However, absence of the conglomeratic horizon southeast of the Needle suggests erosion prior to red-bed deposition.

The Mesozoic sandstone is believed to correlate temporally with the Moenkopi or Chinle Formation of the Colorado Plateau. Volcanic rocks interpreted to be related to Jurassic volcanics overlie the Mesozoic sandstone in the southern Little Harquahala Mountains. In southern Arizona and southeast California the Aztec-Navajo Sandstone is correlated with the Glen Canyon Group which overlies the Chinle Formation on the Colorado Plateau. This sandstone interfingers with volcanic rocks also interpreted to be related to Jurassic volcanism (Bilodeau and Keith, 1979; Grose, 1959; Miller and Cameron, 1982). Precambrian crystalline and Paleozoic sedimentary clasts are present in the Chinle Formation, and Paleozoic chert clasts in the Moenkopi Formation were derived in part from a source on the southwest side of the Colorado Plateau, and indicate the onset of uplift in this region. This same uplift was probably the source for clasts in the Mesozoic sandstone (Stewart, Poole and Wilson, 1972). Correlation of the Mesozoic Sandstone with the Continental Red Beds in the southern Plomosa Mountains (Robison, 1980; Miller, 1966, 1970) is undesirable because the Red Beds overlie Jurassic volcanic rocks, and lack evidence of igneous or metamorphic rocks in their source area (Robison, 1980). In summary, stratigraphic position and petrology suggest correlation of the Mesozoic sandstone with the Moenkopi or Chinle Formation.

Lower Volcanic Unit

Up to 210 meters of unnamed and previously undescribed volcanic and volcaniclastic rocks overlie the Mesozoic sandstone. This sequence is referred to as the lower volcanic unit. It depositionally overlies the Mesozoic sandstone on a surface of low relief; probable interfingering of lithologies suggests that the contact does not represent a significant hiatus. The upper volcanic unit overlies the lower unit on a poorly understood intrusive-extrusive contact. The lower volcanic unit is assigned a Jurassic(?) age because all dated volcanic sequences in similar stratigraphic positions occurring in southern Arizona and California have Jurassic ages (compilation by Kluth, 1982; Pelka, 1973). The unit is best exposed in the vicinity of the Needle.

The lower volcanic unit comprises silicic flows, ash flow tuffs, agglomerates, massive and laminated tuff, and red volcanic-lithic sandstone and conglomerate. It is characterized by purple-gray, maroon-gray and gray-green colors (Figure 19). No consistent internal stratigraphy within the lower volcanic unit could be ascertained; complex lateral variations are the rule. The various lithologies observed are described in the schematic stratigraphic column of Figure 17. Conglomeratic red beds consisting of chaotic maroon sandstone, feldspathic-lithic sandstone and conglomerates are present at the base of the lower volcanic unit in the vicinity of the Needle and on Mixmaster Hill. Clasts in the conglomerate include limestone, volcanic rocks, quartzite, and uncommon intrusive rocks.

Figure 19. Volcanic rocks of the southern Little Harquahala Mountains.

Samples on the left are rocks of the lower volcanic unit: a subaqueous(?) tuff disrupted by later flow activity and a maroon-red flow or ash flow. On the right are three samples of the rhyodacite porphyry of the upper volcanic unit.

The intrusive rock fragments are rounded, coarsely crystalline to porphyritic granitoid up to about 20 cm. in diameter. South and southeast of the Needle, three large recrystallized limestone blocks with sheared contacts are intercalated in the basal part of the lower volcanic unit. They are lithologically similar to limestone in the upper Kaibab Limestone and are either gravity slide blocks emplaced during deposition of the lower volcanic unit, or are tectonic slivers emplaced along a shear zone between the volcanic and sedimentary rocks. The absence of abundant smaller Paleozoic limestone clasts within the surrounding volcanic and volcaniclastic rocks suggests a later, probably tectonic origin, but since there is no other evidence for repetition of units along faults near the blocks, the author favors a slide block origin. The presence of maroon siltstone partings in the Mesozoic sandstone, and probable lenses of sandstone in the basal part of the volcanic section suggests that there was no time break between the deposition of the two units; uplift and the onset of volcanism led to a rapid transformation of the source area.

Other lithologies in the lower volcanic unit include flows or welded tuff, massive and laminated tuff, agglomerates or volcanic conglomerates, and red beds (see figure 17). The flows, tuffs and agglomerates are interbedded. Flows and agglomerates commonly appear to intrude or disrupt bedded sedimentary rocks. Red beds occur as lenses both overlain and intruded by the volcanic rocks. The abundant fragmental volcanic deposits indicate explosive volcanism. Laminated tuffs are probably water lain, but evidence for subaqueous eruption of

the flows is absent. Thus, the lower volcanic unit is interpreted as a sub-areal explosive volcanic pile deposited in an area of local shallow water.

A unit Miller (1970) mapped as a latite dike in the central part of the Quartzite Quadrangle may be a volcanic unit correlative with the lower volcanic unit. Its lithology and stratigraphic position are similar to that of the lower volcanic unit. No other possibly correlative rock units are known.

Upper Volcanic Unit

A maximum of 335 meters of intrusive-extrusive rhyodacite porphyry overlies the lower volcanic unit. The contact is at least locally intrusive but is obscured by alteration; its trace is irregular in detail but at the scale of the map (Figure 5) it parallels other depositional contacts in the central part of the map area, suggesting a depositional contact. The porphyry is overlain gradationally by volcaniclastic conglomerate of similar composition; this contact is also obscured by alteration. The Jurassic(?) age assigned to the upper volcanic unit is based on correlation with other volcanic sequences in southern and western Arizona. A similar rhyodacite porphyry in the McCoy Mountains yielded an age of 175.8 ± 2.7 m.y. (K-Ar, plagioclase, Pelka, 1973).

The upper volcanic unit is a massive and homogeneous gray-green porphyry; no bedding or flow structure is visible (Figure 19 and see detailed description in Figure 17). It is correlated with quartz

porphyry lying between Paleozoic carbonates and the Apache Wash Formation near Apache Wash and on the north side of Black Mesa in the southern Plomosa Mountains (Figure 7) (Miller. 1970). Other quartz porphyry bodies in the southern Plomosa Mountains which are associated with sediments derived from quartz porphyry and the basal conglomerate of the Apache Wash Formation, are also considered correlative. Rhyodacite porphyry associated with the McCoy Mountains Formation of Harding (1982) in ranges west of the Plomosa Mountains (Pelka, 1973) is probably also of the same age.

Volcaniclastic Sediments

In the central part of the map area, up to 335 meters of volcaniclastic sediments overlie the upper volcanic unit. The lower contact is gradational and apparently conformable. The volcaniclastic sediments are conformably overlain on a locally gradational contact by the Apache Wash Formation. However, variable relationships are present at the contact due to facies changes in the lower member of the Apache Wash Formation (see Figure 17). A Jurassic or Cretaceous age is inferred for this unit based on its close association with and similarity to the Jurassic(?) upper volcanic unit.

Lithologically the volcaniclastic sediments closely resemble the upper volcanic unit. They comprise drab light to medium gray-green volcanic sandstone and conglomerate. Outcrops are generally blocky and strongly jointed. The sediments form a fining upward sequence, from a lower conglomerate to sandstone to a local capping

shale unit. The agglomerate-conglomerate unit is composed of medium- to coarse-grained lithic sand with abundant angular volcanic clasts, less common round to subround, tan, vitreous, quartzite and rare Paleozoic limestone clasts. The conglomerates are generally massive, chaotic and matrix supported; bedding is rarely visible. The contact with the sandstone member is placed where sandstone becomes the dominant lithology. The sandstone is generally featureless, massive and unsorted. Petrographically, it consists of altered volcanic rock fragments and sericitized feldspar, with disseminated 1 to 2 mm quartz grains, tiny opaques and altered biotite flakes. Pebble conglomerate lenses occur with decreasing abundance up section. Cross-bedding present in some magnetite rich beds indicates that the sediments were occasionally subject to subaqueous transport. The overall massive unbedded character of the volcanic conglomerate and sandstone suggests that it is mostly reworked pyroclastic sediment. The shale member includes white-weathering, silty, calcareous shale and siltstone interbedded with brown, thin-bedded, porcelaneous dolomite. Interbedded fine-grained volcaniclastic sandstone and siltstone are present near the base and in the upper part of the shale. Lithofeldspathic sandstone replaces volcaniclastic sandstone toward the top. Contacts are placed above and below the highest and lowest white shaly beds. This member was most likely in a shallow, fresh-water environment. It is probably a facies of the lower member of the Apache Wash Formation (see below), but is lithologically more closely

associated with the fining upward sequence of the volcaniclastic sediment unit and is thus included here.

The volcaniclastic sediments are distinguished from the upper volcanic unit by the presence of clastic textures. Miller's (1970) sediments derived from quartz porphyry are believed to be of similar age and origin.

Apache Wash Formation

A minimum of 750 meters of brown weathering fine- to coarse-grained lithofeldspathic sandstone interbedded with siltstone, shale and pebble to cobble conglomerate forms the youngest sedimentary unit deposited before major deformation within the map area. These sediments are correlated with the Apache Wash Formation of Harding (1982). The formation comformably overlies the shale member of the volcaniclastic sediments on the northwest, but uncomformably overlies units as old as the Coconino Sandstone in the Limestone Hills (Figure 17). It is overlain in angular unconformity by Quaternary gravels. Deformation of Mesozoic strata in the southern Little Harquahala Mountains is interpreted to be the result of the same event affecting rocks intruded by the undeformed Granite Wash Pass granodiorite, dated at 65 and 69 m.y. (K-ar, biotite; Damon, 1968; Eberly and Stanley, 1978). Since the sandstones overlie Jurassic (?) volcanic rocks, the age of the unit is Jurassic or Cretaceous (?).

The Apache Wash Formation is divided into two members. The lower member comprises interbedded volcaniclastic sandstone,

lithofeldspathic sandstone and massive conglomerate; the upper member consists of interbedded sandstone and siltstone, with conglomerate lenses in the lower part. The lower member is transitional between volcanic and volcaniclastic rocks below and lithofeldspathic sandstones above. It is present where the shale member of the epiclastic sediments is absent; where the shale is present, the upper member of the Apache Wash Formation directly overlies it (Figure 17). The lower member is in gradational contact with both the underlying volcaniclastic sandstone and the overlying upper member of the Apache Wash Formation. Contacts are placed below the lowest well-bedded or conglomeratic strata and at the top of the highest volcaniclastic sandstone. The volcaniclastic sandstone is generally gray-green to olive drab, medium- to thin-bedded, and composed of very poorly sorted angular fine sand to grit; clasts are mostly volcanic rock fragments and feldspar with minor quartz. It is distinguished from the underlying epiclastic sediments by the presence of obvious bedding and greater abundance of quartz, and from lithofeldspathic sandstone of the Apache Wash Formation (described below) by its distinctive lithic-rich petrology and drab gray-green color. The stratigraphy of the lower unit is variable (Figure 17). In the northwest, where the unit pinches out, it is only slightly conglomeratic, with lenses of Paleozoic limestone- and quartzite-clast conglomerate. To the southeast, along strike, the base of the unit is progressively more conglomeratic, until in the Limestone Hills, massive conglomerate is present at the base of the lower member. To

the west, on the opposite side of the Sore Fingers crystalline assemblage (Figure 5), the volcaniclastic sediment is overlain by bedded volcaniclastic rocks characteristic of the lower member; these are overlain by conglomerate. The conglomerates in the Limestone Hills and west of the Sore Fingers have different clast compositions. Quartzite and volcanic rock fragments up to 30 cm in diameter in the western conglomerate are set in a matrix of volcaniclastic sandstone identical to other volcaniclastic sandstones of the lower member. Conglomerate in the Limestone Hills is composed of clasts of Supai, Coconino, and Kaibab Formations in a matrix of calcareous quartz-rich sandstone and siltstone. A thin, sandy limestone interbedded in the limestone conglomerate in center west Sec. 28, T. 4N., R. 12W. contains algal structures similar to those described by Miller (1966) in the basal conglomerate of his Livingston Hills Formation, now assigned to the Apache Wash Formation (Harding, 1982). The sedimentary-clast conglomerate grades upward into poorly exposed mixed sedimentary-and volcanic-clast conglomerate, resembling those in the western exposures; this conglomerate is overlain by the upper member of the Apache Wash Formation. The lower contact of this conglomerate is a shear zone. On the southeast of Hill B in the Limestone Hills, the fault separating the Supai and Coconino Formations from the Kaibab Limestone (see Figure 34) does not offset the shear zone as much as the underlying rock. This relationship, along with truncation of the volcanic unit and upper part of the Kaibab Limestone and coarsening of conglomerates to the south suggests

that the contact is a sheared unconformity at the edge of an uplift that was a source of the conglomerates. In summary, the lower member is absent along the northwest edge of outcrops, where the shale member of the volcaniclastic sediment unit is present. Where the lower member is present, it becomes more conglomeratic to the southeast, with a predominance of Paleozoic clasts on the northeast, and volcanic clasts on the southwest. These relations suggest that the shale member of the volcaniclastic sediment unit is a lateral facies equivalent to the lower member of the Apache Wash Formation. Alluvial fans formed along the margins of an uplift graded laterally into a lacustrine environment in an adjacent basin.

The upper member of the Apache Wash Formation comprises lithofeldspathic sandstone, siltstone and pebble to cobble conglomerate. In general the unit is non-resistant and forms low outcrops. The sandstone is characteristically gray on fresh surfaces and medium-to dark-brown on weathered surfaces (Figure 20). The major detrital components of the sandstone are mono- and polycrystalline quartz, feldspar, rock fragments, and chert. Sandstone point count data for four thin sections, all from samples low in the stratigraphic section, are presented in Figure 18 along with data from Harding (1978) for sandstone in the southern Plomosa Mountains. Point counts from sandstones of the Little Harquahala Mountains resemble the Plomosa Mountains section of Harding (1978), now assigned to the Apache Wash Formation (Harding, 1982). The sandstone is fine- to coarse-grained, poorly sorted and thin- to thick-bedded. Beds are

Figure 20. Upper member of the Apache Wash Formation.

Note the cleavage in the siltstone beds.

normally massive or vaguely plane laminated; cross bedding is present but not common. Siltstone and silty shale are light brown or gray weathering and generally medium to dark gray on fresh surfaces, commonly with a micaceous sheen. Siltstone beds in NW Sec. 30, T. 4N., R. 12W. contain locally abundant poorly preserved shell remains; these have not been identified. Conglomeratic beds contain clasts up to 15 cm in diameter, but generally are coarse sand or grit dominated. Clasts are mostly vitreous tan quartzite, but limestone and volcanic rock fragments are present, along with rare intrusive rock fragments. The Apache Wash Formation forms a gross fining upward sequence. Coarse-grained sandstone and conglomerate predominate at the base, with minor interbedded thin siltstone layers. Siltstone is progressively more abundant higher in the section. Individual sand-shale packages form fining upward sequences. Above this sequence, in the western part of the outcrop area, gray and medium gray-green, medium- to thin-bedded, and quartz-rich sandstone with quartzite and volcanic pebbles and light grey-green silty or muddy partings is present. The lithofeldspathic sandstone occurring in the southern Little Harquahala Mountains is correlated with the Apache Wash Formation based on similar stratigraphic position, internal stratigraphy and sandstone petrology.

Rocks of Harquar Peak

Clastic and volcanic rocks below the Hercules thrust are included in the rocks of Harquar Peak. They underlie and are named

for Harquar Peak, the highest point in the Little Harquahala Mountains. The assemblage is intruded by the Granite Wash Granodiorite on the north and is in fault contact with Precambrian rocks on the east and south; Quaternary alluvium and Tertiary volcanic rocks bound outcrops on the west. Depositional contacts with identifiable pre-Mesozoic rocks have not been found. Within the study area the sequence includes porphyritic andesite flows or sills and volcaniclastic sandstone, siltstone and conglomerate. The contact between these units is not exposed and may be a fault or a depositional contact. The andesite is dark gray-green, with white feldspar phenocrysts up to 3 mm long; no bedding is visible. The clastic rocks comprise lithofeldspathic sandstone, siltstone and conglomerate. The sandstone weathers gray or maroon-gray, and is light gray on fresh surfaces. It is fine- to coarse-grained, well indurated, and thin- to thick-bedded. Maroon shaly siltstone partings, which locally contain mudcracks, are abundant. Interbedded conglomerates commonly occur in channels cut into the sandstone and contain angular volcanic rock clasts and subrounded to subangular quartzite, limestone, and rare intrusive rock clasts ranging in size up to 10 cm in diameter. The sandstone petrology was not studied in thin section, but feldspar, volcanic rock fragments, and variable amounts of quartz were observed in hand samples. Quartzite, quartz-rich sandstone and conglomerate similar to the continental red beds in the southern Plomosa Mountains (Miller, 1966, 1970; Robison, 1980) are present within the assemblage north of the map area. The association

of lithofeldspathic sandstone and conglomerate with quartzose clastic rocks and the absence of a pre-Mesozoic substrate suggests that the rocks of Harquar Peak are more closely related to the McCoy Mountains Formation than to the Apache Wash Formation of Harding (1982).

Cenozoic Rocks

Cenozoic rock units include a breccia, a conglomerate, and older alluvium. The breccia and conglomerate occur exclusively north of the Needle, whereas the older alluvium is present north of the Needle and in the Northeast Hills. The breccia occurs along a northeast-dipping low-angle fault zone, an association considered characteristic of mid-Tertiary low-angle normal faulting; the breccia is thus interpreted to be of Tertiary (?) age. Both the conglomerate and older alluvium depositionally overlie the breccia and are therefore of Tertiary or Quaternary age.

Breccia

Tertiary(?) breccia occurs along a northwest-trending, northeast-dipping, low-angle fault zone north of the Needle (discussed in the structural geology chapter). It is underlain by Paleozoic rocks east of the Needle fault (see Figure 5) and by Precambrian monzogranite to the west. The breccia consists mostly of crushed clasts of Paleozoic carbonates ranging from brecciated blocks several meters long to angular pebbles. Monolithologic horizons can locally be traced, but in general the breccia is polymictic and chaotic. The rock is strongly cemented by calcite or by silica.

A number of isolated outcrops of brecciated rock of probable tectonic origin occur in the Limestone Hills (Figure 5). Southeast of Hills B and C are two low hills of crushed Coconino Sandstone, with associated small outcrops of Apache Wash Formation and Kaibab Limestone. The Coconino Sandstone breccia is strongly indurated, with a sandy matrix indistinguishable in thin section from Coconino clasts in the breccia. Two outcrops of Coconino breccia occur southwest of Hill D. These are apparently fault bound, but contacts are not exposed. North of Hill D are two outcrops of limestone breccia. The southern outcrop is larger, and contains interleaved upper Kaibab and lower Apache Wash lithologies. These breccias are similar in appearance to Tertiary breccia outcrops occurring north of the Needle, but have a more monolithologic character.

Tertiary(?) Conglomerate

Poorly indurated, east-dipping conglomerate underlies one of the hills east to the Needle fault. A veneer of boulders present on Tertiary(?) breccia at the east end of the east ridge of Redwall Hill is interpreted to be a remanent of this conglomerate indicating that the conglomerate overlies the breccia. Near the Needle fault, the conglomerate consists of boulders of Supai and Coconino Formation up to one meter in diameter. To the east above this zone, clast size becomes smaller, and all Paleozoic lithologies, as well as Precambrian monzogranite are present as clasts. The conglomerate becomes finer-grained up section and grades into sandstone, pebble conglomerate, and

mudstone. The Tertiary(?) conglomerate is interpreted to be a fining upward sequence representing the transition from alluvial to playa sedimentation related to a Tertiary faulting episode.

Older Alluvium

Older allumium unconformably overlies Tertiary(?) breccia and Precambrian monzogranite along the Needle fault and along the southeast side of Corral Hill. It is composed of angular cobbles of various Paleozoic lithologies, strongly cemented by caliche. Although good exposures across the bedding are non-existant there is no evidence for tilting of the older alluvium. Its occurrence is limited to areas that are presently drained by Centennial Wash, where it crops out in low, rounded hills.

Sore Fingers Assemblage

Precambrian(?) and Mesozoic(?) intrusive and metamorphic rocks in the southern part of the Little Harquahala Mountains are informally referred to as the Sore Fingers Assemblage, named after Sore Fingers, two low hills in the southernmost part of the range. The assemblage is bounded by the Sore Fingers normal faults and Sore Fingers thrust on the northeast, southwest, and northwest, and by alluvium on the southeast (see Figure 5). The most abundant lithology is a coarsely porphyritic monzogranite that intrudes a complex, heterogeneous assemblage of metamorphic rocks. Medium-grained granite and diorite intrude the monzogranite. Rocks of the Sore Fingers assemblage are variably altered and fractured; secondary biotite, chlorite, silica

and epidote are the most common alteration products. In the following sections, rock units are described in order of abundance, intrusive rocks first, then metamorphic rocks.

Porphyritic Monzogranite

The southern part of the Sore Fingers assemblage is dominated by a coarsely porphyritic monzogranite that unit intrudes heterogeneous metamorphic rocks on the northeast, and is in faulted and gradational contact with metamorphosed porphyritic monzogranite on the north. The monzogranite is faulted against Mesozoic and Paleozoic strata along short segments of the Sore Fingers thrust The age of the unit is Precambrian or Jurassic, based on the presence of similar coarse porphyritic granitoids of both ages in southeast California and western Arizona. A minimum age of 140 m.y. (K-Ar, biotite) was reported by Rehrig and Reynolds (1980). The rock consists of coarse-grained quartz, plagioclase and potassium feldspar, with chloritized biotite and minor opaque minerals. Flesh pink subequant potassium feldspar pheoncrysts up to 8 cm in diameter are ubiquitous. Mineral composition of the monzogranite groundmass determined in thin section is 28% quartz, 36% potassium feldspar, 23% plagioclase, 9% biotite, and 4% opaque and other minerals. The potassium feldspar content of the whole rock must be greater due to the abundant megacrysts. The texture is variable and locally the rock is almost equigranular. Outcrops of unaltered monzogranite are bold and rounded with boulder-strewn slopes covered with grus and feldspar phenocrysts weathered

from the rock (Figure 21). Slight alteration throughout the intrusion is concentrated along joints commonly filled by chlorite and epidote. As alteration becomes more extensive, the rock becomes more resistant, and darker in color, forming blocky outcrops with dark desert varnish coatings. Internally, the overall grain size is reduced and feldspars become red-pink as alteration advances. In the most intensely altered areas, the monzogranite becomes a dense, black, highly fractured, siliceous rock in which biotite clots surround relict feldspar and quartz. In these areas, pods of white bull quartz, dense gray aphanitic rock and microdiorite are common. Silicification and biotitization are the major effects of the alteration.

Other Intrusions

A series of small, equigranular to slightly porphyritic granite plugs intrude the porphyritic monzogranite and meta-monzogranite along the southwest side of the Sore Fingers area. Contacts are gradational, but rare monzogranite inclusions are present in the granite, and a fine grained contact phase of the granite is locally developed. The composition of the rock is similar to the monzogranite and plots near the center of the granite field on the Q-A-P plot (Figure 22). The rock consists of medium-grained quartz (36%), potassium feldspar (39%), plagioclase (19%), and biotite (6%). Elongate potassium feldspar phenocrysts up to 2 cm long are locally present. The grain size is variable, but the granite is

Figure 21. Porphyritic monzogranite of the Sore Fingers Assemblage.

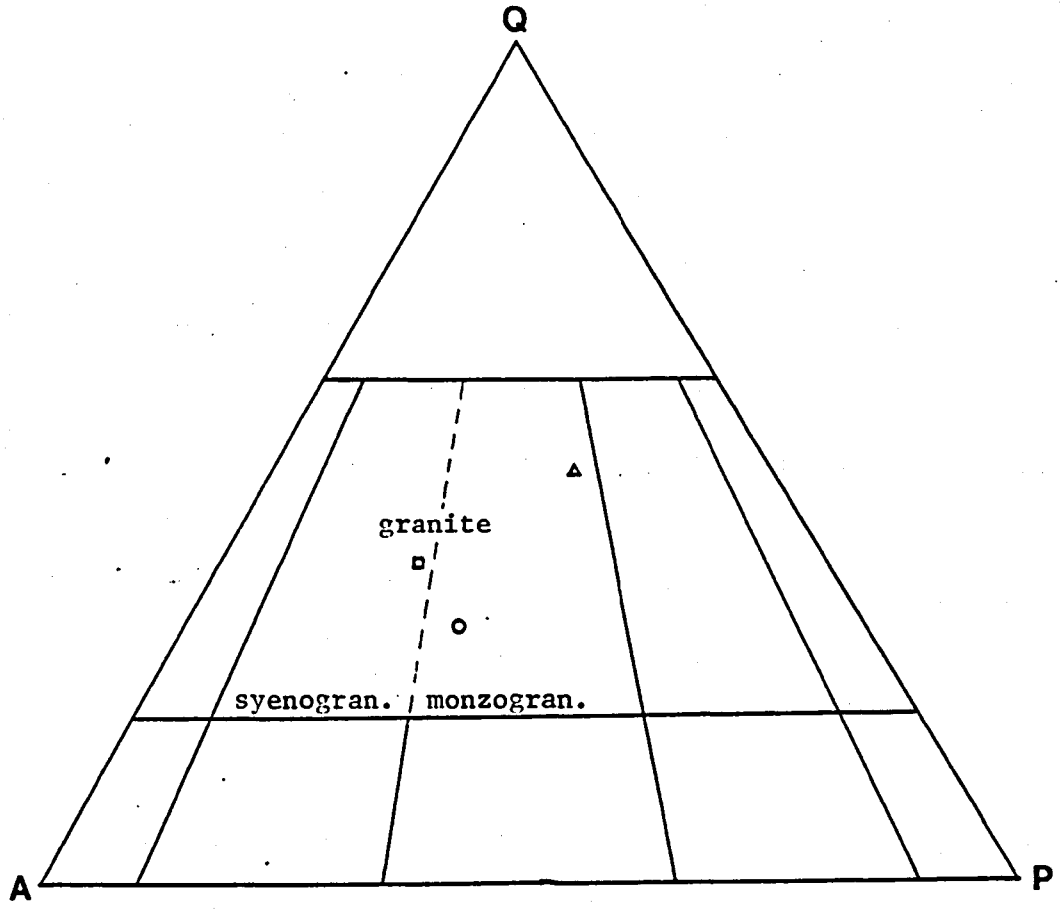

Figure 22. Composition of Granitic Rocks.

Shows approximate composition of three intrusive rocks in the southern Little Harquahala Mountains. Triangle is Precambrian Monzogranite; square is Sore Fingers granite; circle is groundmass of Sore Fingers Porphyritic Monzogranite. Triangle is I.U.G.S. General classification of plutonic rocks. Poles are quartz (Q), alkali feldspar (A) and plagioclose (P).

always finer grained than the porphyritic monzogranite. The southwesternmost exposures of the granite are highly fractured and altered. The similiarity of the granite and monzogranite suggests that they are related to the same intrusive event.

At the northern end of exposures of the Sore Fingers assemblage a dioritoid intrudes meta-monzogranite. The contact is poorly exposed, and is complicated by minor faulting. Inclusions of meta-monzogranite occur in the dioritoid near the contact. The rock consists of fine- to medium-grained plagioclase, chloritized biotite or hornblende, and quartz, with abundant secondary epidote. The mafic content and grain size of the rock is variable, but a characteristic equigranular texture allows identification of the unit even where it is strongly altered and fractured.

A small outcrop of granodiorite occurs west of the Sore Fingers. The contact with porphyritic monzogranite is not exposed but the relatively unaltered condition of the granodiorite suggests that it intrudes the monzogranite. The rock consists of quartz, plagioclase, hornblend, in blades up to 5 mm long, and biotite. It forms a low rounded outcrop with a grussy cover. The granodiorite is similar in appearance to parts of the Granite Wash Granodiorite and is believed to be related to that intrusion.

Meta-monzogranite

Along its northern margin, the porphyritic monzogranite becomes weakly metamorphosed. The contact between metamorphosed and

unmetamorphosed rock is gradational, commonly modified by faulting. Low-grade metamorphism predates intrusion of the granite plugs; since these are interpreted as late stage intrusions related to the monzogranite, the metamorphism is probably a syn- to slightly post-intrusive event. The meta-monzogranite is mineralogically identical to its protolith; it is characterized by red staining, zones with weak crystalloblastic foliation, pinkish-red slightly rounded potassium feldspar phenocrysts, abundant quartz veins, and small bodies of light colored, fine-grained granite. Attitudes of the crystalloblasitc foliation are highly variable (Figure 23) indicating that fabric development is a very local phenomena.

Metamorphic Rocks

The porphyritic monzogranite intrudes an extremely heterogeneous assemblage of igneous, meta-igneous and metasedimentary rocks in the east central part of the Sore Fingers area (Figure 24). Unfaulted contacts are gradational with interleaving of various lithologies, and locally appear migmatitic. The unit is the oldest exposed in the Sore Fingers area, and is probably Precambrian. Composition of the metamorphic rocks ranges from quartz-muscovite schist to plagioclase-biotite gneiss and uncommon lenses of biotite schist. Porphyritic monzogranite, variably altered or foliated, and alaskitic granitoid are a widespread component; swarms of microdiorite bodies are locally present. Gradational contacts with the porphyritic monzogranite bodies suggest that the monzogranite may have been

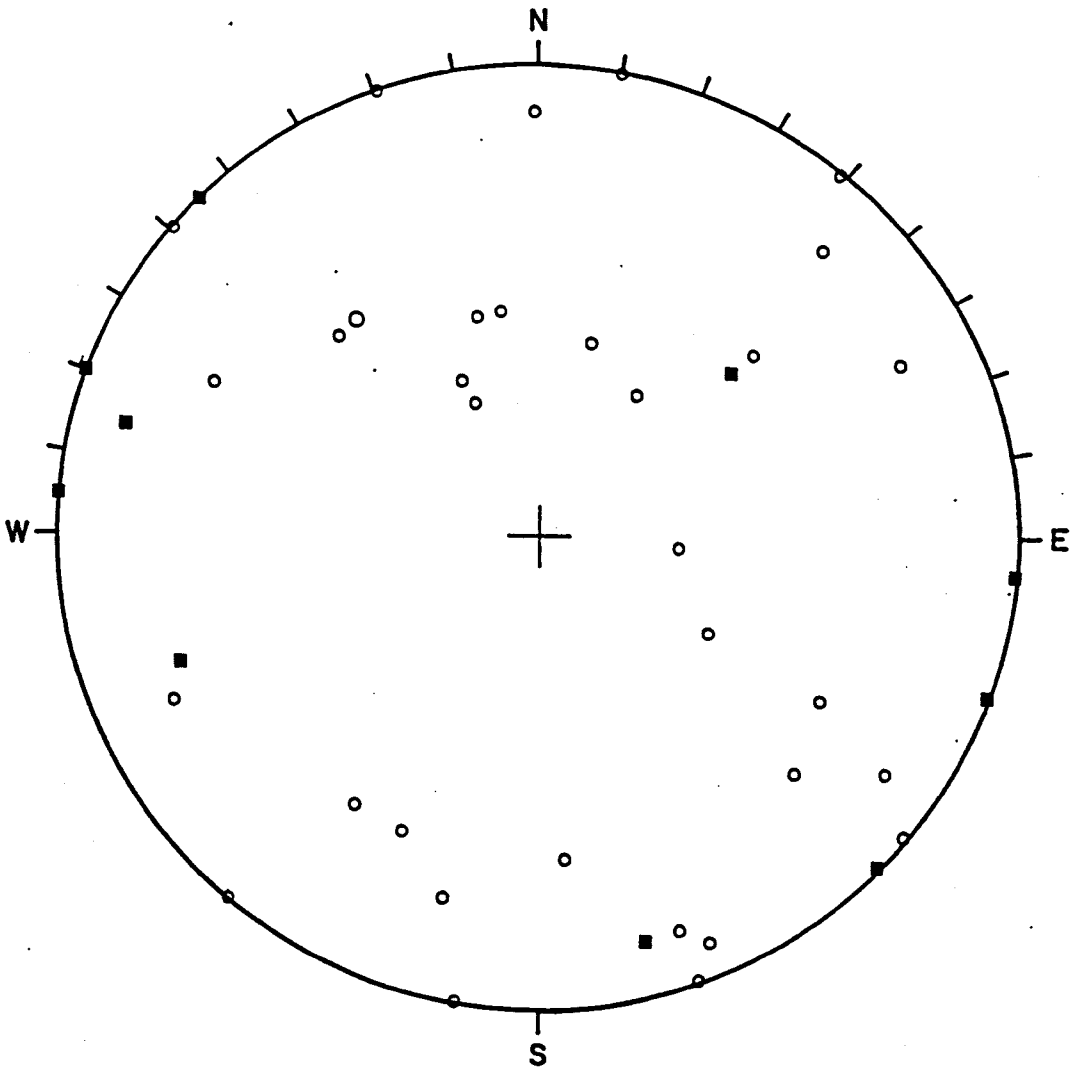

Figure 23. Foliations in Metamorphic Rocks.

Solid squares-foliation in meta-monzogranite; circles-foliation in other metamorphic rocks.

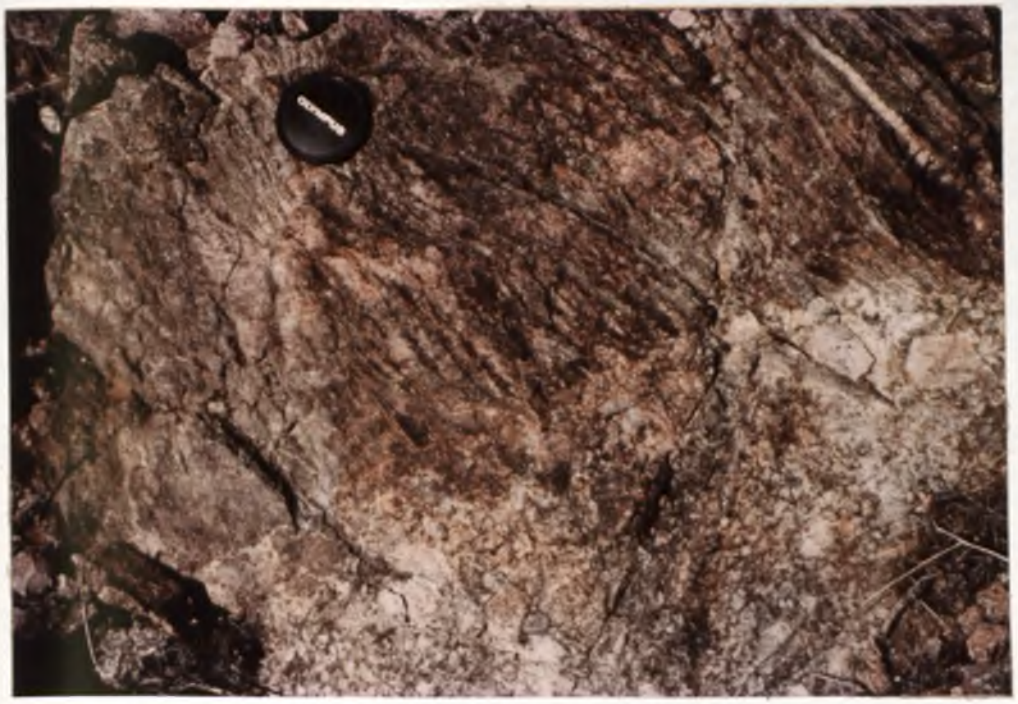

Figure 24. Intrusive contact between porphyritic monzogranite and foliated metamorphic rock.

derived by partial melting of the metamorphic rocks. Alteration is widespread and similar in character to that described in the porphyritic monzogranite. Foliation is weakly developed in general and is irregular in orientation (Figure 23).

Dikes

Six dike lithologies were mapped in the southern Little Harquahala Mountains. Lithologies occurring only in the Sore Fingers assemblage include aplite-pegmatite, andesite porphyry and rhyolite. Lithologies occurring only in the upper plate of the Sore Fingers thrust include rhyodacite porphyry and dacite. Microdiorite dikes occur within the Sore Fingers assemblage and in Mesozoic volcanic rocks above the Sore Fingers thrust. These dikes are described in Table 1. Structural characteristics are described in Table 2. Andesite porphyry dikes in the Sore Fingers area and dacite dikes in the Paleozoic rocks are similar in mineralogy and texture and may be related. Quartz was not observed in the andesite porphyry dikes, but is locally present in dacite dikes.

Table 1 DIKE LITHOLOGIES

TYPE	TEXTURE	MINERALOGY	OUTCROP	AGE, CORRELATION
IN SORE FINGERS ASSEMBLAGE				
Aplite-pegmatite	sucrose, equigranular, very fine- to very coarse-grained, locally porphyritic	quartz, potassium feldspar, minor plagioclase, biotite, magnetite	up to 5 m long, and 30 cm thick; white, more resistant than monzogranite	Occur in swarms. Seem to be related to granite plugs, intruding monzogranite and meta-monzogranite in the Sore Fingers area.
Andesite Porphyry	slightly porphyritic fine grained	chloritized hornblende or biotite phenocrysts up to 5 mm long, in chloritic, sausseritized feldspar-rich groundmass	Up to 150 m long, approx. 1.5 m thick; non-resistant grey, grussy outcrop; green-grey on fresh surface; also in irregular masses.	Intrusion postdates development of meta-monzogranite and most intense alteration of porphyritic monzogranite
Rhyolite	very fine-grained, locally porphyritic	grey, chloritic quartz, feldspar groundmass, phenocrysts of potassium feldspar and chloritized hornblende or biotite up to 4 mm long	1 km long, 1-2 m thick; crops out as low ledges and smooth blocky rubble, weathering tan or brown varnished, medium grey on fresh surfaces	Intrussion postdates porphyritic monzogranite and major alteration and fracturing; little deformed.
Microdiorite	very fine- to fine-grained	plagioclase and hornblende, local biotite, variably altered	lenses and pods in metamorphic rocks; dark grey weathered and fresh surfaces.	related to original metamorphism of metamorphic rocks (?)
Microdiorite	same as above	same as above	small sills and dikes; dark grey color	Intruded before major fracturing and alteration of Sore Fingers Assemblage
IN SORE FINGERS ASSEMBLAGE AND MESOZOIC VOLCANIC ROCKS				
Microdiorite	fine- to medium-grained	same as above, but little or no alteration	sub-vertical dikes, up to 650 m long, 10 m thick, dark grey	crosses Sore Fingers Thrust
IN PALEOZOIC ROCKS				
Rhyodacite porphyry	porphyritic, slightly to intensly sheared	Most intensly altered dikes are red, siliceous clay with white, argillized relict feldspar phenocrysts and quartz eyes. Less altered dikes have rounded phenocrysts of embayed quartz up to 7 mm, plagioclase up to 5 mm, subhedral to euhedral potassium feldspar to 2 cm long and biotite to 2 mm in diameter in a very fine-grained siliceous groundmass.	non-resistant; weather pink grey or light grey and occur only in Paleozoic rocks	Shearing indicates intrusion before major deformation of Paleozoic rocks. Probably related to Mesozoic volcanic rocks
Dacite	fine-grained, locally slightly porphyritic; locally have cleavage	chloritized hornblende or biotite, argillized feldspar, minor quartz; in coarser phases contains limonite after pyrite cubes	non-resistant, medium dark grey on weathered and fresh surfaces	Similar in appearance to microdiorite, distinguished by presence of quartz and generally coarser grain size. Resembles andesite prophyry of Sore Fingers area, but contains more quartz.

Table 2 STRUCTURAL CHARACTERISTICS OF DIKES

LITHOLOGY	ORIENTATION	NOTES ON OCCURRANCE
SORE FINGERS DOMAIN		
Microdiorite	Irregular	Lenses and pods in metamorphic rocks
Microdiorite	Irregular	Fractured, deformed dikes occur throughout domain.
Microdiorite	Generally NW strike, steep dip	Occur along SW side of domain. Cut by Faults of A set; Cross Sore Fingers Thrust.
Andesite Porphyry	Northerly strike, vertical. Also sill/like irregular mass	
Rhyolite	NE strike, near vertical	Set of three parallel dikes and a fourth discontinuous zone of nearly aligned dikes. May be intruded along NE-trending fracture zones of A or E fault set (Figure 26). Appear less deformed and altered than other types.
LIMESTONE HILLS DOMAIN		
Rhyodacite Porphyry	Sills and dikes, variable orientation	Sheared and altered; generally follow fault zones of A or B fault set (Figure 27). Discontinuous along strike.
SOME FINGERS WEST DOMAIN		
Microdiorite	approx. N 50° W strike, steep dip	Aligned with similar dikes in SW Sore Fingers Area.
MARTIN PEAK DOMAIN		
Dacite	Northeast to northwest strike, moderate dips, some irregular masses.	Dike on SW corner of Martin Peak has NW-trending, SW-dipping cleavage.
GOLDEN EAGLE HILL DOMAIN		
Rhyodacite Porphyry	Sill	In basal Martin Formation and Redwall Limestone; very discontinuous
MIXMASTER HILL DOMAIN		
Rhyodacite Porphyry	Easterly strike near vertical	Intrudes lower Kaibab Limestone
Dacite	N 60° W 65° SW	Altered; cut by NW-trending high-angle fault which is cut by NW-dipping normal faults
ELBOW HILL DOMAIN		
Rhyodacite Porphyry	Sill	Intrudes lower Redwall Limestone, discontinuous along whole strike belt.
NEEDLE DOMAIN		
Rhyodacite Porphyry	Sill	Discontinuous; intrudes basal Martin Formation
Dacite	NNW-trending dike	Occurs along Needle Fault, may intrude fault post strike-slip, pre dip-slip
Microdiorite	North-trending, near vertical dike	Post-dates disruption of bedding in Martin and Redwall Formations on east side of Redwall Hill
SPLIT MOUNTAIN DOMAIN		
Rhyodacite Porphyry	Sills	Intrude lower Redwall Limestone, less common in lower Martin Formation
Dacite	Sills, dikes, small intrusion	Near small intrusion in Redwall and lower Supai Formations, Redwall is altered to white recrystallized limestone, Supai is silicified. Dike south of Fault F (Figure 33) cuts fabric in Supai Formation but is slightly deformed; it is late or post kinematic.

STRUCTURAL GEOLOGY

Seven major deformational events are recognized in the southern Little Harquahala Mountains. From oldest to youngest they are 1) probable high-angle faulting before or during deposition of the Apache Wash Formation; 2) large-scale south to southeast-vergent folding; 3) refolding of earlier folds about steeply north-northeast-plunging axes; 4) thrust faulting; 5) northwest-dipping normal faulting; 6) north- to northwest-striking strike- or oblique-slip faulting; and 7) northeast-dipping normal faulting. In the first part of this chapter major structures related to each of these events will be described in chronologic order. In order to simplify this discussion, minor structures are treated separately in a final section. The second part of the chapter describes evidence bearing on the kinematics of deformation in the area. The map area has been divided into 11 structural domains (Figure 25) bounded by structural and physiographic features and characterized by unique assemblages of rocks or structures. Figures 26 through 33 and accompanying tables 3 through 12 label and describe faults within the various domains. These figures and tables can be used in conjunction with the descriptive part of this chapter to provide a more detailed description of the structure.

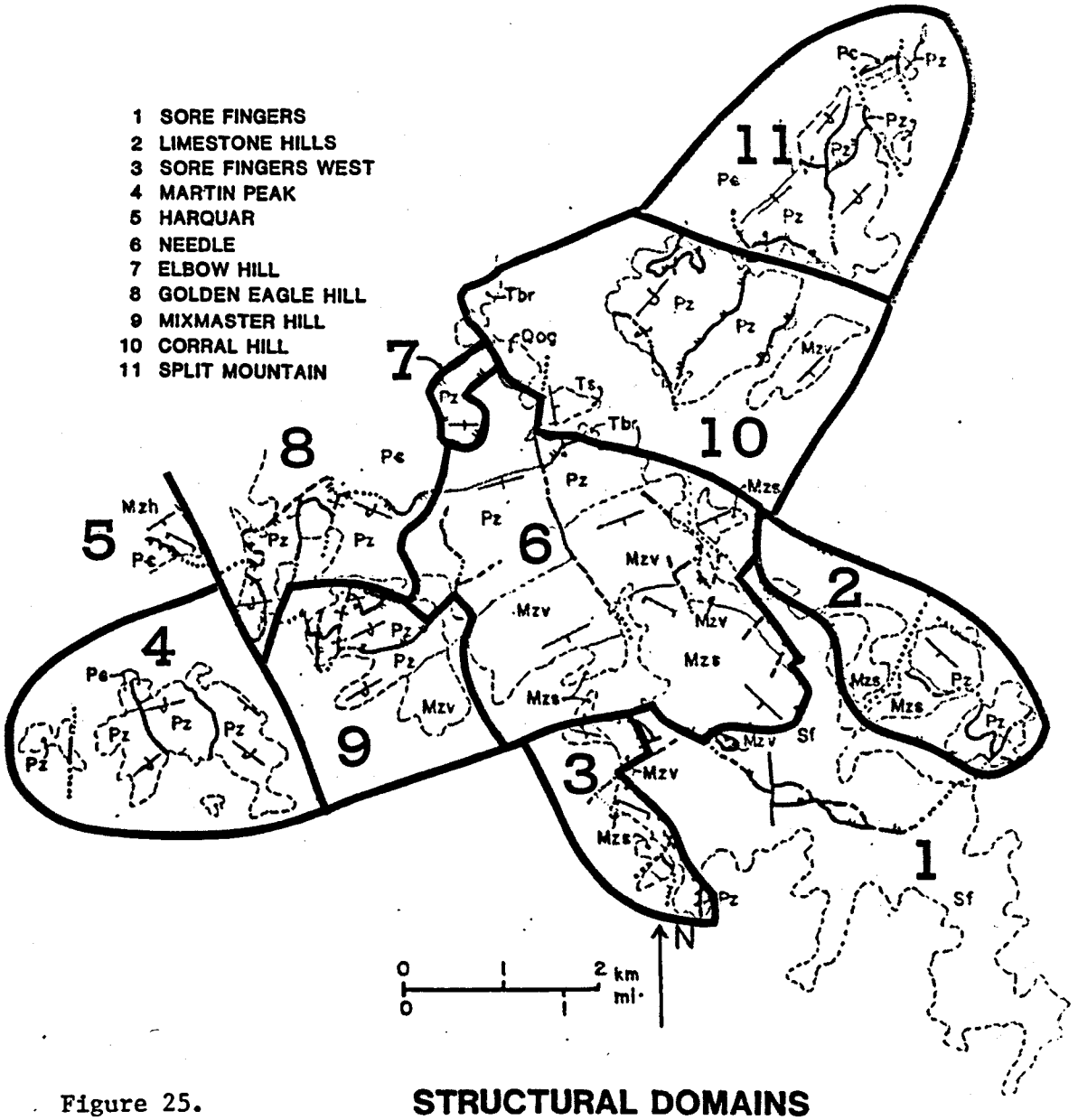

Figure 25. **STRUCTURAL DOMAINS**

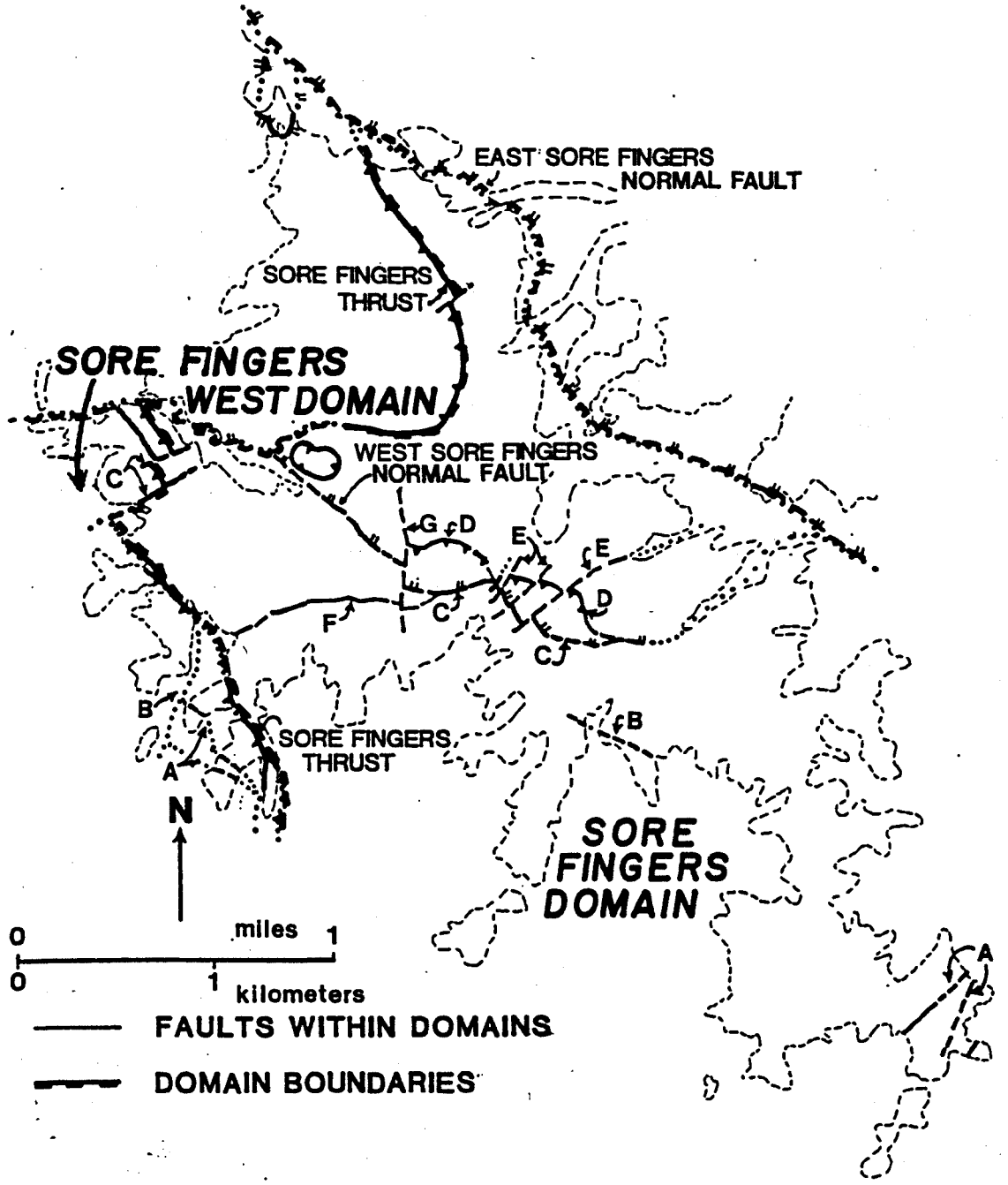

Figure 26. Faults in the Sore Fingers Domain and Sore Fingers West Domain

Table 3 FAULTS IN THE SORE FINGERS DOMAIN

FAULT	ATTITUDE	SEPARATION	DESCRIPTION
A	approx. N 35° E 90°	right separation about 20 meters	Set of faults about 180 m spacing, progressively closer together to SE. Faults accompanied by intense jointing. They cut microdoirite dike and granite
B	approx. N 55° W 90°	?	Zones of intense jointing seem to control physiography. One fault of this set truncates a rhyolite dike. They occur throughout Sore Fingers area.
C	N 50° W 40° NE	normal	West Sore Fingers Normal Fault. Local intense brecciation in fault zone; absence of markers makes interpretation difficult. Cuts fault D
D	SE segment N 30° W 20–45° SW	thrust (?)	Fracture cleavage is present in rocks adjacent to fault. Fault becomes steeper to SE and cleavage disappears. Monzogranite to meta-monzogranite contact in upper plate is eroded away in pass between NW and SE segments.
E	N 50° E 90°	oblique; left and/or up on NW	Cuts C and D. Similar to A, but opposite lateral offset.
F	approx. N 90° E 90°	up on south?	Vertical striations present on slickensided joint or fault surfaces on steep south face of hill. Apparent increase in alteration upward to west in porphyritic monzogranite suggests meta-monzogranite may lie above it, thus indicating normal separation. May not have significant offset as monzogranite is increasingly altered towards the fault zone, apparently transitional to meta-monzogranite
G	N 0° E 90°	oblique, right and/or down on east	Separation is based on offset of faults C, D and F
	approx. N 30° W, 30–70° SW	thrust (?)	Sore Fingers Thrust - fracture cleavage developed in crystalline rocks of Sore Fingers Assemblage and Mesozoic volcanic rocks along the fault.
	gentle dip to east	normal(?)	East Sore Fingers Normal Fault. Fault zone strongly brecciated in one exposure.

Table 4 FAULTS IN THE LIMESTONE HILLS AND SORE FINGERS WEST DOMAINS

FAULT	ATTITUDE	SEPARATION	DESCRIPTION
LIMESTONE HILLS DOMAIN			
A	N 25° E 60° NW	oblique; right and/ or down on NW	Sharp planar fault surface. Ofset by hidden fault between hills D and C. Series of NE to NNE trending faults with similar orientation but variable separation. Cuts B faults, but major offset occurred before B set.
B	strikes NW, gentle to moderate SW dip	reverse	Sharp fault surface. Set of low-angle shears imbricate various Kaibab lithologies and basal Apache Wash conglomerates. Fabric in conglomerate is subparallel to shear zones.
C	N 55° W, steep	down on NE	Poorly exposed. Minor splay has N 25° W trend. Cuts B faults on Hill A. Relation to fault A interpretive. Fault between hills B and C interpreted to be of this type.
D	unknown	unknown	Poorly exposed. Coconino breccia is juxtaposed against Apache Wash Formation and may be a slide block in Apache Wash conglomerate or Tertiary breccia.
SORE FINGERS WEST DOMAIN			
A	approx. N 60° W, steep SW dip	reverse?	Poorly exposed, obscure. Probably related to adjacent Sore Fingers Fault zone.
B	northerly strike	right	Fault not exposed
C	approx. N 60° E, steep dip	right	Fault not exposed

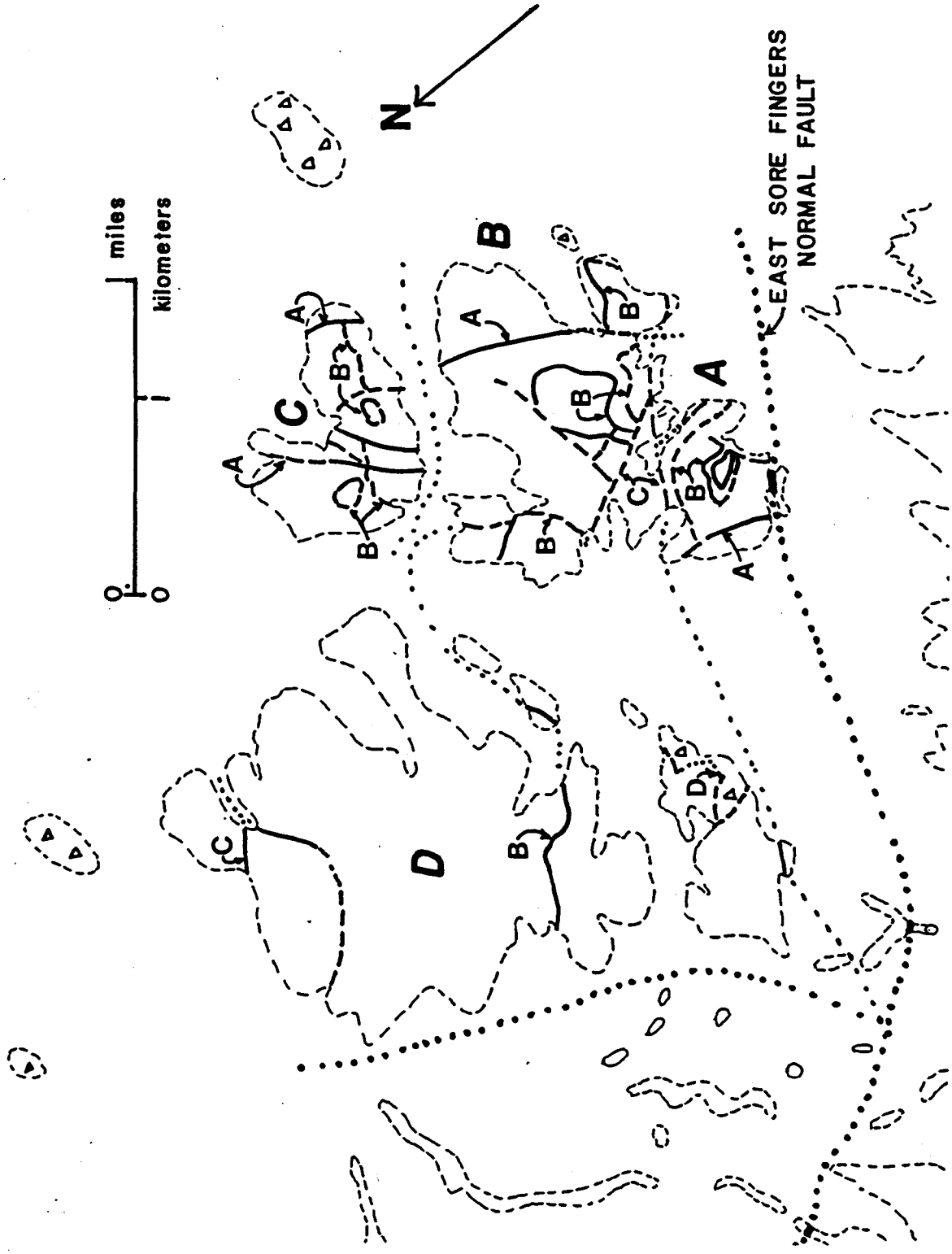

Figure 27. Faults in the Limestone Hills Domain

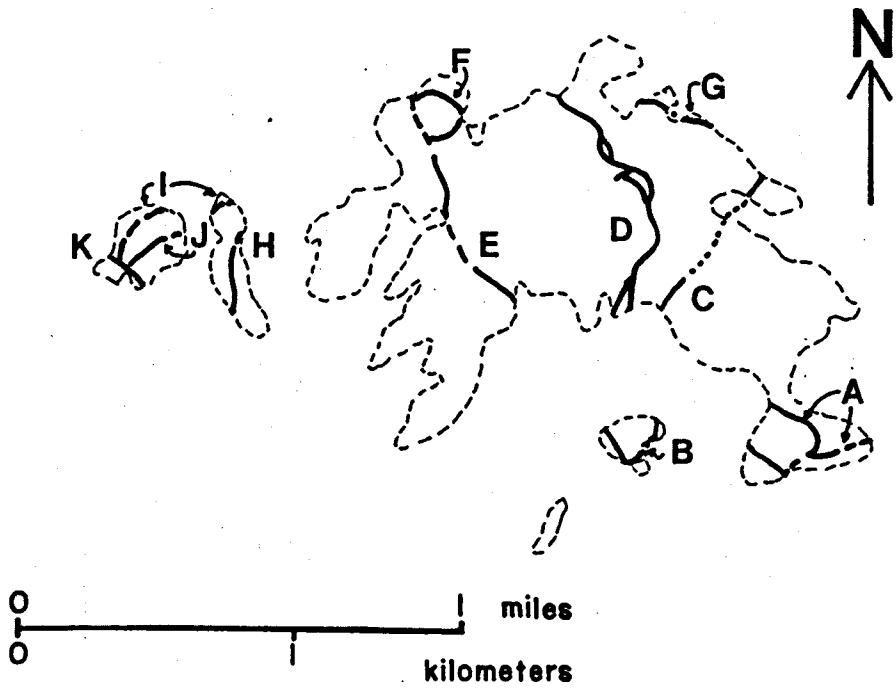

Figure 28 Faults in the Martin Peak Domain

Table 5 FAULTS IN THE MARTIN PEAK DOMAIN

FAULT	ATTITUDE	SEPARATION	DESCRIPTION
A	variable, dips approx. 10° to the N or W	Reverse, upper plate to N	Sharp, unbrecciated fault surface. Imbricate normal-separation faults. Cut by minor NW trend reverse fault.
B	Low dip	?	Poorly exposed. Supai formation brecciated and sheared. May be intersection of north and east trending high-angle faults. Coconino-Kaibab contact repeated in upper plate by NW-trending high-angle faults.
C	N 30° E, 62° NW	Normal	Sharp fault surface
D	Strikes N to NW dips approx. 60° W	Reverse	Sharp fault surface, slivers of formations along fault caught in fault zone. Interpreted to be related to space problems in core of F_2 fold.
E	N 20-45° W, 60° NE to Vert.	Left or Normal	Brecciated fault zone. Cuts fault bounding Bolsa Quartzite klippe
F	NE strike, very low NW dip	Normal	Breccia along fault, locally sheared carbonate in fault zone. Bedding in upper plate Bolsa Quartzite is totally disrupted.
G	N 62° W, approx. 20° SW	Reverse	Mineralized shear zone about 2 meters thick. Mine shaft follows shear zone; mineralization in the Harquahala Mine may follow the same fault. Martin-Bolsa contact on N side of Peak west of Fault D is also a minor south-dipping reverse fault.
H	N 0° E, 45° E	Right or Normal	Brecciated fault zone
I	N 60° E, 30-60° SE	Reverse	Poorly exposed. Bolsa Quartzite is disrupted and brecciated near contact. Basal Bolsa Quartzite beds are absent, fault cuts across bedding.
J	N 62° E, steep SE dip	?	Sharp fault surface (?), poorly exposed.
K	N 45° E, Near vertical?	Left or down on SW	Sharp fault surface(?). Relations in this area are obscure.

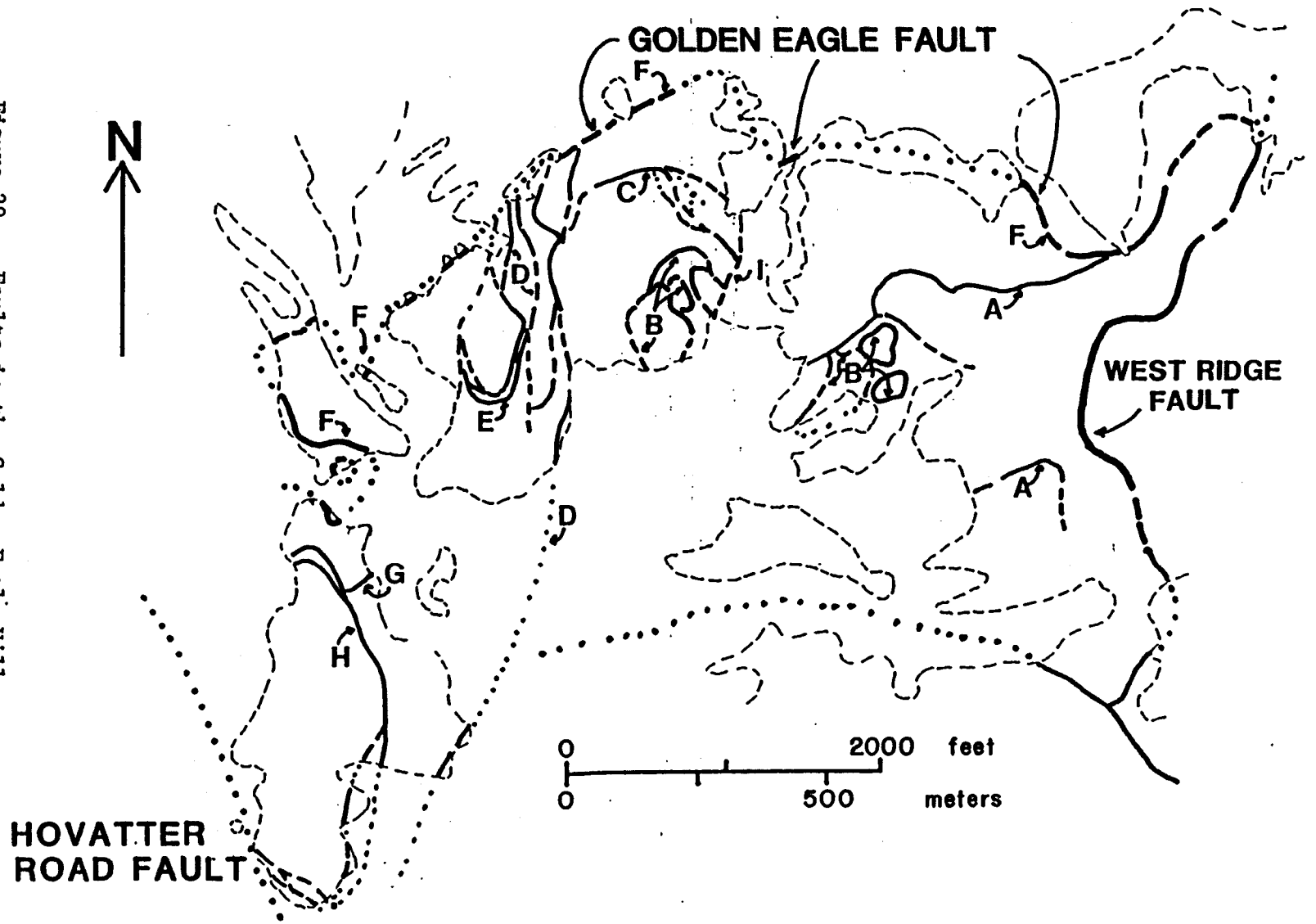

Figure 29 Faults in the Golden Eagle Hill Domain

Table 6 FAULTS IN THE GOLDEN EAGLE HILL DOMAIN

FAULT	ATTITUDE	SEPARATION	DESCRIPTION
A	N 62-75° W, 30-35° SW	Reverse	Sharp fault surface. Two faults in set occur on west ridge, Redwall Hill.
B	Moderate SSW dip	Reverse	Sharp fault surface. Stacks of thin plates shuffled. Basal fault probably of A set. 'Shingled structure'.
C	N 70° W, 22° SW	Normal	Sharp fault surface, locally there are slices of various lithologies in fault zone. Upper plate moved south. Thin lenses of Bolsa, Martin, Redwall and Supai Formation along fault
D	approx. N 0° E zone, faults commonly dip 60° E	Left separation across zone	Anastamosing faults in zone about 150 meters thick.
E	sub-horizontal	?	Slivers of various lithologies in fault zone; sharp, fault surfaces. No stratigraphic separation, but abrupt dip discontinuity. Beds below fault dip south, beds above dip to north. Slivers of Redwall and Supai Formations in fault zone require significant transport for their emplacement.
F	upper plate to north	near flat (?)	Golden Eagle Fault. Exposures of fault are highly variable in attitude due to later disruption; trace of fault indicates a low-angle contact, Monzogranite below fault is altered; overlying Bolsa Quartzite is altered and brecciated; Redwall and Martin Formation sheared in fault zone. Abrigo Formation is mineralized in the fault zone. Mine shafts penetrate monzogranite below the fault
G	N 70° E, 65° S	Reverse	Sharp, heavily altered rhyodacite porphyry intrudes. Some mineralization in breccia along fault. Cuts F_2 fold. Fault disappears to east. Cut by Fault H.
H	N 15° W, 20° W	Upper plate to S?	Sharp contacts, slivers in fault zone. Rhyodacite porphyry intrudes. Coconino sliver at S end highly brecciated.
K	N 15° E trace steep dip?	Left separation	Poorly exposed
	N 30° E, near vertical at north end, decreases to approx. 15° E to south	left separation	West Ridge Fault. Merges with Northern Boundary Fault. Intruded by rhyodacite porphyry at northern end. Dike has been brecciated by later movement on fault. Interpreted to cut Golden Eagle Fault.
	NNW trend, steep dip	left separation	Hovatter Road Fault. Truncates all other structures. Fault not exposed.

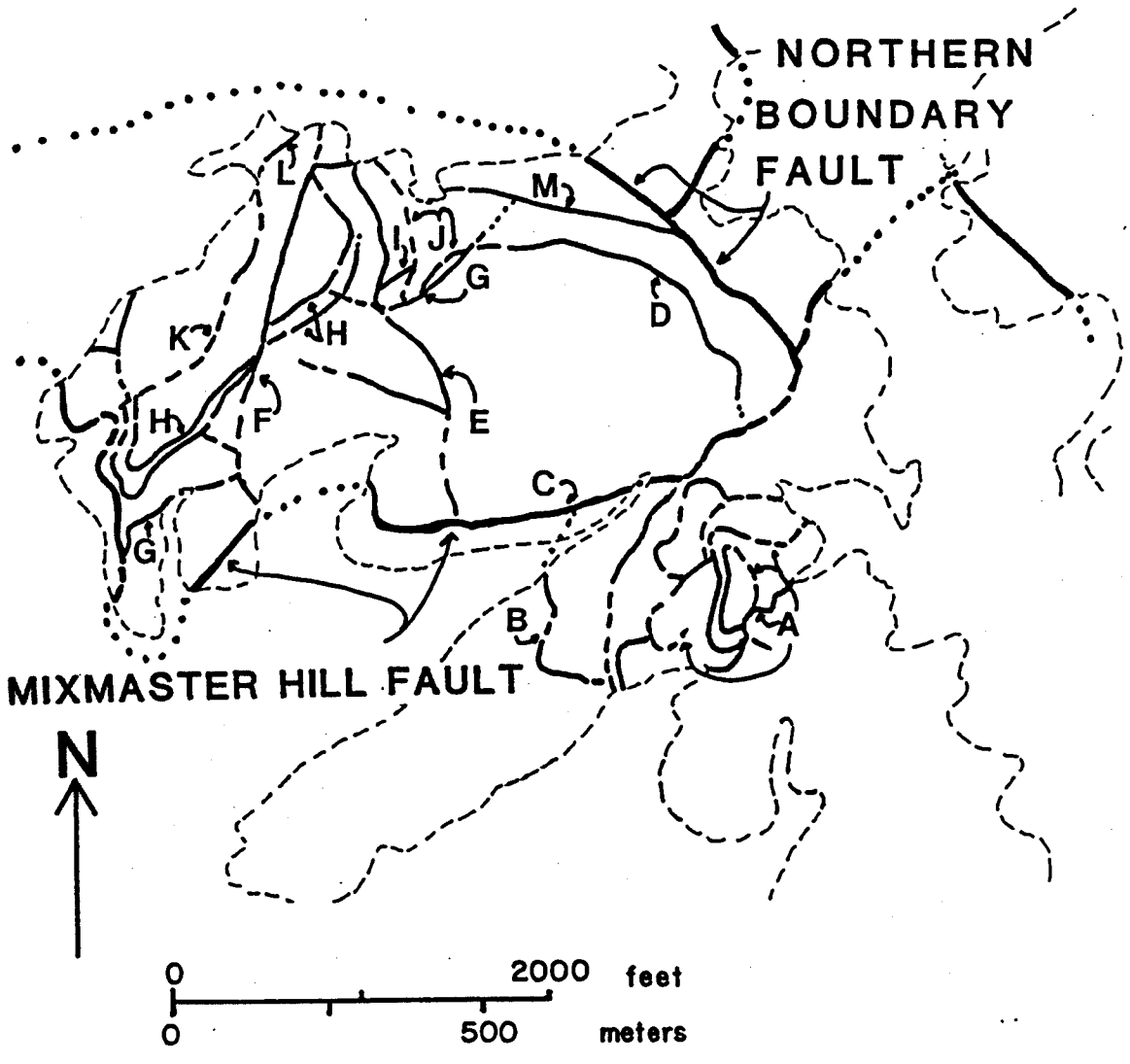

Figure 30 Faults in the Mixmaster Hill Domain

Table 7 FAULTS IN THE MIXMASTER HILL DOMAIN

FAULT	ATTITUDE	SEPARATION	DESCRIPTION
A	approx. N 50° E 25° SE	Reverse	Sharp fault surface. Stack of thin plates, shingled structure. Disrupts Kaibab unit 3 to base of lower volcanic unit.
B	N 17° W 30° E	Left, reverse?	Brecciated fault zone, planar fault surface. Probable reverse component. Cut by Mixmaster Hill Fault (C).
C	NE strike, 40° NW to near flat	Normal, upper plate to north	Mixmaster Hill Fault. Sharp fault surface, some local brecciation along fault. Flattens down dip to west. Fault dies out along strike to NE.
D	N 45° W, 45° SW	Right, reverse?	Sharp fault surface, Kaibab unit 2 partially transposed near fault. Dies out into crushed rock near Mismaster Hill Fault, cut by or merges with Fault G.
E	N strike, steep dip	Right and left	Coconino brecciated, sharp fault surface in Kaibab. Series of minor faults in upper plate of Mixmaster Hill Fault. Left separation of dike mostly due to left slip, using intersection of dike and Pkl-Pc contact.
F	N 15° E, steep to vertical	Left, but conflicting indicators at north end	Brecciated fault zone. Relations difficult to interpret. Contacts and structures truncated along a nearly continuous zone of brecciated rock.
G	Low angle, arched	Upper plate displaced south	Coconino brecciated above limestone sheared below the fault. May merge with Fault D. Dips to north on north and to south on south.
H	N 35-40° E, approx 15° NW	Normal, upper plate NW	Coconino brecciated, Kaibab sheared, fault surface sharp. Thin slices of Pkl and Pk2 occur in fault zone.
I	55-65° southerly dip	Normal	Sharp fault surface. Cut by low-angle faults of G and J set.
J	Near flat, warped surface	Upper plate to north	Coconino brecciated, sharp fault surface. Faults G and J sandwich a thin plate of Kaibab transported relatively north. Upper plate of G is south relative to lower plate of J. J may correlate with the West Ridge Fault.
K	N 45° E, 50-80° NW	Up on NW	Brecciated fault zone. Obscure breccia zone similar to F.
L	NE strike, moderate SE dip	?	Coconino brecciated, Kaibab disrupted. Part of low-angle imbricate fault set (Faults G,H,J)
M	approx. N 75° W steep SW dip	?	Sharp fault surface. Juxtaposes upright and overturned Kaibab, probably part of Northern Boundary Fault zone.
	N 50° W, dips steeply to SW	?	Northern Boundary Fault. Offsets Mixmaster Hill Fault about 25m left, offsets Kaibab Limestone Unit 1 - Unit 2 contact 90 m right. Projected northeast along wash on the north side of Mixmaster Hill. Merges with or truncates the West Ridge Fault zone.

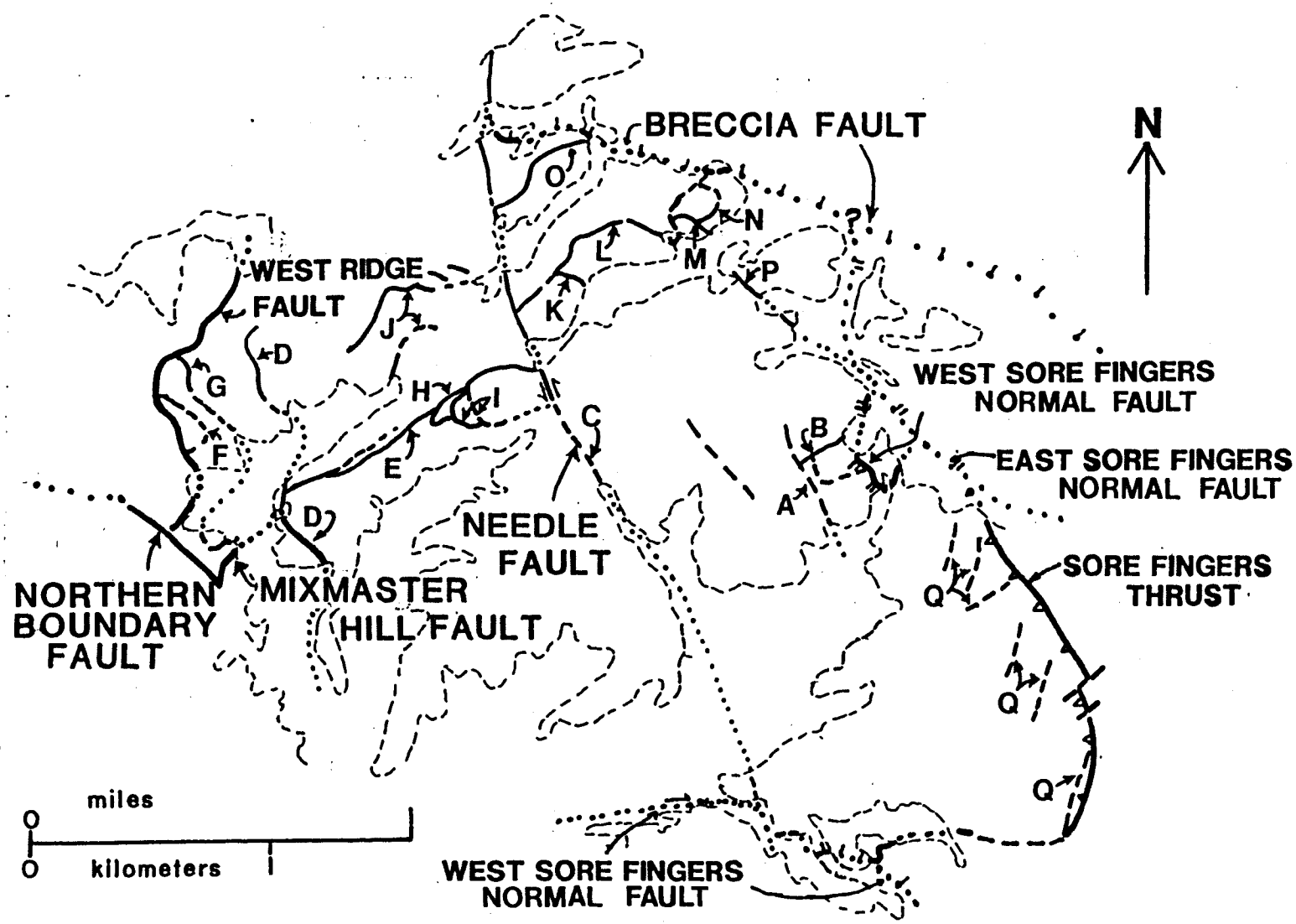

Figure 31. Faults in the Needle Domain

Table 9 FAULTS IN THE NEEDLE DOMAIN

FAULT	ATTITUDE	SEPARATION	DESCRIPTION
A	N 25° W trace	?	Poorly exposed. Cuts Fault B, juxtaposes lower Apache Wash conglomerate with shale unit of volcaniclastic sediments.
B	NE strike, steep dip	?	Poorly exposed. Upper volcanic unit and volcaniclastic sediments repeated. Presence of lower volcanic unit requires significant displacement.
C	N 10–30° W near vertical	Right, down on east	Needle Fault. Poorly exposed, some brecciation of Paleozoic rocks along fault. Correlation of Fault Q with Elbow Hill Fault and offset of Breccia Fault requires some dip slip.
D	N 0–30° W, 35–50° E	Left	Local brecciation in Redwall, Coconino and Kaibab; planar fault zone. Relations at west end of west Needle Ridge are obscure. Chosen as a domain boundary because Mixmaster Hill fault dies out rapidly to the east. Correlation of the fault from west ridge, Redwall Hill to west ridge of Needle is based on similar orientation and separation.
E	N 58° E, near vertical	Down on NW	Sharp fault surface. Coconino brecciated, thin slivers of Pk1 and Pk2 along fault. Cut by Mixmaster Hill Fault, dies out to west. May be same as fault L.
F	NW strike, moderate SW dip	Reverse	Sheared Supai Formation along fault. Cut by West Ridge Fault.
G	N 65° W, 18° SW	Contradictory indicators, both normal and reverse	Brecciated, difficult to map in Supai Formation. Change in dip in upper plate may explain inconsistent separation. Extension to Mixmaster Hill Fault is tenuous.
H	N 40° E, 30° SE to subhor., steeper to NW	Normal?	Limestone sheared along fault. Steeper part is a series of planar surfaces forming a sub-planar zone. Pk1 forms a slight drag fold. Cuts Fault E. Problem with offset is that motion on fault E removed Pk1 from a position from which it could be faulted on to Pk2. Faults must have recurrent motion.
I	NE strike, 20–50° SE dip	Reverse	Breccia to incipient transposition along fault. Two similar faults probably related to H but have opposite separation.
J	approx. N 60° E, 45° SW	Reverse	Sharp fault surface. Other minor reverse faults in vicinity commonly strike N 35–70° W in outcrop.
K	approx. N 80° E, 40–75° S	Reverse	Sharp fault surface. Complex relations in brecciated rock at west end of east Needle Ridge. Probably a continuation of structures on Needle. Associated minor faults strike N 70–85° E.
L.	N 35–80° E, 40–70° S	Reverse	Sharp irregular fault surface. Fault is steep at west end, flattens to east. Complex irregular cross cutting faults form fault zone. Slivers occur in fault zone at east end.
M	East strike, dips steeply north to vertical	Reverse?	Brecciated fault zone.
N	N 0° E, 25° W	Upper plate to N	Relations at east end of east Needle Ridge obscured by brecciation in vicinity of Breccia Fault.
O	N 45° E, 32° NW	Normal, upper plate to north	Sharp fault surface. Correlated with Elbow Hill Fault, is based on similar stratigraphic separation and structural position. Disruption in vicinity of Breccia Fault causes apparent southerly dip.
P	N 50° W, steep	Left	Poorly exposed. Upper volcanic unit greatly thinned across this zone; suggests hidden faults or original thickness variation.
Q	NE strike	Right	Poorly exposed. Series of stratigraphic discontinuities. Largest juxtaposes volcanic rocks and lower member of Apache Wash Formation. Responsible for continuity of volcaniclastic sediments along Sore Fingers Thrust, although they strike into the fault.
	NW strike, dips a minimum of 15° NE	Normal	Breccia Fault. Poorly exposed. Characterized by crushed Paleozoic strata along fault zone.

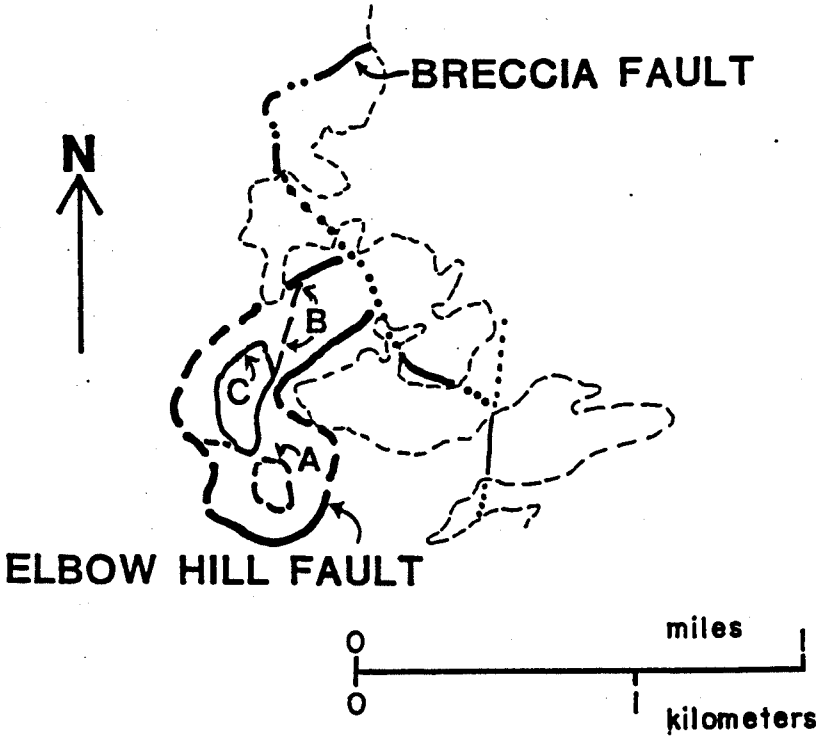

Figure 32. Faults in the Elbow Hill Domain

Table 8 FAULTS IN THE ELBOW HILL DOMAIN

FAULT	ATTITUDE	SEPARATION	DESCRIPTION
A	Subhorizontal, slight E dip	?	Difficult to locate exactly in Supai. Dip discontinuity, beds steep, overturned to N below fault, and upright S dips above. Slice of Coconino occurs in fault zone at south end.
B	Approx. N 50° E 37° NW	Upper plate to S	Siliceous breccia, 30 cm thick where fault cuts Martin formation. Redwall limestone sheared. Minor normal faults in Redwall and Martin occur in center east of peak and offset this fault. They trend N 2-67° W.
C	Curviplanar	?	Sharp fault surface in Abrigo and Martin Formation, Bolsa is brecciated near fault. Fault surface is an east-plunging synform.
	curviplanar; gentle dip to north and east	Normal	Elbow Hill Fault. Dip decreases to north. Redwall Limestone is transposed near fault; Precambrian Monzogranite is granulated near fault.

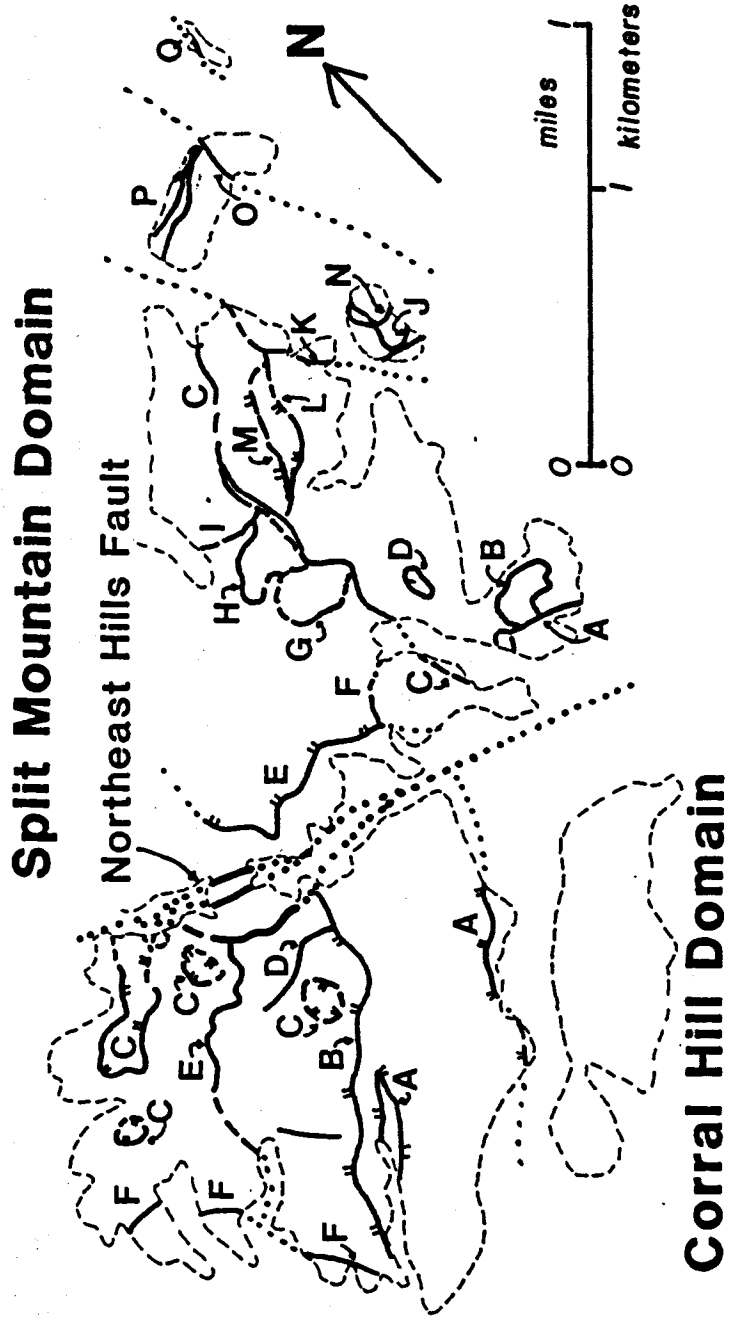

Figure 33. Faults in the Corral Hill Domain and the Split Mountain Domain

Table 10 FAULTS IN THE CORRAL HILL DOMAIN

FAULT	ATTITUDE	SEPARATION	DESCRIPTION
A	Arched: N 60°E 26° SE on south N 55° W, 12° SW in window	Upper plate to north	Sharp fault surface, Pk2 is transposed above fault in window. Fold axes in Pk2 tectonite above fault in window: 33° S 20° E, 28° S 24° W, 23° S 28° W. Tectonite cut by minor normal faults trending N 50° W.
B	N 50° E, 32° NW, N 18° E, steeper at SW end	Normal, upper plate to north	Sharp fault surface, Pc is brecciated near fault. Fault seems to change orientation to near vertical at SW end. Fault in upper plate may be related.
C	Shallow NW dip	Normal, upper plate to north	Sharp fault surface, beds in Pk2 and Pk3 seem to be warped near fault. Upper plate occurs as a series of klippen.
D	N 63° W, 90° to N 15° W, 58° E	Left	Sharp fault surface. Disappears into Pk1-Pc contact. Cut by Fault B.
E	Approx. N 50° E, 30° SE	Reverse	Pc is brecciated above fault. Disrupted, flattened in vicinity of Fault C.
F.	NNW-NW trace, steep	Left and Right	Brecciated fault zone. Discontinuous faults, senses of offset are not consistent. May be separate minor faults.
	N 70° W, subvertical	Right	Northeast Hills Fault. Series of faults across fault zone, right separation accumulates progressively. Correlation of Fault A (Corral Hill) with Fault E (Split Mountain) makes dip slip component small. Some brecciation along fault.

Table 11 FAULTS IN THE SPLIT MOUNTAIN DOMAIN

FAULT	ATTITUDE	SEPARATION	DESCRIPTION
A	approx. N 60° W 50° NE	Right	Sharp fault surface, but difficult to locate. Minor offset.
B	Subhorizontal	Upper plate to north	Sharp fault surface.
C	N 0° E, 30-58° E	None in Coconino or Supai Formations	Split Mountain Fault. Intensely brecciated fault zone. Moderate angle normal faults in NE part of domain do not correlate across this fault. Separation is between simultaneously active faults.
D	N 60° E, 15° SE	Upper plate to north	Sharp fault surface. Probably a klippe of the upper plate of Fault L.
E	Arched, N 33° W 20° E to N 25° E, 20° W	Upper plate to north	Sharp fault surface. Correlated with Fault A in Corral Hill Domain.
F	NE strike, steep	?	Poorly exposed, Supai Formation disrupted in vicinity of fault. Supai is very thick, must be repeated. Thin Coconino outcrops occur between Supai sections.
G	N 10° W, 22° E	Upper plate to north	Sharp fault surface. Cut by Fault C. Offsets small dacite intrusion 180 meters to north.
H	N 26-54° W, 30° NE, warped.	Upper plate to north, reverse?	Sharp fault surface. Cuts Fault G.
I	N 73° W, 55° NE	Left	Sharp fault surface, Bolsa brecciated. Rock is brecciated at intersection of Faults H and I. Difficult to determine cross-cutting relations.
J	Low-angle, dips east	Upper plate to north	Sharp fault surface. Pk2 in upper plate is silicified, breccia.
K	N 10-30° W, moderate dip to east	Left, normal?	Intense brecciation along fault. Strata northeast of fault is upright; strata southwest of the fault is overturned.
L	approx. N 32° E 30° NW	Normal	Sharp fault surface. Cuts Fault M on SW, then merges with M on the NE. Relations obscure at intersection with K due to brecciation.
M	N 25° E, vertical to low-angle	Normal	Sharp fault surface. Fault is vertical at east end, but abruptly becomes low-angle. Minor reverse faults in Redwall below fault: N 6° E, 45° E; N 0° E, 62° E.
N	Low-angle, dips east	Upper plate to south	Sharp fault surface. Stratigraphic facing in upper plate is opposite to that in the rest of the map area.
O	Strikes N, steep E dip	Left	Brecciated fault zone.
P	approx. N 60° E, low-angle to south	Reverse ?	Slivering of lithologies including Precambrian Monzogranite to Supai Formation. North side of hill is a south-dipping fault zone unlike any other in the area.
Q	N 10° E, 40° E	Right	Brecciated fault zone. Very small exposure.

Major Structures

Early Faulting

The earliest structural events in the region are apparent only in the stratigraphic record. Precambrian and Paleozoic rocks were uplifted and exposed to erosion in the source area of the Mesozoic sandstone, but the absence of both coarse conglomerate and angular clasts in the sandstone indicates that the uplift lay at some distance from rocks exposed in the Little Harquahala Mountains. Upper Paleozoic rocks were eroded from nearby uplifts to provide conglomerate in the lower member of the Apache Wash Formation. Sheared contacts at the base of the conglomerate in the Limestone Hills (Figure 17 and 34) are interpreted to be disrupted depositional contacts. Overlap of the conglomerate across northeast-trending faults in the Limestone Hills Domain (Figure 34) suggests that these faults may be related to uplift of the source area of the conglomerate. No other structures formed during these early periods of deformation can be identified. The effect of early high-angle faulting on later structures is thus difficult to gauge, but is believed to be significant. In particular, uplift of Precambrian rocks would allow later thrust faults to juxtapose Precambrian and Mesozoic rocks with considerably less displacement than stratigraphic relations alone would suggest.

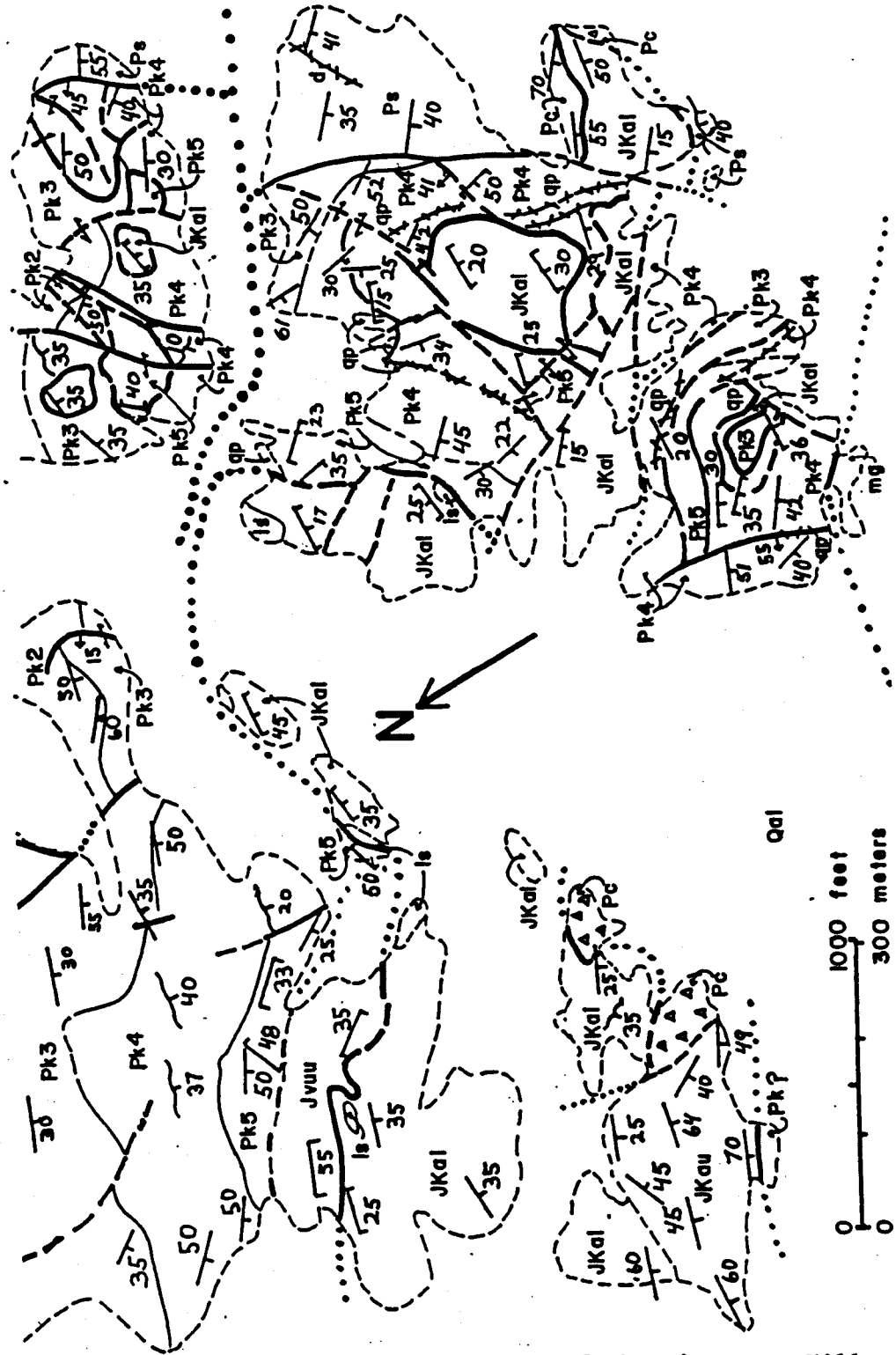

Figure 34. Detailed Geologic Map of the Limestone Hills

See Figure 5 for explanation of symbols

Southeast-vergent Folding

Variations in dip of bedding from upright south dips to extremely overturned north dips (Figure 5) are due to a large-scale southeast-vergent recumbent fold referred to as F_1. A synclinial hinge of this fold is present on eastern Martin Peak (Figures 35 and 36). Northwest trend of the axis is due to later refolding. In other sections of the main Paleozoic outcrop belt, the hinge of this fold is not exposed due to the lack of topographic relief. The anticlinal hinge of the fold structure is present in beds of the Supai Formation on Elbow Hill (Figure 37). Approximate axes of F_1 folds were stereographically determined (see Ragan, 1973, p. 116 for method) in sub-domains of the Martin Peak Domain and are plotted in Figure 38. Although attenuated stratigraphic sections are present in the map area, their location bears no relation to F_1 fold geometry. The F_1 fold has a concentric geometry and is interpreted to have formed primarily by flexural slip (Ramsay, 1967, p. 392). Disruption of bedding throughout the area is attributed at least in part to bedding-plane shear during development of the fold.

Refolding and Associated Structures

The F_1 fold was refolded about steeply plunging axes referred to as F_2 axes. The refolding is most apparent in the change from northeast to northwest strike on Martin Peak (Figure 35) and in the southern Needle Domain (Figure 5). Northwest strike of strata in the Limestone Hills and Sore Fingers West Domains also results from this

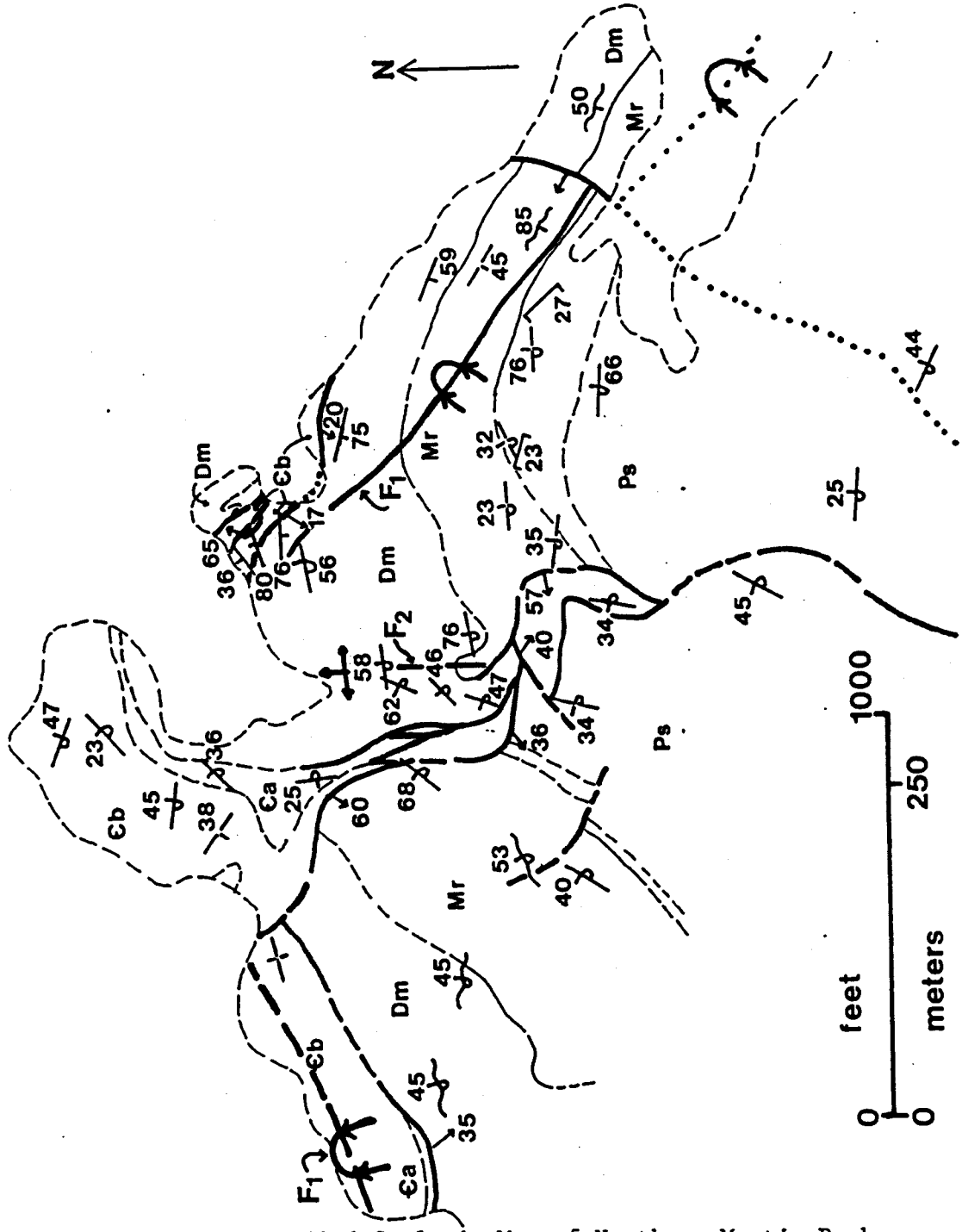

Figure 35. Detailed Geologic Map of Northern Martin Peak.

F_1 and F_2 Folds are labeled. For an explanation of symbols see Figure 5.

Figure 36. Aerial view of Martin Peak.

The view is to the west. The synclinal hinge of the F_1 fold can be seen in Redwall Limestone on the right side of the peak.

deformation. The major fault cutting the central part of Martin Peak (Fault D, Figure 28) follows the axial plane of the F_2 fold, separating the east and west limbs and gaining separation to the south. This fault is interpreted to have formed during F_2 folding. A broad antiform and synform in extremely overturned beds south of Golden Eagle Hill (Figure 5), and a synformal anticline above fault C on Elbow Hill (Figures 32 and 37) are also included as F_2 structures based on similar geometry, axial trend, and similar age relative to other structures. Approximate F_2 fold axes, determined using Pi plots of bedding, fall on a great circle girdle (Figure 38) that defines the axial plane of F_2 (Ramsay, 1967, p. 538-540), oriented at about N 30° E, 60° NW. Distribution of F_1 fold axes in a poorly defined subhorizontal girdle indicates that the F_2 axis is steep. Structures related to F_2 deformation are summarized in Figure 39.

Structural complexity at the southeast end of northwest-trending strike belts in the Sore Fingers area suggests a second phase of high angle faulting. In the Limestone Hills, the southeast corner of the Needle Domain, and in the southern Sore Fingers West Domain, (Figure 5), north- to northeast-trending, moderate- to high-angle faults with right and/or reverse separation are present. These are interpreted to be subsidiary faults in a northeast-trending fault zone which originally juxtaposed the Paleozoic and Mesozoic strata against the Sore Fingers Assemblage. The relationship of this zone to other major structures is not clear. Northeast-trending faults in the Limestone Hills (A set, Figure 27) which may be pre-Apache Wash

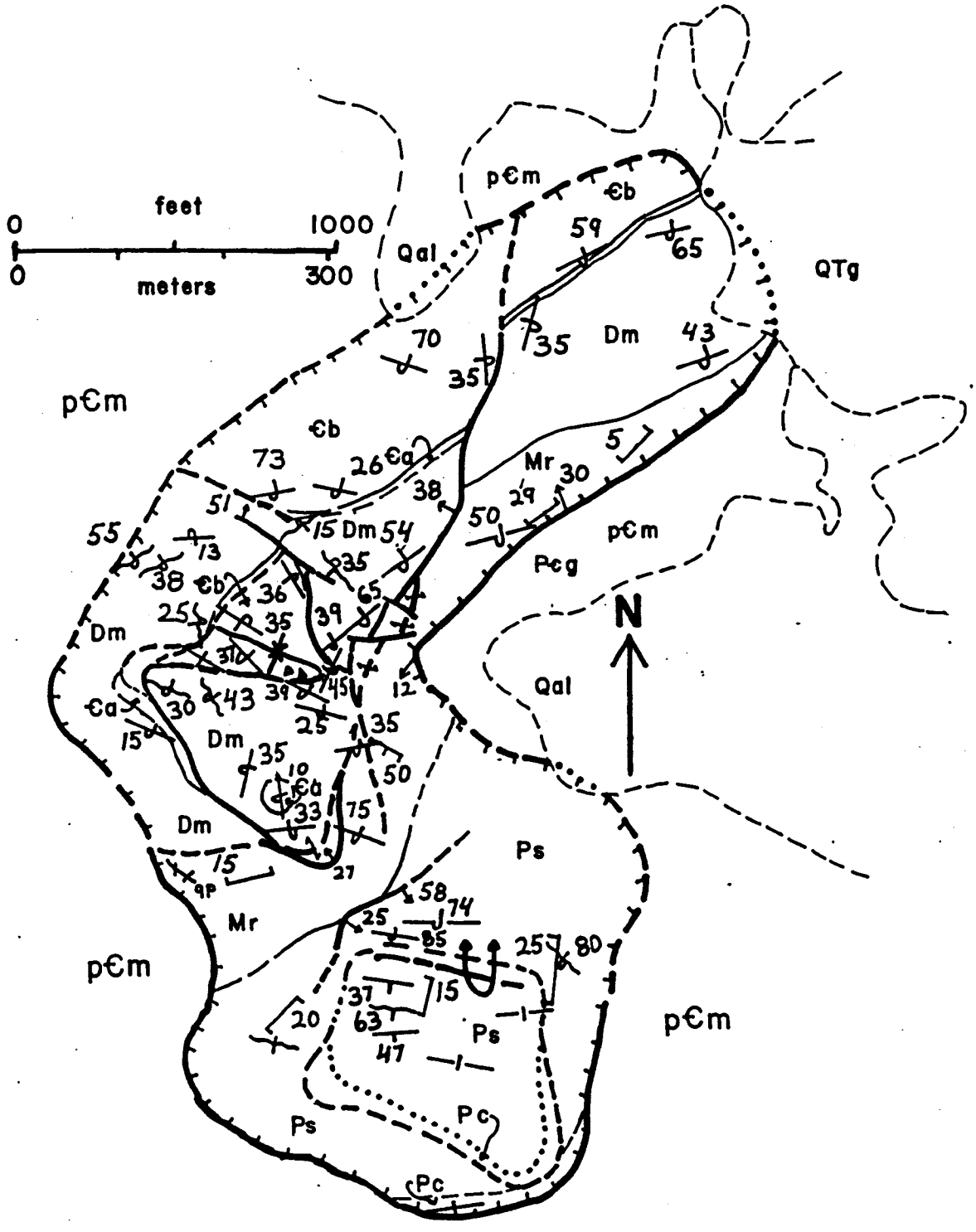

Figure 37. Detailed Geologic Map of Elbow Hill.
For an explanation of symbols, see figure 5.

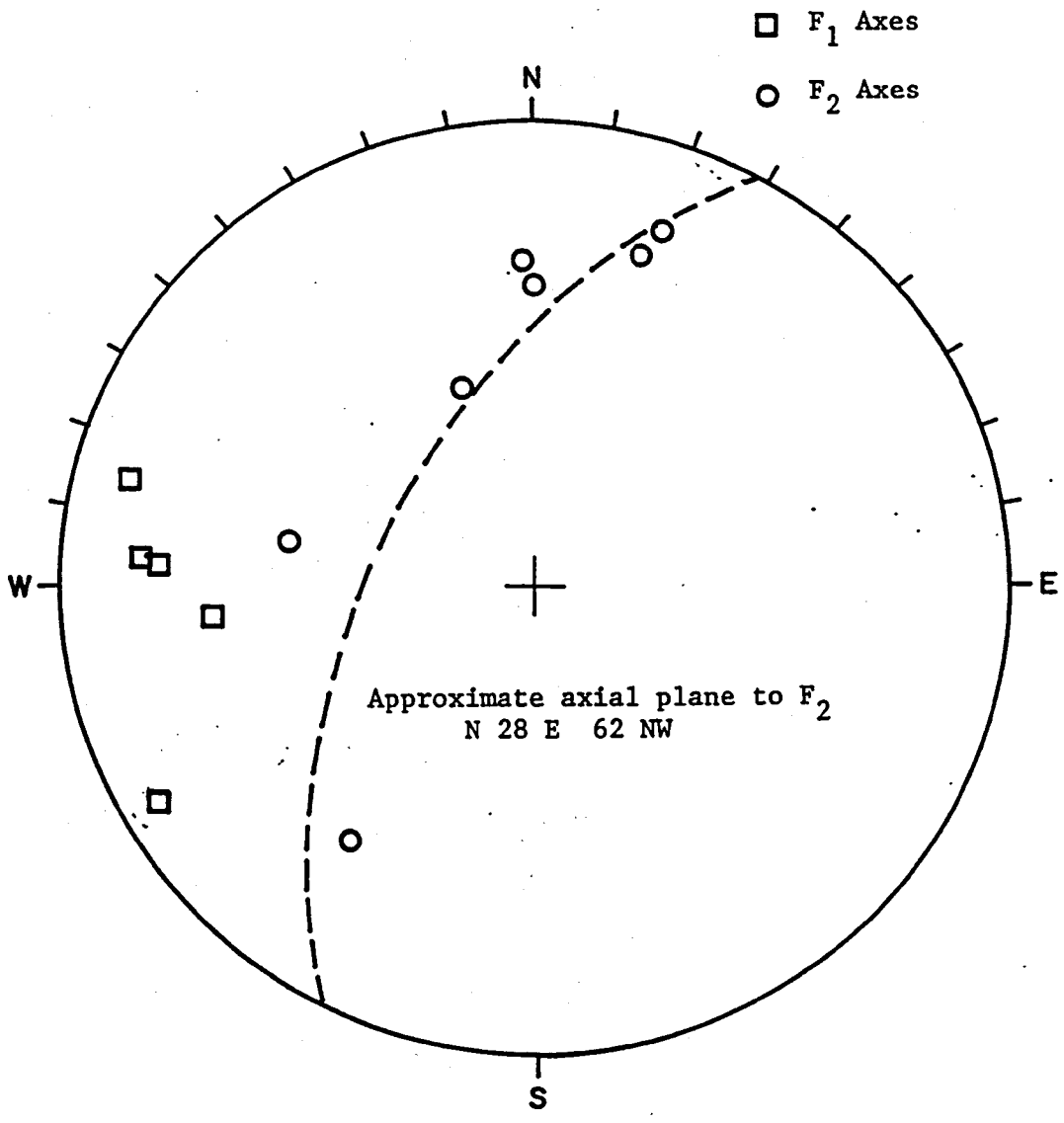

Figure 38. Axes of Major Folds.

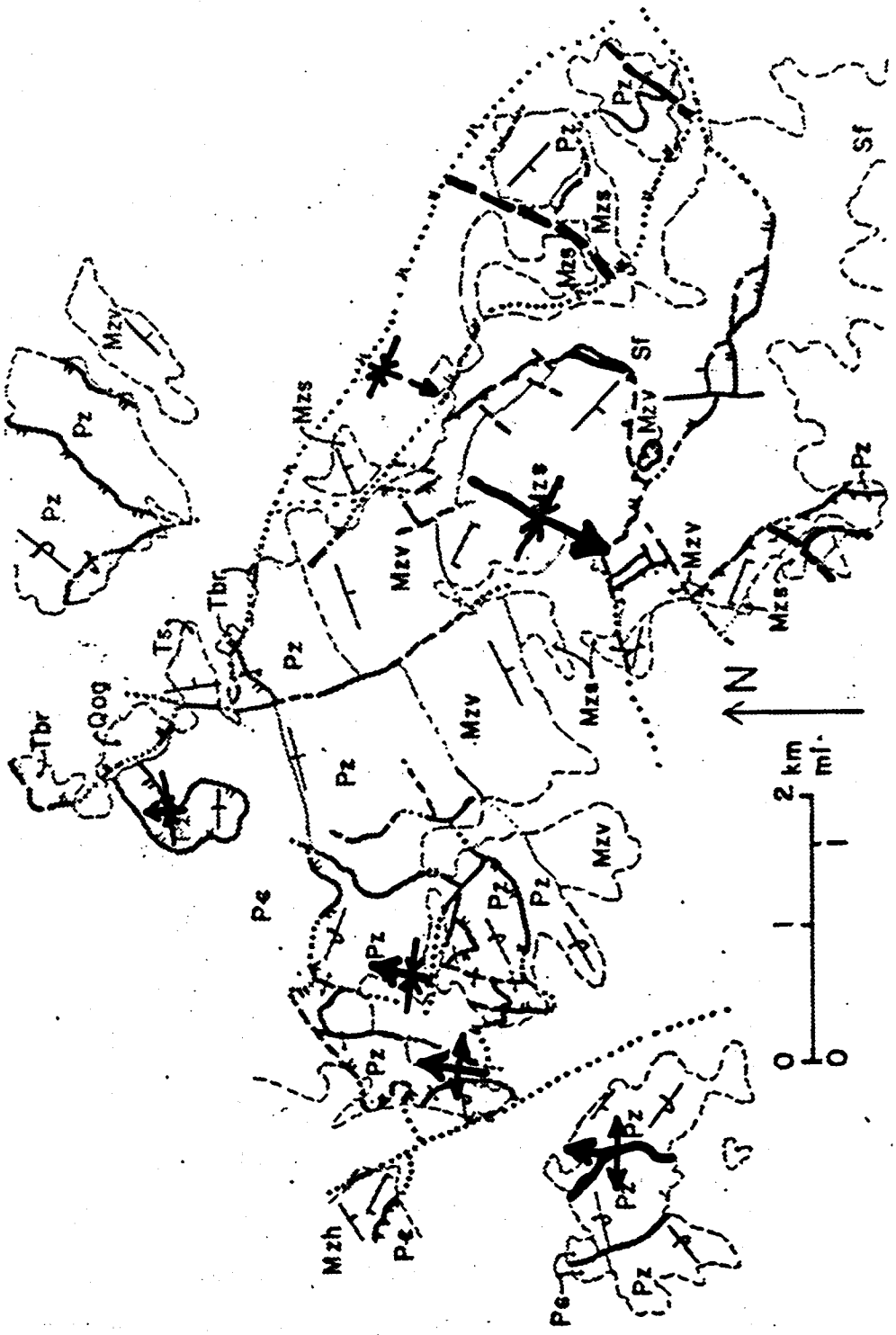

Figure 39. Structures related to F_2 folding.

structures are parallel to this trend, suggesting that later faults which do cut the Apache Wash Formation are reactivated structures. However, the present distribution of structures related to this event on northwest-trending limbs of F_2 folds indicates that the fault zone is syn- or pre-F_2. The clockwise rotation of these limbs is consistent with drag on a northeast-trending, right-slip fault. Presence of both sedimentary rocks and rocks of the Sore Fingers Assemblage in what is interpreted as the upper plate of the Sore Fingers thrust (discussed below) indicates that the northeast trending fault was active before thrusting. Since the faults which can be observed or confidently inferred have right separation as well, this fault zone is interpreted to be a right slip fault which formed along with the F_2 folds and juxtaposed the sedimentary rocks with the Sore Fingers Assemblage. At least part of this fault zone may be reactivated Pre-Apache Wash structures.

Foliations and thrust faults

Tectonic foliations are common throughout the area and are related to thrust faulting. Fabrics present include fracture cleavage in siliceous rocks, transposition layering in limestones, and flattening in limestone conglomerates. Fracture cleavage, defined as "a cleavage consisting of closely spaced microfaults or fractures that divide the rock into a series of tabular bodies or microlithons" (DeSitter, 1964, p. 268), is best developed along the Sore Fingers thrust (Figure 40) and in Mesozoic clastic and volcaniclastic rocks

Figure 40. Fracture cleavage along the Sore Fingers thrust.

The pencil lays on the contact, with the upper volcanic unit above the fault, and crystalline rocks of the Sore Fingers Assemblage below it.

(Figure 20). Cleavage is present within about 10 meters above and below the Sore Fingers thrust. Its development in crystalline rocks of the Sore Fingers Assemblage is accompanied by a reduction in grain size as the fault is approached; volcanic rocks above the fault show little change in grain size. Lineation was not observed in the cleaved rocks. The cleavage is apparently best developed where volcanic or volcaniclastic rocks occur adjacent to the fault; it is not prominent in the southernmost exposures of the fault, where Paleozoic carbonates occupy the upper plate, or along the west-trending segment in central Sec. 30, T. 4°N., R.12°W., where sandstone of the Apache Wash Formation is present above the fault. However, this west-trending segment may also be the trace of a younger north-dipping normal fault (discussed below). Poles to cleavage along the fault are plotted in Figure 41; the average strike of the cleavage is about N 55° W.

Fracture cleavage in Mesozoic volcanic and clastic rocks is identical in appearance and orientation (Figure 42) to that along the Sore Fingers thrust. The cleavage becomes parallel to bedding in the southern Needle Domain (Figure 5) and cannot be distinguished from the bedding. Cleavage in the rocks of Harquar Peak is subparallel to the Hercules thrust and to cleavage in the rocks of the southern Little Harquahala Mountains.

Foliations in Paleozoic rocks are more variable in style and more scattered in orientation than the cleavage in Mesozoic rocks (Figure 44); in general, they dip at lower angles. Fracture cleavage

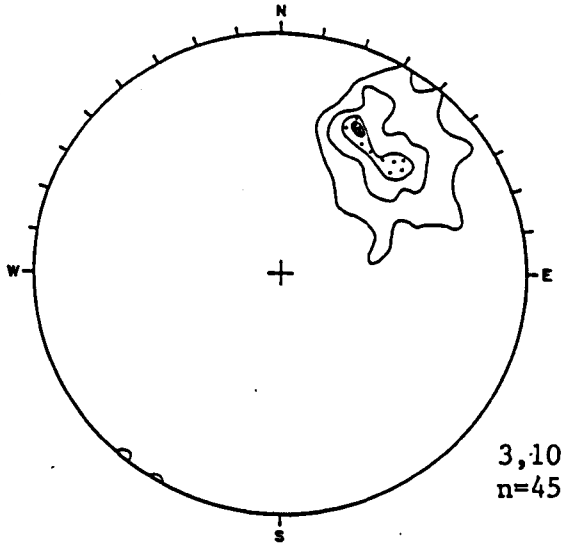

Figure 41. Contoured equal area plot of poles to cleavage along the Sore Fingers Thrust.

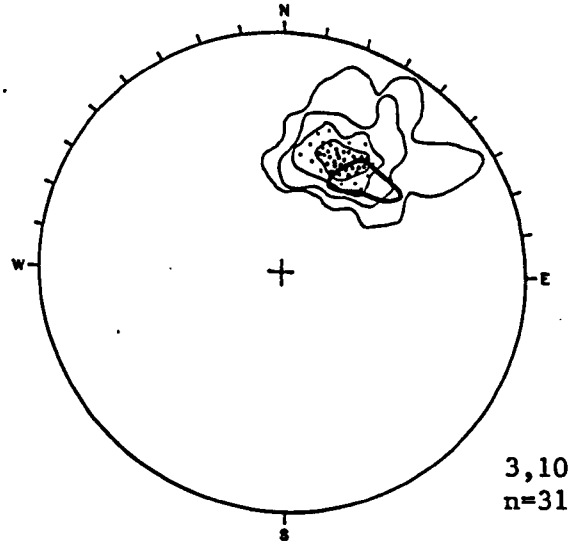

Figure 42. Contoured equal area plot of poles to cleavage in Mesozoic rocks.

Light contours are for 31 poles in Apache Wash formation. Heavy contour is for 4 poles in rocks of Harquar Peak.

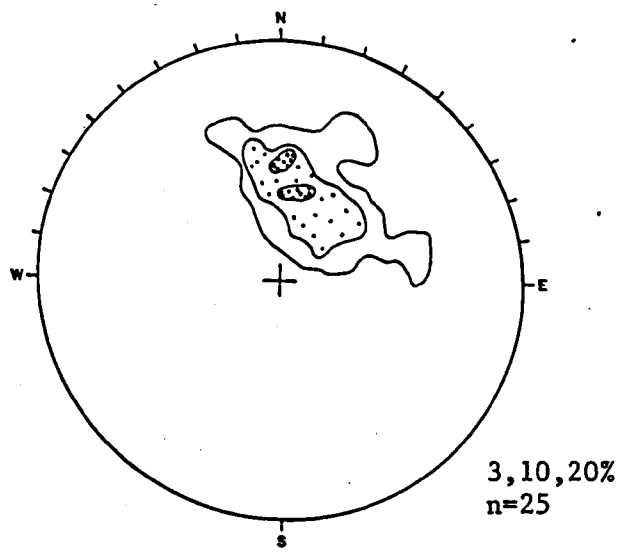

Figure 43. Contoured equal area plot of poles to foliation in the Limestone Hills Domain.

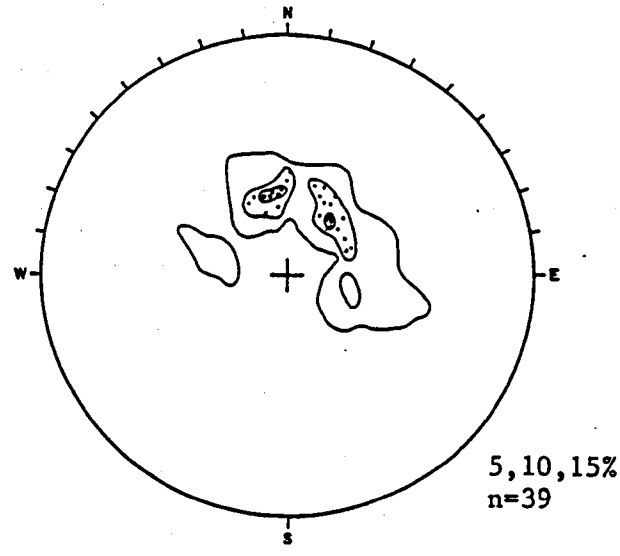

Figure 44. Contoured equal area plot of poles to foliation in Paleozoic rocks of the Main outcrop belt.

is present in fine-grained siliceous clastic rocks of the Supai Formation and Kaibab Limestone. Transposition layering is present in cherty limestones of the Redwall and Kaibab Limestone. Limestone clast conglomerate at the base of the Supai Formation and Apache Wash Formation has a planar fabric defined by flattened, but not preferentially elongated clasts. Low-angle shear zones (B fault set, Figure 27) and foliations in the Limestone Hills are sub-parallel and spatially associated (Figure 34). There is no indication that the foliation is folded by or related to either fold event. The difference in orientation of foliation between Paleozoic and Mesozoic rocks is attributed to greater lithologic variability of Paleozoic rocks and the effects of later deformation.

Two major thrust faults are present in the map area. The Hercules thrust (Reynolds, Keith and Coney, 1980; Keith and others, 1981) places Precambrian monzogranite on Mesozoic volcanic and clastic rocks of Harquar Peak at the northern edge of the map area. The Sore Fingers thrust places Mesozoic volcanic rocks, clastic rocks of the Apache Wash Formation and rocks of the Sore Fingers Assemblage on rocks of the Sore Fingers Assemblage in the southern part of the area. The relationship between these two faults is not revealed by outcrops in the map area and remains a fundamental unsolved problem.

The Hercules thrust strikes northwest and dips gently southwest within the map area. Near vertical gneissic foliation in amphibolite gneiss of the upper plate is folded and disrupted within about 10 meters of the fault, but the geometry of the folds does not

indicate transport direction on the fault. Clastic rocks near the fault are comminuted and sheared; the planar fabric in these rocks is oriented sub-parallel to cleavage present below the fault zone. The age of the Hercules thrust is poorly constrained (Reynolds, 1982). The Hovatter Road Fault is the only structure which cuts the thrust.

The Sore Fingers thrust is separated into two segments by a poorly exposed low-angle normal fault described later (Figure 45). Both segments strike about N 35° W and dip southwest at 30° to 65°. At the south end of both segments, the strike changes to a northerly orientation, and the dip of the fault decreases. The thrust is characterized by well developed fracture cleavage in rock along the fault. The average strike of this cleavage (N 55° W, Figure 41) diverges from the strike of the thrust (N 35° W). Lenses of Paleozoic limestone and Paleozoic-clast conglomerate occur at several places along the thrust (Figure 45). Fault D in the Sore Fingers Domain (Figure 26) is correlated with the Sore Fingers thrust based on the presence of identical cleavage along the fault and the similar orientation of the fault zone. The northern segment of the thrust is thus extended south below the klippe of upper volcanic unit in the center of Sec. 30 T.4°N., R.12°W., and into rocks of the Sore Fingers Assemblage. The poorly exposed west-trending fault north of the klippe may be a younger structure related to the northwest-dipping normal faults, or an uncleaved segment of a curviplanar Sore Fingers thrust. Northeast-trending faults similar to those in the southern Sore Fingers West domain (Figure 5) and the Limestone Hills are

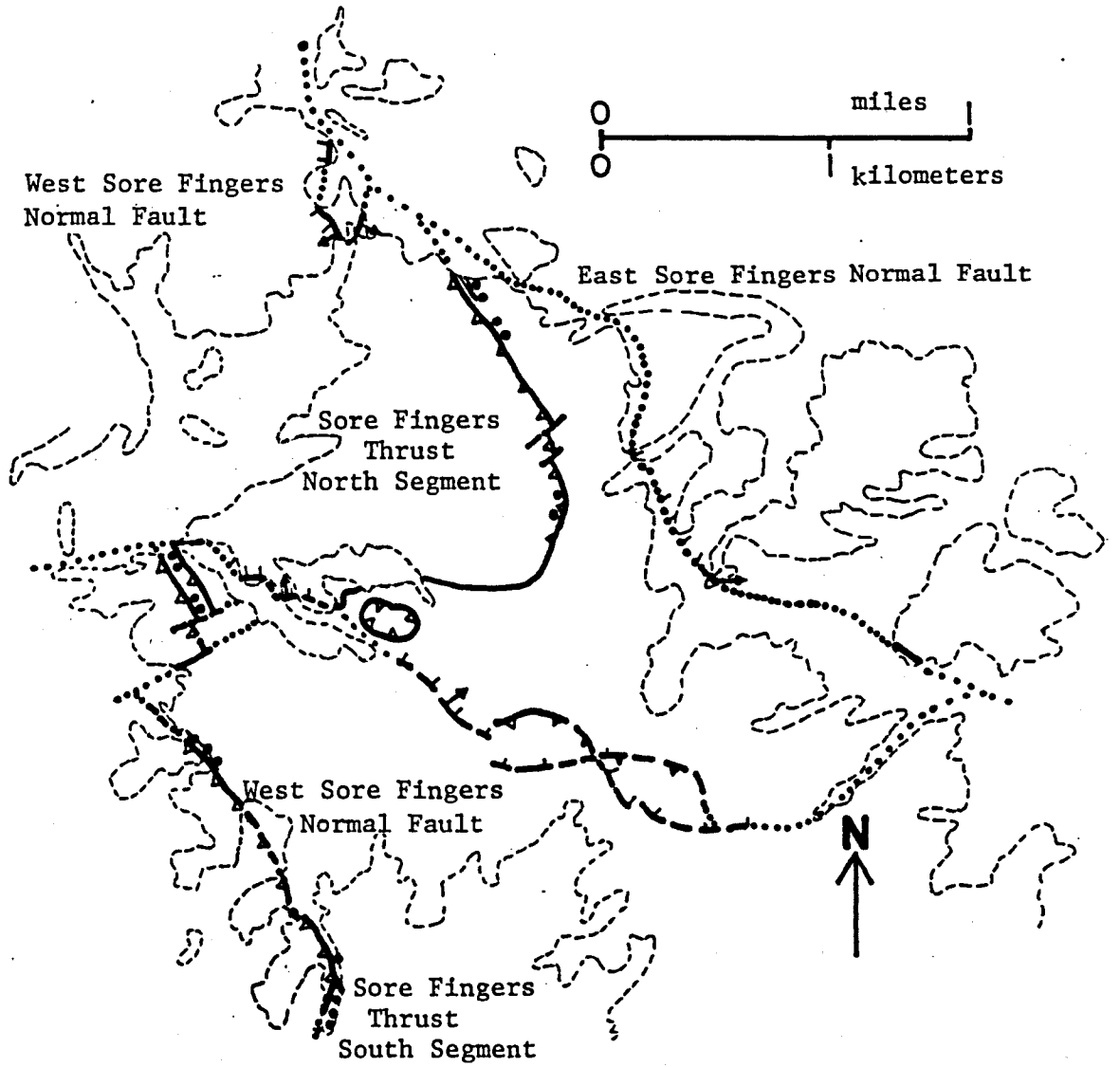

THRUST FAULT; Solid dots indicate presence of limestone or limestone conglomerate in fault zone.

LOW-ANGLE NORMAL FAULT; Arrows show dip direction where fault is exposed.

Fault not exposed, no adjacent cleavage

Figure 45. Sore Fingers Thrust and normal faults.

interpreted to separate the Sore Fingers Assemblage and Mesozoic volcanic rocks in the upper plate of the Sore Fingers thrust, indicating that the thrust cuts the northeast-trending fault which originally juxtaposed these two lithologic assemblages. Alternatively, if the cleaved fault zone in the Sore Fingers domain (Fault D, Figure 26) is not a continuation of the northern segment of the Sore Fingers thrust, then the complex faulting along the southeast termination of the rocks of the southern Little Harquahala Mountains may indicate that the Sore Fingers thrust intersects an older fault zone which was reactivated during thrusting. A third possibility is that the complex faulting at the southeast end of the strike belt is related to either minor Pre-Apache Wash Formation high-angle faulting, or to deformation accompanying thrusting. In the first two cases, the Sore Fingers thrust is a relatively minor fault imbricating rocks in the upper plate of the Hercules thrust and the Sore Fingers and Hercules thrusts are related. In the third case both thrusts are major structures and may not be related.

Uniform orientation of foliation across the area and absence of cross-cutting foliations indicates a single, post-folding foliation-forming event. Spatial association of foliation with low-angle faults in the Sore Fingers, Limestone Hills and Harquar Domains suggests that the fabrics formed in connection with faulting (Figure 46), and the presence of similar fabric in the lower plate of the Hercules thrust indicate that the foliations formed during or after the Hercules thrust. Rhyodacite porphyry sills in Paleozoic rocks are

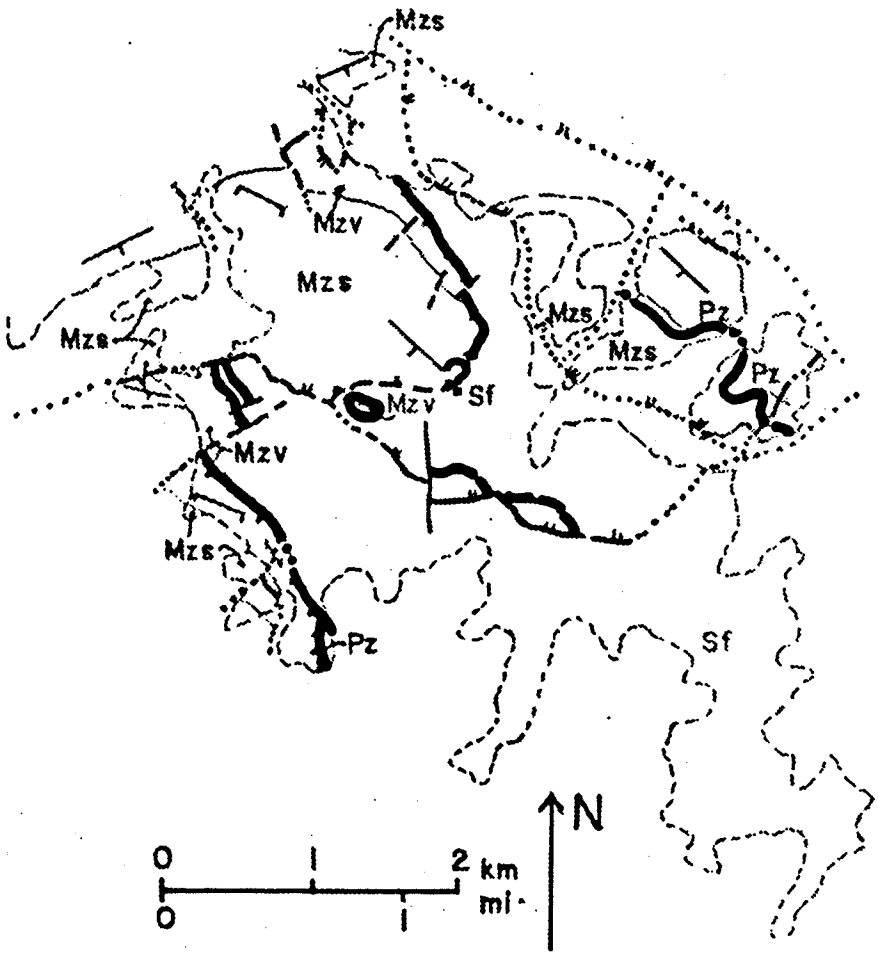

FAULTS RELATED TO THE FOLIATION-FORMING EVENT

Figure 46.

locally foliated and are deformed by the low-angle faults associated with the foliation; the absolute age of the sills is unknown. Northwest-trending microdiorite dikes in volcaniclastic sediments along the southern segment of the thrust are aligned with similar dikes in rocks of the Sore Fingers Assemblage below the thrust (Figure 5), suggesting that the dikes were intruded after movement on the Sore Fingers thrust. Similar dikes in the Harquahala Mountains are dated at 22 and 28 m.y. (K-Ar, biotite, hornblende; Shafiqullah and others, 1980). In summary, foliation development and thrusting occured after folding and intrusion of rhyodacite porphyry sills, but before intrusion of microdiorite dikes and the latest movement of the Hovatter Road Fault.

South Dipping Reverse Faults

Complex faulting in overturned strata of the main Paleozoic outcrop belt can be bracketed in age between the early fold events and the development of northeast-dipping low-angle normal faults, but the relative age of these faults with respect to the thrust events cannot be confidently established. South- to southeast-dipping reverse faults are the oldest faults cutting the northeast-trending Paleozoic outcrop belt (Figure 56). The consistent orientation of these faults indicates that they formed after both fold events. In the area of the intersection of West Redwall Ridge and the Golden Eagle Hill stacks of very thin, fault-bounded plates, called shingled structures (Figure 56), are apparently related to south-dipping reverse fault A of the

Golden Eagle Domain (Figure 29). Less extreme stacking of the reverse faults occurs on the Needle and on east Needle Ridge. Minor faults of this set have beem mapped on Redwall Hill. Similar stacking of thin sheets of rock in the shingled zones and on Limestone Hill A (Figure 34), sharp, unbrecciated fault surfaces, and early development of the south-dipping reverse faults suggest correlation with the low-angle faults in the Limestone Hills and thus with the Hercules and/or Sore Fingers thrusts.

Northwest-dipping Normal Faults

The most abundant faults in the area are northeast-striking, northwest-dipping normal faults (Figure 47). Their geometry is best displayed in the Corral Hill Domain (Figure 5 and 25). Northeast-striking, vertical to extremely overturned strata are separated into four structural plates by faults A, B, and C (Figure 33 and cross section G-G in Figure 6). Bedding is progressively more overturned in successively higher plates (Figure 48), suggesting rotation of beds associated with northwest transport on listric normal faults, or juxtaposition of beds from different parts of the large-scale F_1 fold structure. The Elbow Hill Fault (Figure 32), which underlies and bounds the Elbow Hill Domain is also a relatively simple member of this set. The fault is a subhorizontal, warped surface; northward dip of the fault increases to the south (Figure 37). Where the fault surface is exposed, the Redwall Limestone is transposed in the fault zone, while the underlying Precambrian monzogranite is granulated and altered; one fold axis along the fault trends N 83° W.

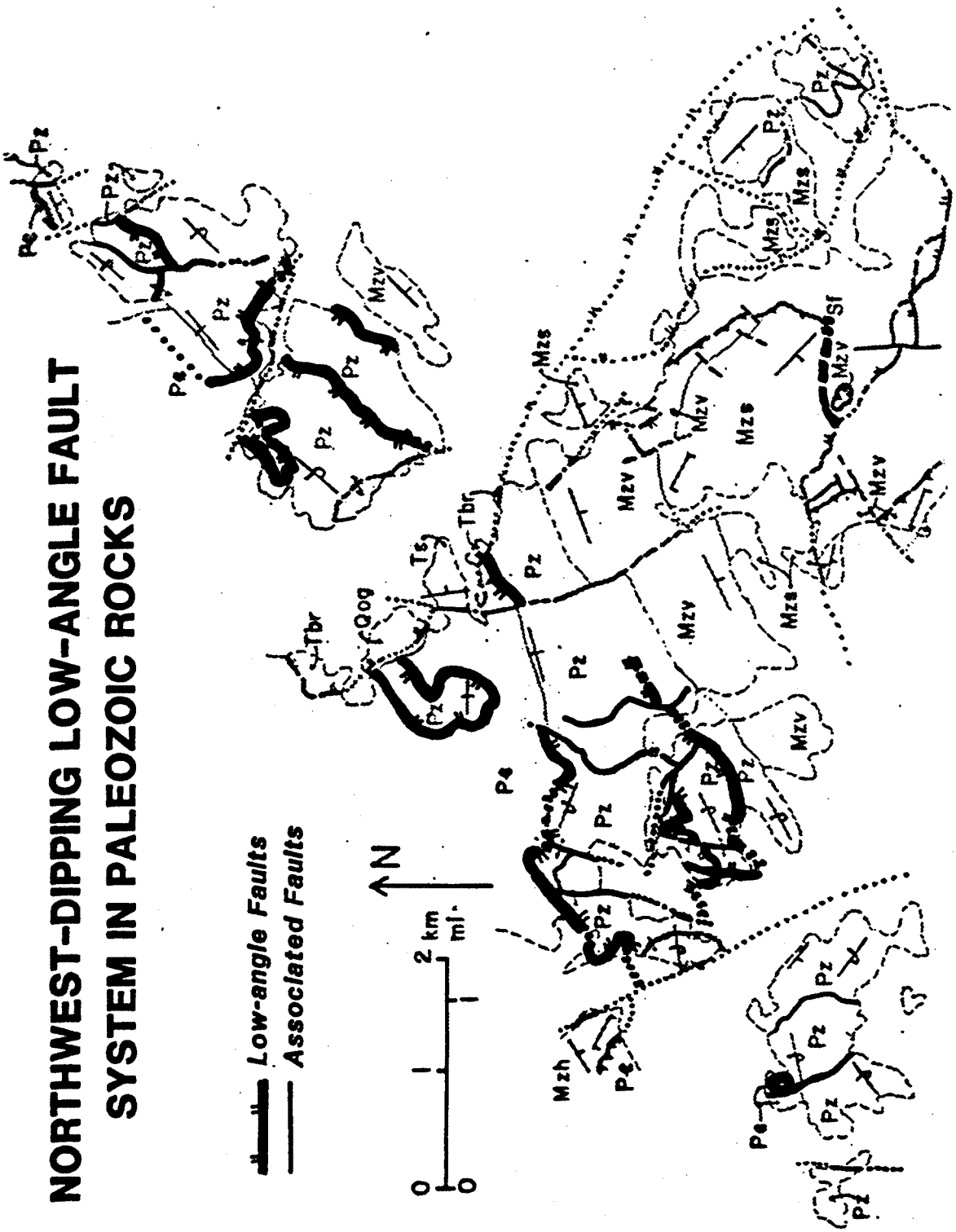

Figure 47. Northwest-dipping normal fault system in Paleozoic rocks.

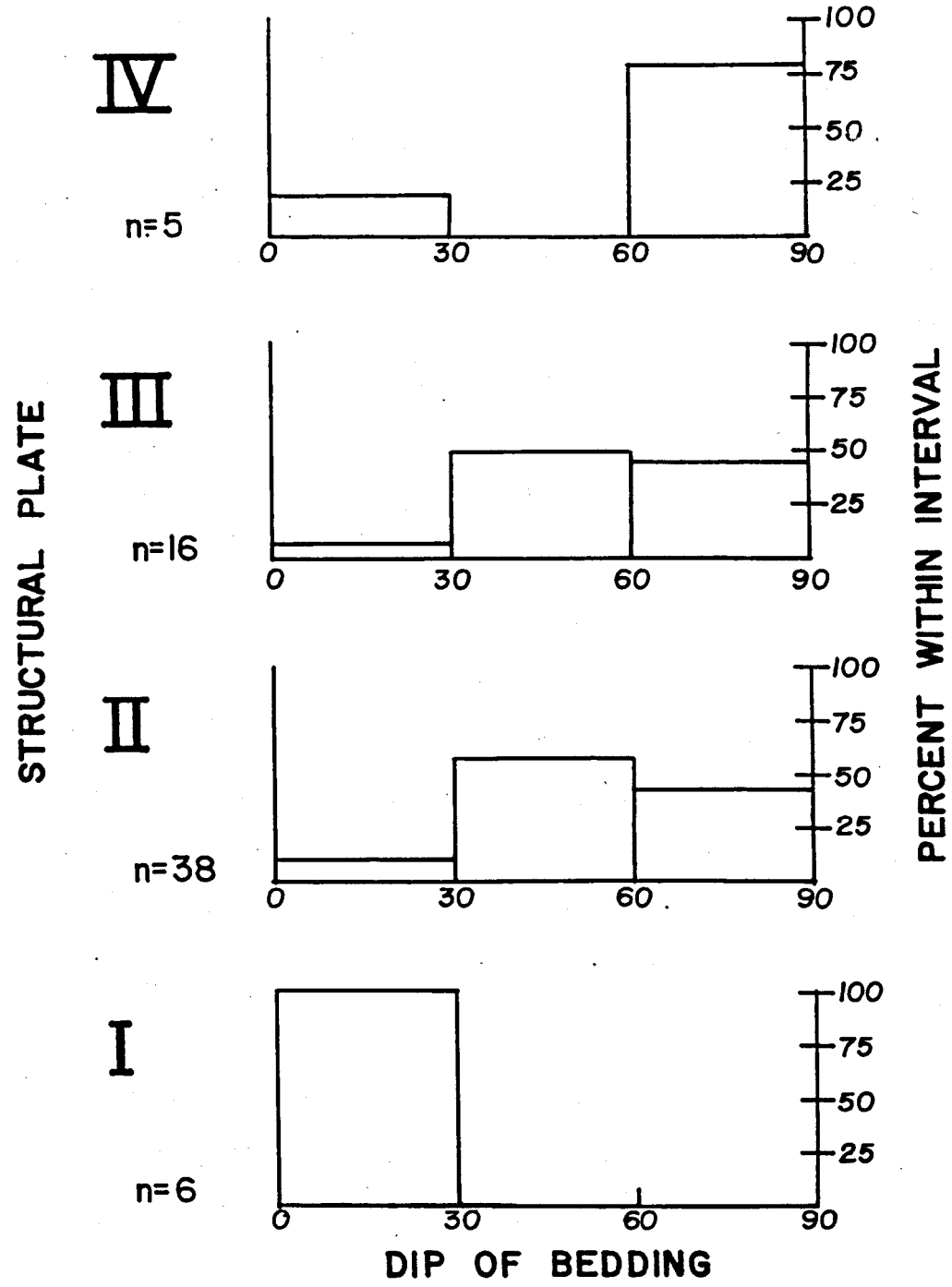

Figure 48. Distribution of Dips of Bedding on Corral Hill. 'n' is the number of readings. I is the highest structural plate, IV is the lowest.

On Split Mountain and in the Golden Eagle Hill-Mixmaster Hill area, the northwest-dipping normal separation faults are associated with north- to northwest-trending, low- to high-angle faults. Conflicting cross-cutting relations between these two groups of faults can only be resolved if they both formed at the same time. On Split Mountain (Figure 5), the Split Mountain Fault (Fault C, Figure 33) truncates stacked faults present on both its east and west sides. Specific faults on opposite sides cannot be correlated because the stratigraphic offsets across the normal faults and cross-cutting relations between faults are not consistent. Also, there is no separation across the Split Mountain Fault south of the stacked normal faults, although a breccia zone can be traced a short distance. The Split Mountain Fault does not cut a pre-existing set of normal faults. Thus, the separation on its northern part must be related to movement on the stacked normal faults; and all of the faults in question (Split Mountain Domain, faults C, G, H, I, L, and M; Figure 33) are interpreted to have formed together.

The Mixmaster Hill Fault is a northwest-dipping normal separation fault which becomes nearly flat and emerges on the northwest as the Golden Eagle Fault (cross section C-C′ on Figure 6). On west Needle Ridge the Mixmaster Hill Fault is steep and repeats the Kaibab Limestone-Coconino Sandstone contact with only a small stratigraphic separation. On Mixmaster Hill the separation increases rapidly due to right separation on the Northern Boundary fault and fault D (Mixmaster Hill Domain, Figure 30), and the dip decreases to

the west and down hill (Figure 50). The fault dips about 13° north where the Kaibab Limestone overlies Redwall Limestone. The Mixmaster Hill Fault cuts across bedding at angles of from 0° to 50°. The poorly exposed Golden Eagle Fault places Paleozoic rocks on Precambrian monzogranite along the northern boundary of the Golden Eagle Domain. The trace of the fault indicates that it is subhorizontal (Figure 5); steep contacts observed locally are interpreted to be the result of later, minor fracturing. These two faults underlie an allochthon transported in a northerly direction off the main Paleozoic strike belt.

On Mixmaster Hill four north-northwest-dipping normal faults divide this allochthon into five plates (Figure 49). North and northwest-trending, high-angle faults cut rocks in plates III and IV, but are truncated by the Mixmaster Hill Fault; the thickness of plate IV changes across these faults. The thickness of plates II and III is variable due to anastamosing of their bounding faults (Figure 50 and cross section C-C in Figure 6). Faults of the northwest-trending set accomodate increased separation across the Mixmaster Hill Fault, but are cut by overlying low-angle faults in the imbricate stack, indicating that they formed during the normal faulting. North-trending brecciated fault zones (fault F and K; Figure 30) are similar in style to the Split Mountain Fault, and cut all other faults except the Mixmaster Hill Fault and the Northern Boundary fault. The West Ridge Fault is interpreted to be an important member of this north-trending set; it bounds the allochthon on the east, and merges with

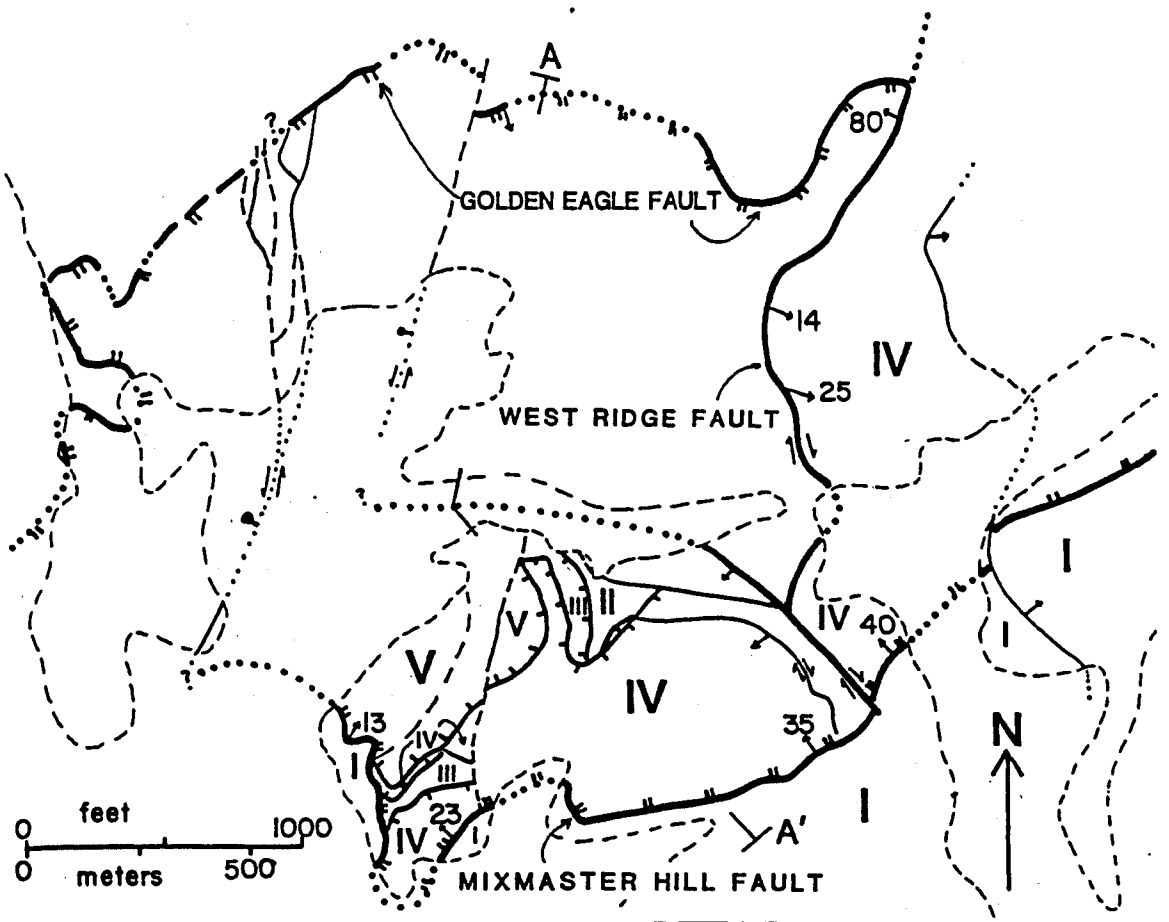

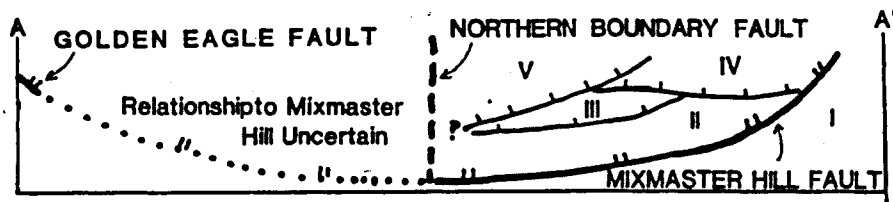

SCHEMATIC CROSS SECTION SHOWING RELATIONSHIP OF FAULTS

EXPLANATION

Boundaries of the Mixmaster Hill–Golden Eagle Hill Allochthon

Other Low-angle Faults on Mixmaster Hill

Associated Tear Faults

FOR EXPLANATION OF OTHER SYMBOLS SEE PLATE 1

Figure 49. Simplified geologic map of the Mixmaster Hill-Golden Eagle Hill Allochthon

the Northern Boundary fault to the south. The north-trending faults formed during late-stage movement on the Mixmaster Hill Fault. Change in strike from northeast to west-northwest from west Redwall Ridge to Golden Eagle Hill and on Mixmaster Hill is interpreted to be the result of rotation related to increased displacement on the Mixmaster Hill Fault.

The west-trending fault between the Apache Wash Formation and Sore Fingers Assemblage in central section 30, T.4°N, R.12°W may be a fault of this set, based on its orientation and the possible offset of the Sore Fingers thrust. Presence of such a fault would explain the klippe of upper volcanic unit lying south of the fault.

The Golden Eagle Fault of this report is the type Golden Eagle thrust of Keith and others (1981). Reinterpretation of the type Golden Eagle thrust as a normal fault requires that the structural analog of the Golden Eagle thrust present in the western Harquahala Mountains lies within the Precambrian monzogranite northwest of the Paleozoic rocks of the Little Harquahala Mountains. This structural position is analogous to the postion of the thrust in the westernmost Harquahala Mountains (S. B. Keith, personal communication, 1982).

Northeast-dipping, low-angle normal faults

The Breccia Fault and the East and West Sore Fingers Normal Faults are interpreted to be part of a set of generally northwest-trending, northeast-dipping normal faults (Figure 51). These faults are characterized by low dips, intense brecciation and poor exposure

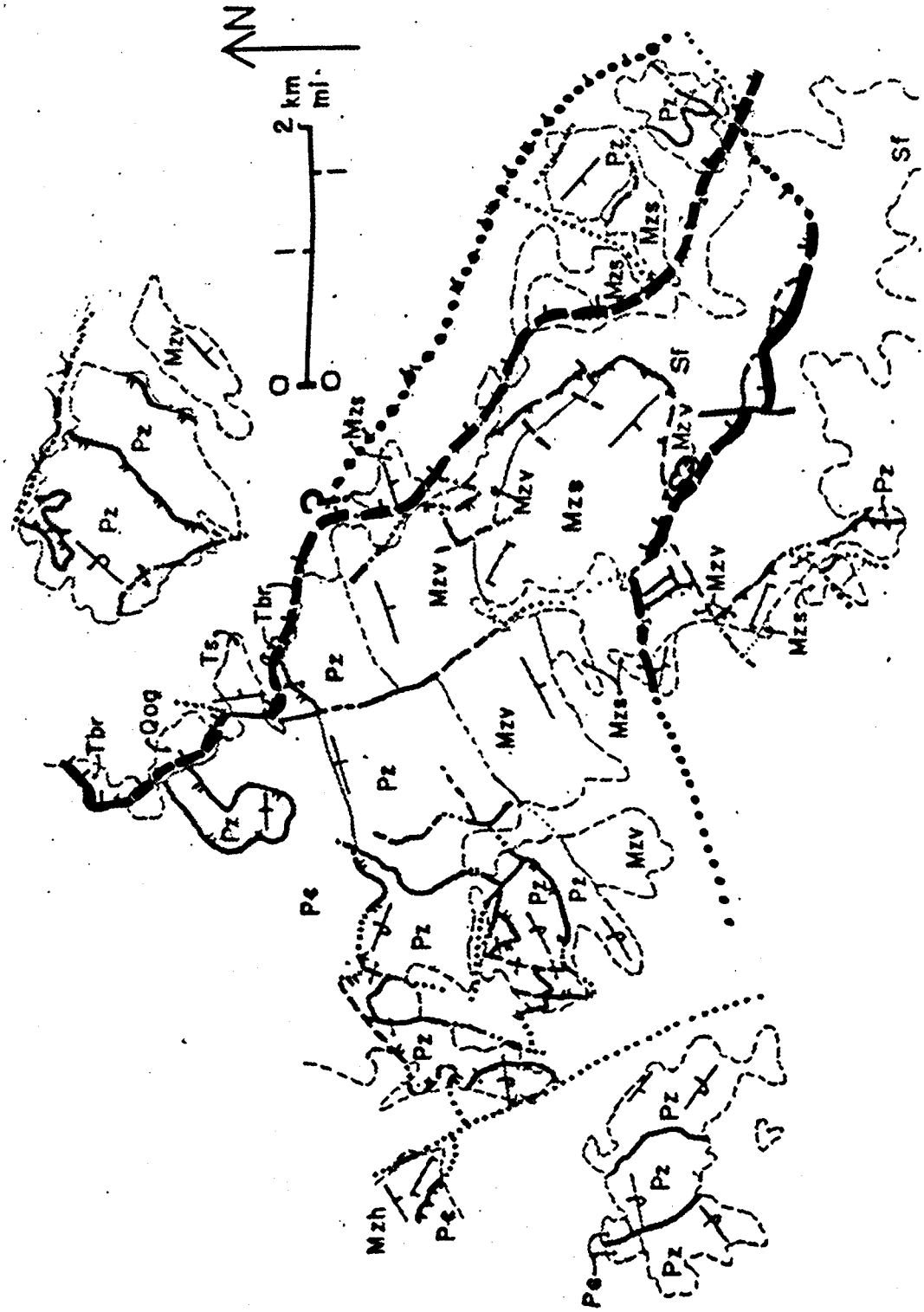

Figure 51. Northeast-dipping normal faults.

(Figure 52). The Breccia fault dips gently to the northeast. Where the location of the fault is well constrained, near East Needle Ridge and Elbow Hill (Figure 5) it must dip a minimum of 15° in order to pass over the ridge tops. Along the northern part of the fault, limestone breccia in the upper plate is up to 15 meters thick and is shown at Tertiary(?) breccia on Figure 5. The presence of similar breccia on the east side of the Limestone Hills (Figure 5) suggests extension of the Breccia fault into that area. The fault may lie just east of and above the Limestone Hills, or join the East Sore Fingers Normal Fault, in which case the breccias indicate proximity to a near flat fault zone. Both possibilities are shown on Figure 5.

Where the Sore Fingers normal faults are exposed (Figure 45), a white, powdery breccia occurs along the fault zone, and rock above and below the fault is crushed (Figure 52). Measured dips range from 10° to 45° and the strike is highly variable; the irregular trace of the east normal fault suggests a general northeast strike and low dip. The nearly flat fault underlying a small klippe in SW Sec. 19, T.4N., R.12W. (Figure 5) is interpreted to be part of the East Sore Fingers Normal Fault. The West Sore Fingers Normal Fault is interpretive southeast of north-striking fault G in the Sore Fingers Domain (Figure 26) because the clearly defined, strongly brecciated zone which characterizes the fault was not observed. The western end of the West Sore Fingers Normal Fault forms the northern boundary of the Sore Fingers West Domain and is interpreted to be an east-trending tear fault connecting the northeast-dipping West Sore Fingers Normal

Figure 52. Fault zone along the east Sore Fingers normal fault.

A sliver of Paleozoic limestone lies above the fault on crystalline rocks of the Sore Fingers Assemblage.

Fault with an inferred detachment fault to the west or southwest. Whatever its nature, the fault along the northern boundary of the Sore Fingers West Domain truncates the Sore Fingers thrust (Figure 5). This fault may be the structural boundary between Martin Peak and the Golden Eagle-Mixmaster Hill area, or lie west of Martin Peak, outside the map area. If Martin Peak is separated from the rest of the area by a detachment fault, then another fault is present which offsets the Sore Fingers West domain from the southeast limb of the F_2 fold on Martin Peak. This fault is dotted in on Figure 5. The base of the Apache Wash Formation is repeated three times by the northeast-dipping normal faults.

Northeast transport is suggested by correlation of northeast-trending Paleozoic rocks in the Northeast Hills with northeast-trending Paleozoic rocks in the Needle area and by correlation of Mesozoic rocks in the northwest striking limbs of F_2 structures. If the West Sore Fingers Normal Fault is interpreted to pass between Martin Peak and Mixmaster Hill, and the Breccia Fault is correlated with the East Sore Fingers Normal Fault, then only one large-scale F_2 fold is present in the area, repeated three times: on Martin Peak; in the Needle Area; and in the Northeast Hills-Limestone Hills area. This correlation requires a long vertical limb of the F_1 fold above the synclinal hinge exposed on Martin Peak. Nevertheless, this interpretation provides a simple way to integrate the large-scale structures in the area.

The low-angle normal faults post-date the Sore Fingers thrust and all structures in the main Paleozoic outcrop belt except late dip-slip movement on the Needle Fault. The Breccia Fault is older than the Tertiary conglomerate unit.

High-Angle Normal Faults

The Needle fault set comprises generally north-trending strike- and dip-slip faults (Figure 53). The Needle Fault shows evidence of early strike slip and later dip slip. Strike slip preceeded movement on the Elbow Hill and Breccia Faults, but late dip slip on the Needle Fault cuts these low-angle faults. Other faults of the Needle set cut structures of all earlier generations. Truncation of tilted Tertiary conglomerate by the Needle Fault demonstrates a Teriary age at least for the late dip-slip movement. Major faults of the Needle set are described briefly below.

The Hovatter Road fault is a north-northwest-trending, left-separation fault which cuts the Hercules thrust. Reconnaissance mapping by Rehrig, Reynolds, Keith and Richard (unpublished, 1981) shows the trace of the Hercules thrust on the east side of the fault offset about 2 km north relative to the west side. This separation is the result of a dip slip down on the northeast and/or left slip.

The Needle Fault cuts conglomerate which overlies the breccia occurring along the Breccia Fault (Figure 5 and 31). Realigning the Paleozoic strike belts by removing left separation on the Needle Fault increases the separation of the Breccia Fault across the Needle Fault

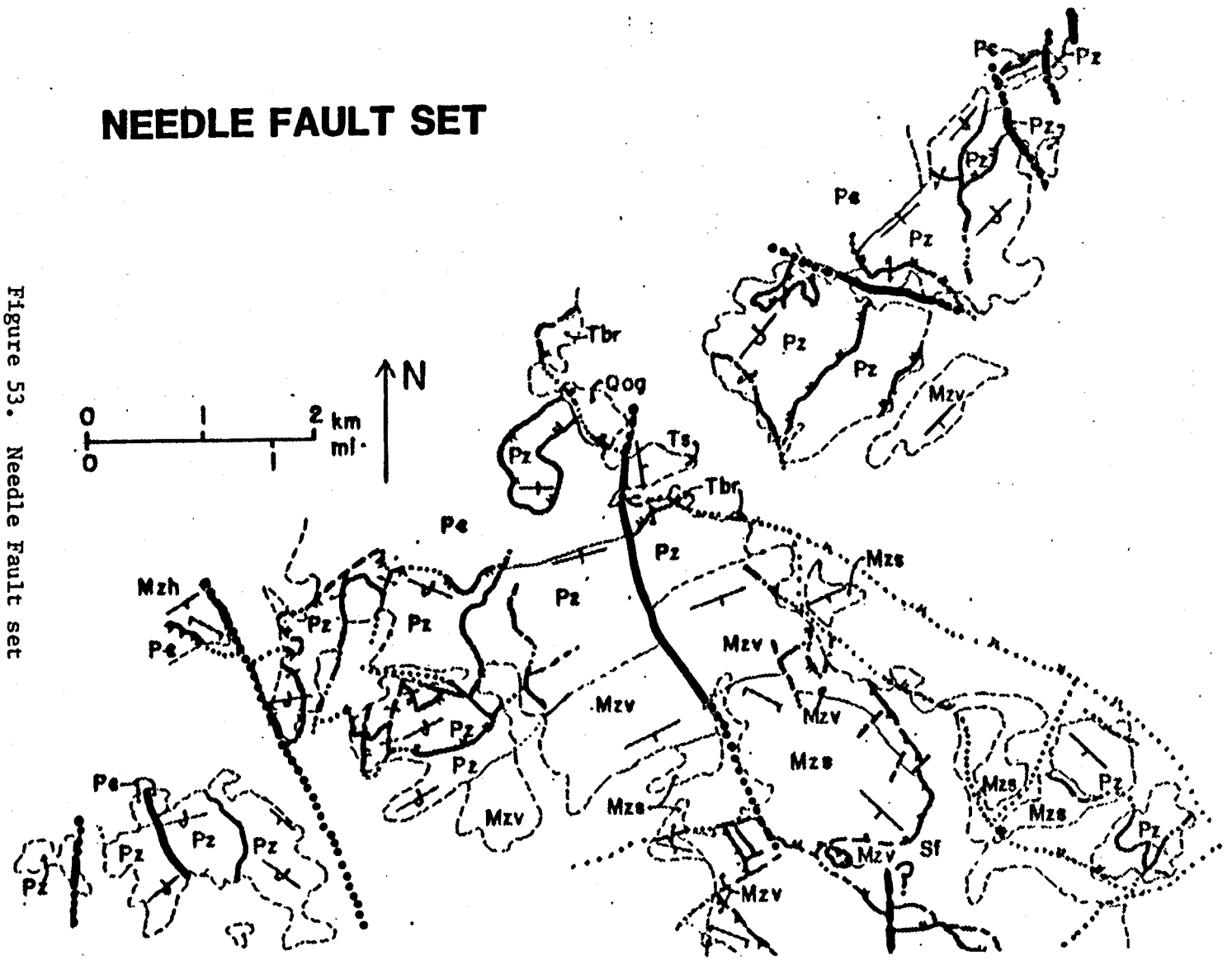

Figure 53. Needle Fault set

trace. Thus, the Needle Fault must have been active before the Breccia fault formed. Correlation of the Elbow Hill Fault with Fault 0 of the Needle Domain (Figure 31) requires that strike slip on the Needle fault occurred before the Elbow Hill Fault was active. This is because the contacts between the Supai, Coconino and Kaibab formations are presently aligned such that little separation between them is required after removing the dip-slip component on the Needle Fault. Late normal slip on the Needle Fault is responsible for present offset of the low-angle faults. Thus, normal separation on the Needle Fault is post-Breccia fault, and strike separation predates the Elbow Hill Fault. The Needle Fault is interpreted to extend south and cut the west Sore Fingers Normal Fault (Figure 5); it can not be traced in the Sore Fingers Domain.

The Northeast Hills Fault trends N 70° W, and is sub-vertical along its main trace, but an associated splay dips about 50° to the northeast. Breccia is present along the fault, but is not a prominent feature of the fault zone. Several faults are present in the fault zone where it is exposed between Corral Hill and Split Mountain (Figure 5). Progressively more right slip accumulates across each fault in the zone. Correlation of Fault A in the Corral Hill Domain with fault E in the Split Mountain Domain (Figure 33) makes dip-slip on the Northeast Hills Fault minimal.

At the northeast end of the main Paleozoic outcrop belt, poorly exposed north-trending dip- and/or strike-slip faults progressively expose structurally higher levels in the F_1 fold to the

northeast. Upright beds at the northeast end of the domain are interpreted to have been faulted down from the upper upright limb of the F_1 fold.

Minor Structures

Minor structures observed in the map area and briefly described here include joints in the Sore Fingers Domain, vein sets in the Apache Wash Formation and several minor fault sets.

Joints

Joint measurements in crystalline rocks of the Sore Fingers Assemblage were taken where prominent sets of sub-parallel fractures cut the rock. The most commonly observed sets were nearly parallel, planar subvertical zones of joints, uniformly spaced at 1 to 20 cm intervals. Alteration commonly increases in intensity in the vicinity of these fractures, indicating that they served as conduits for fluid circulation. A contoured stereonet plot of orientations of 77 measured joints (Figure 54) shows maxima of vertical joints at N 65° W and N 25° E.

Veins

Quartz and quartz-calcite veins occurring in en echelon sets are abundant in the Apache Wash Formation in the Needle Domain (Figure 5 and 25). Groups of veins generally trend near N 70° W and individual veins within the set trend about N 0° E. The veins are 5

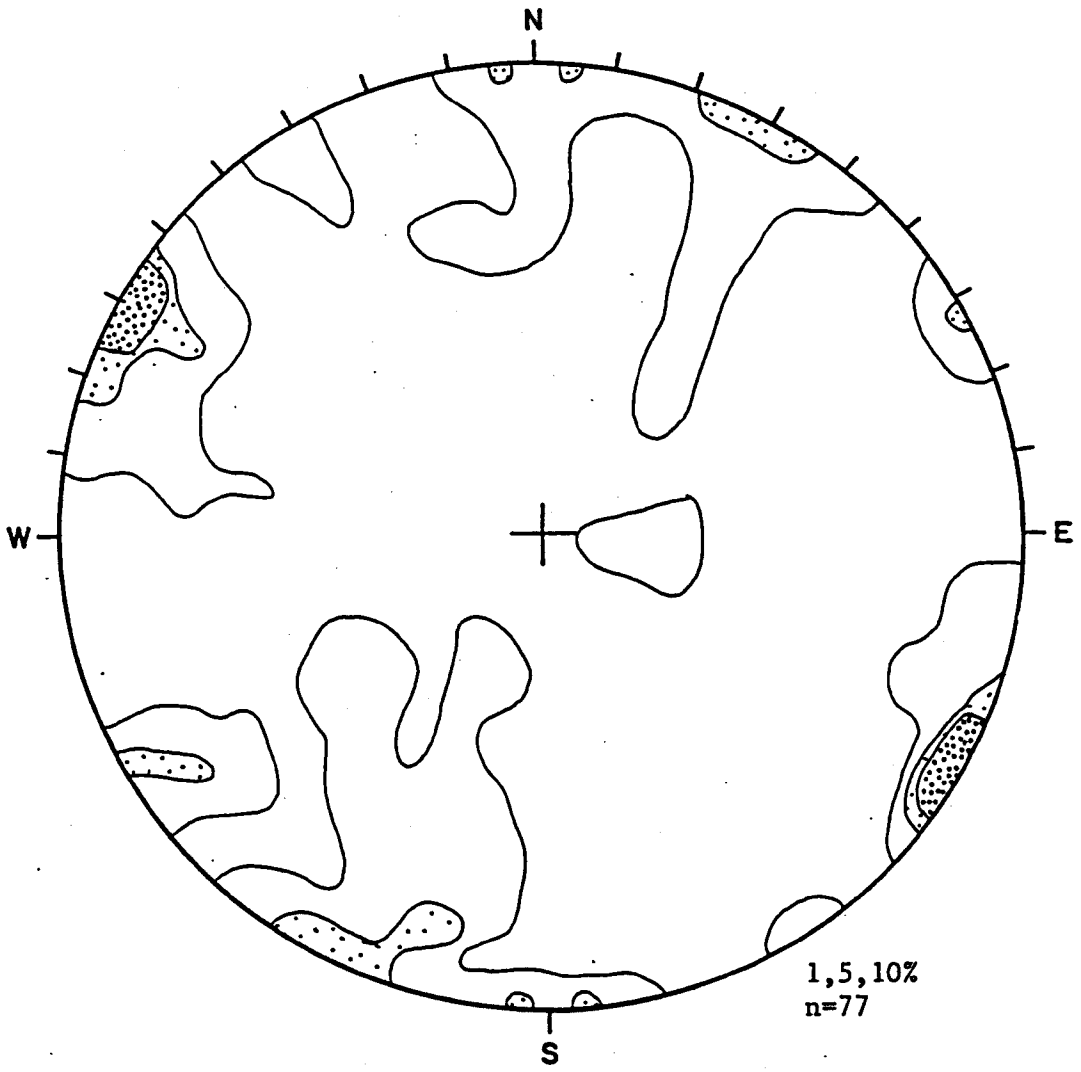

Figure 54. Contoured equal area plot of poles to joint surfaces in the Sore Fingers Domain.

to 15 cm wide and spacing between veins varies from 2 to 5 meters. Similar orientation across the F_2 syncline in the sandstone indicates that the veins formed after folding.

Northeast-trending faults in the Sore Fingers area

Northeast-trending faults of several ages are present in the Sore Fingers area (Figure 55); because they have small separation and can not be correlated with structures of the main Paleozoic outcrop belt, they are all treated here. The oldest of these is cut by the Sore Fingers thrust and has been discussed above along with F_2 structures. Other northeast-trending faults cut low-angle faults associated with thrusting, but do not cut the East Sore Fingers Normal Fault in the Limestone Hills; the youngest faults postdate both thrusting and low-angle normal faulting.

South-vergent, low-angle faults

Four enigmatic low-angle faults with southward transport of the upper plate relative to their lower plate are present in the map area (Figure 56). The West Ridge Fault and fault H in the Golden Eagle Hill Domain (Figure 29) are interpreted to be part of an originally continuous fault surface belonging to this set. The surface is now arched on a northerly-trending axis, and intense brecciation along the West Ridge Fault is the result of reactivation of that fault discussed previously. This correlation is indicated by alignment of stratigraphic contacts in the upper plate, and by the presence of similar south-dipping reverse faults in the lower plate.

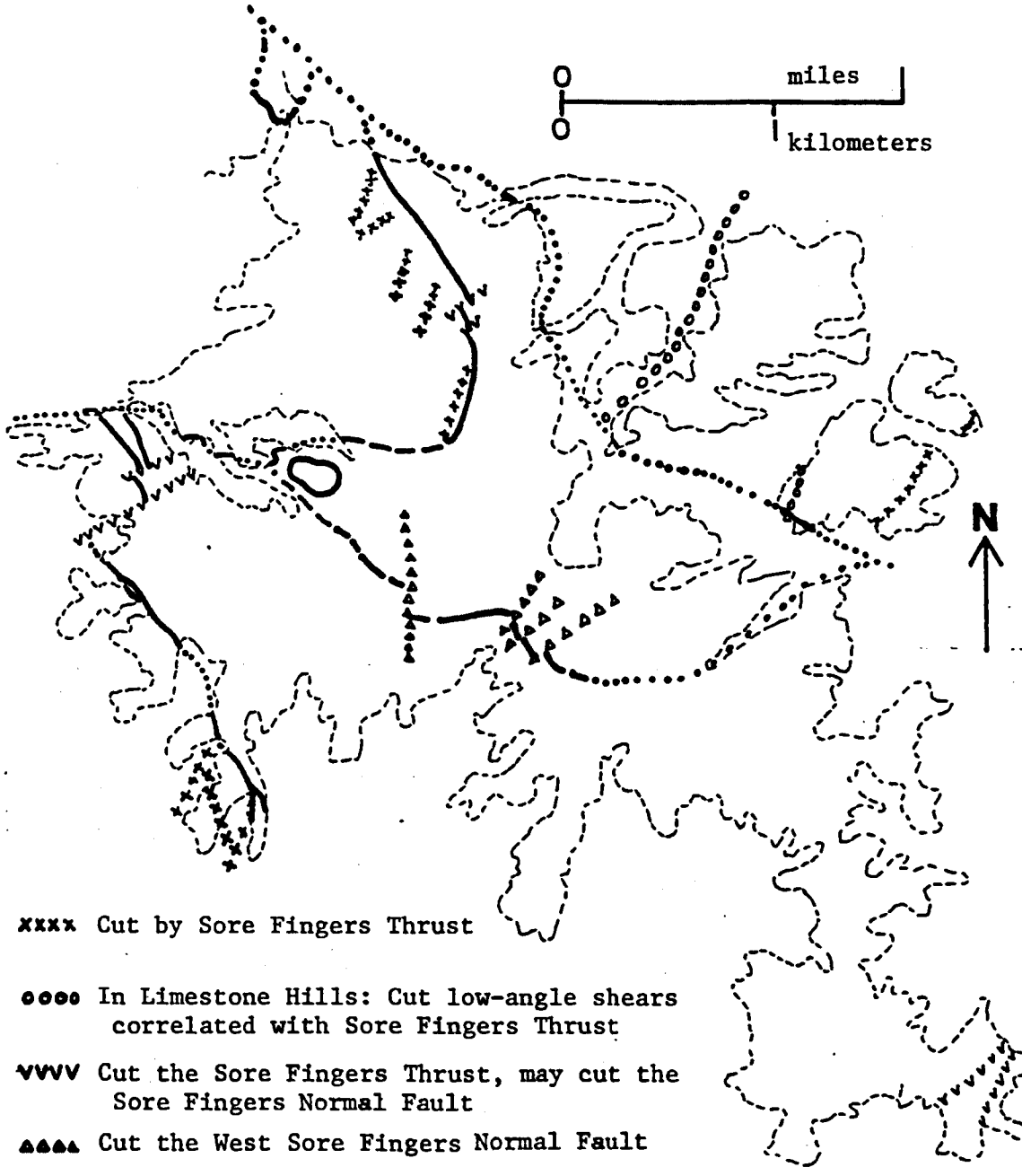

Figure 55. Northeast-trending faults in the Sore Fingers area.

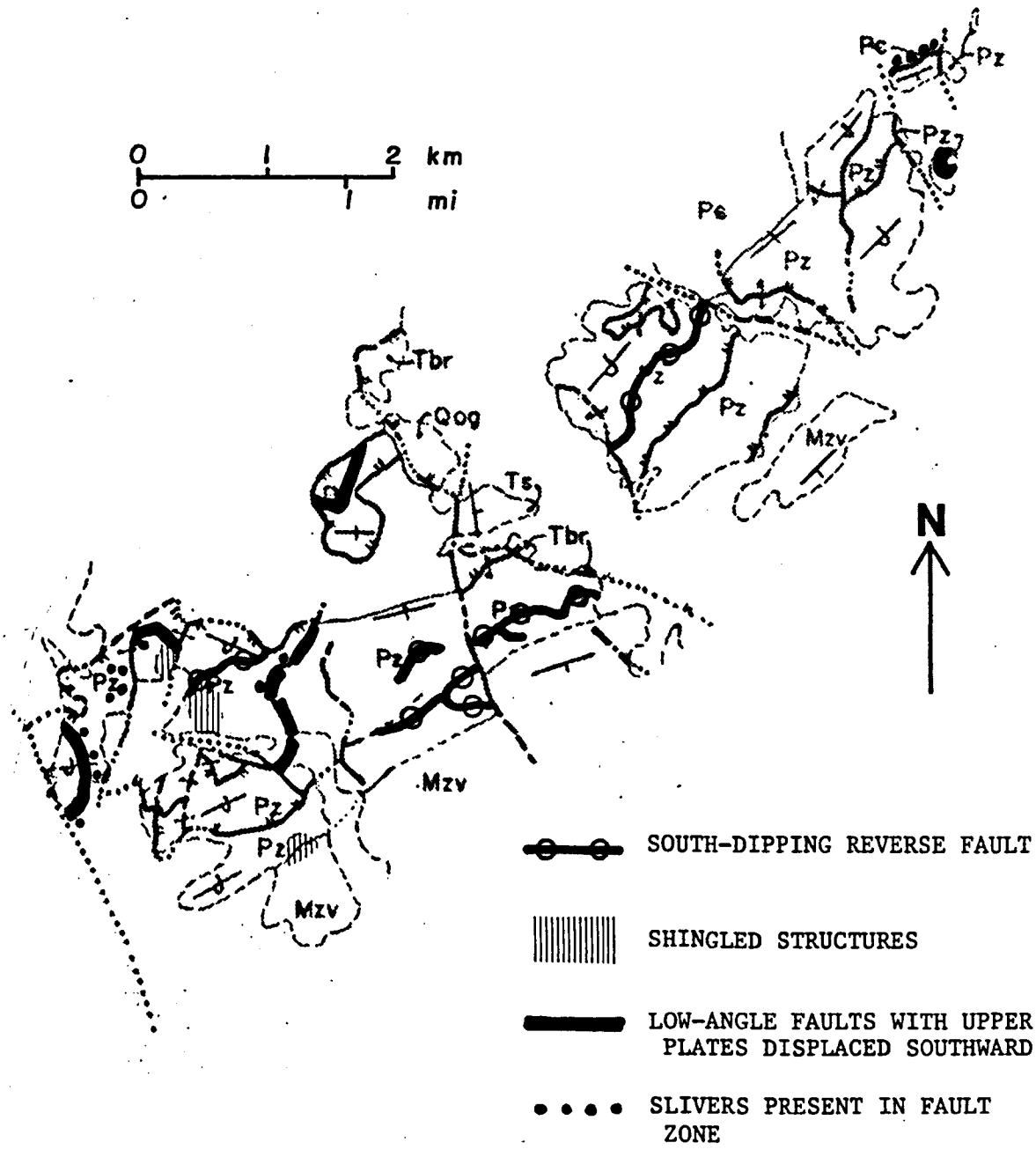

Figure 56. South-dipping reverse faults and minor structures in the main Paleozoic outcrop belt.

Table 12 CHRONOLOGY OF FAULTS

	Sore Fingers Domain	Sore Fingers West Domain	Limestone Hills Domain	Martin Peak Domain	Needle Domain	Elbow Hill Domain	Golden Eagle Hill Domain	Mixmaster Hill Domain	Corral Hill Domain	Split Mountain Domain
MESOZOIC										
Northeast-Trending high-angle faults		A(?), B	A set		Q set					
Thrust Faults	Sore Fingers D	Thrust	B set							
MESOZOIC or CENOZOIC										
South-dipping reverse faults				I,G(?)	E,F,G,I,J, K,L,M		A,G,B(?)	A	E	
Low-angle faults, upper plate to south						B	C,H,west Ridge Faults			
Northwest-dipping normal faults				A,B,F	O	Elbow Hill Fault	Golden Eagle Fault	C,G,J,H,	A,B,C	B,E,G,H,I L,M
Tear faults associated with northwest-dipping normal faults				E(?)	D(?)		D,I Northern Boundary Fault	D,E,F,K	D	C
MIDDLE TERTIARY(?)										
Northeast-dipping low-angle normal faults	East and West Sore Fingers Low-angle Normal Faults				Breccia Fault					
LATE TERTIARY										
High-angle Normal faults	G(?)		C set(?)	E(?),H Hovatter Road Fault	Needle Fault (Dip Slip)					Northeast Hills Fault I,O,Q

Table 13. CHARACTERISTICS OF FAULT SETS

FAULT SET	CHARACTER	ATTITUDE	NOTES
Thrust Faults	cleavage developed along fault	present dips 20° - 70° strike variable	
South-dipping reverse faults	generally sharp contact, minor or no breccia	dip 30-50°. Near vertical on W. Needle Ridge. East to northeast strike	
Low-angle faults upper plate to south	slight Brecciation silicified breccia on Elbow Hill and Split Mountain Domain Faults	strike variable, dip 10-37°, West Ridge fault arched	
Northwest-dipping normal faults	generally sharp, local transposition in limestones, brecciation in other places particularly in Coconino. Associated north- to northwest-trending faults are highly brecciated	Northwest dip at 10-40°. Elbow Hill and Mixmaster Hill Fault become steeper to SE. Arched in Northeast Hills	Associated with north to northwest-trending tear faults
Northeast-dipping low-angle normal faults	crushing of rock along fault	northeast trend, gentle east dips	northeast-trending tear zones linking faults are not exposed
High-angle normal faults	generally poorly exposed; brecciated	north-trending, 60° to vertical	

The klippe of Redwall and Martin Formations above fault N in the Split Mountain Domain (Figure 33) has been transported a minimum of 630 meters to the south, the greatest separation on any fault of this set. Stratigraphic facing of upper plate strata is opposite to that observed throughout the area; the younger Redwall Limestone lies north of the Martin Formation requiring greater than 90° of overturning.

Complex fault zones

A number of faults in the Golden Eagle Hill-Mixmaster Hill area are characterized by the presence of thin lenses of various stratigraphic units within the fault zones (Figures 5 and 56). The shingled structures mentioned in the discussion of the south-dipping reverse faults are an extreme case of this phenomena. Scrambling of stratigraphic units may be the result of thinning of structural plates between converging fault zones, or of repeated movement in a fault zone on slightly different planes with variable transport directions.

Table 12 presents a summary of relative chronology of fault systems in the map area, ennumerating the faults included in each set, and Table 13 summarizes the characteristics of faults in each set.

Kinematics

Superimposed multiple deformation of brittle rocks makes interpretation of kinematics in the southern Little Harquahala Mountains difficult. Minor folds are not common, and the carbonate

rocks are not susceptible to development of slickenside striations; crushing of rock is the most common mesoscopic to microscopic reflection of deformation. Minor fold data will be discussed first to indicate some of the difficulties in interpretation, followed by a chronologic discussion paralleling the synthesis of the last section.

Orientations of minor folds in the southern Little Harquahala Mountains are highly variable (Figure 57). This is due to the presence of several types of folds with different origins and to the effects of superimposed deformation. Fold types observed include: 1) assymetric folds in the Abrigo Formation; 2) broad open to moderately appressed folds in the Martin Formation; 3) drag folds along faults; 4) isoclinal folds in partially transposed limestone units; and 5) chevron folds in the Coconino Sandstone. As discussed in the last section, incipient transposition is related to development of foliation. Because axes of asymetric folds in the Abrigo Formation have east-northeast to east-southeast trends similar to axes of transposition folds (Figure 58), they are interpreted to have formed in connection with foliation development. East to southeast-trending axes of these folds suggests a north-south to northeast-southwest transport direction for faulting associated with the cleavage development, but conflicting assymetry does not allow the direction of transport to be determined. Other transpostion fold axes and drag fold axes trend northeast-southwest; these are associated with northwest-dipping normal faults and suggest northwest transport on these structures.

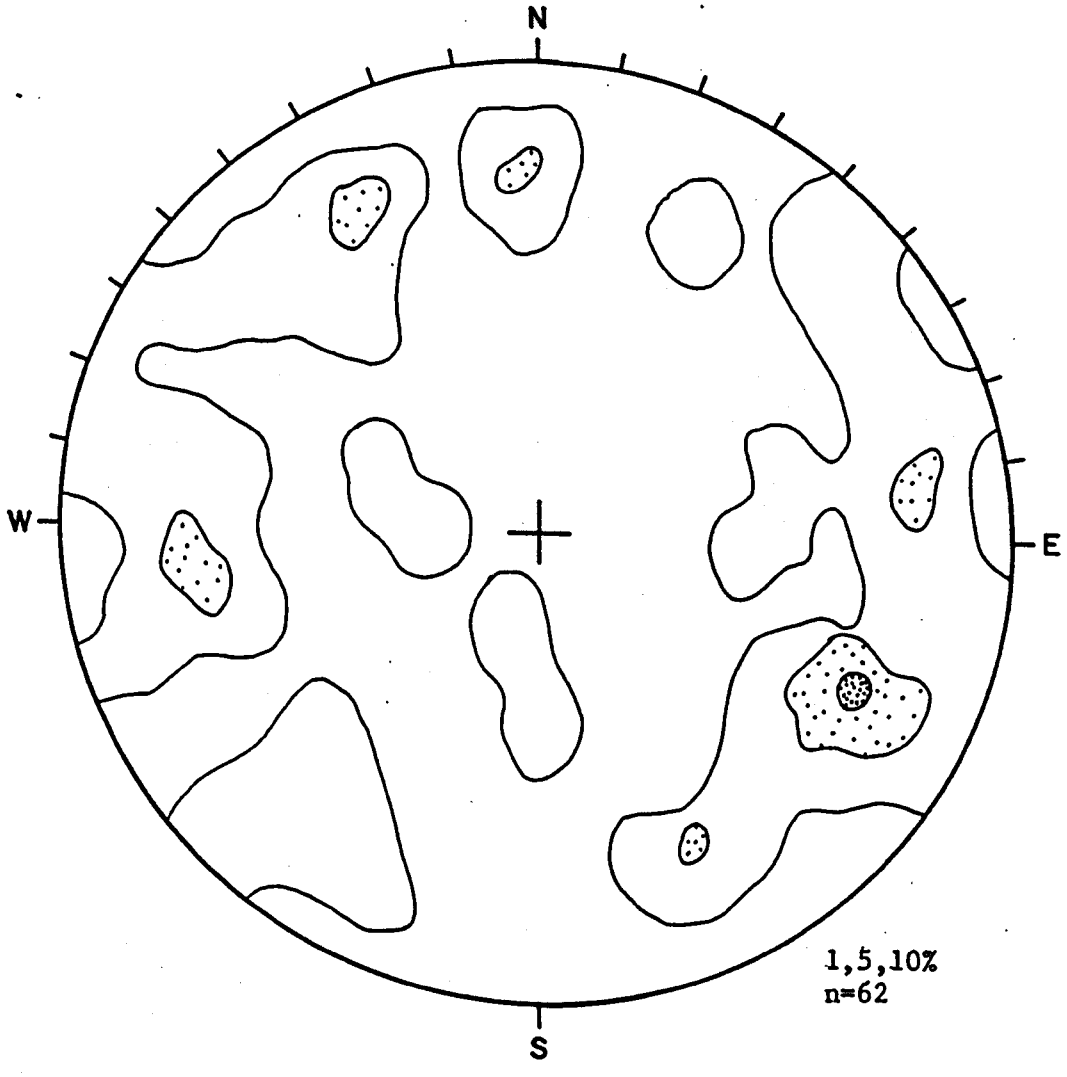

Figure 57. Contoured Equal Area plot of Minor Fold Axes

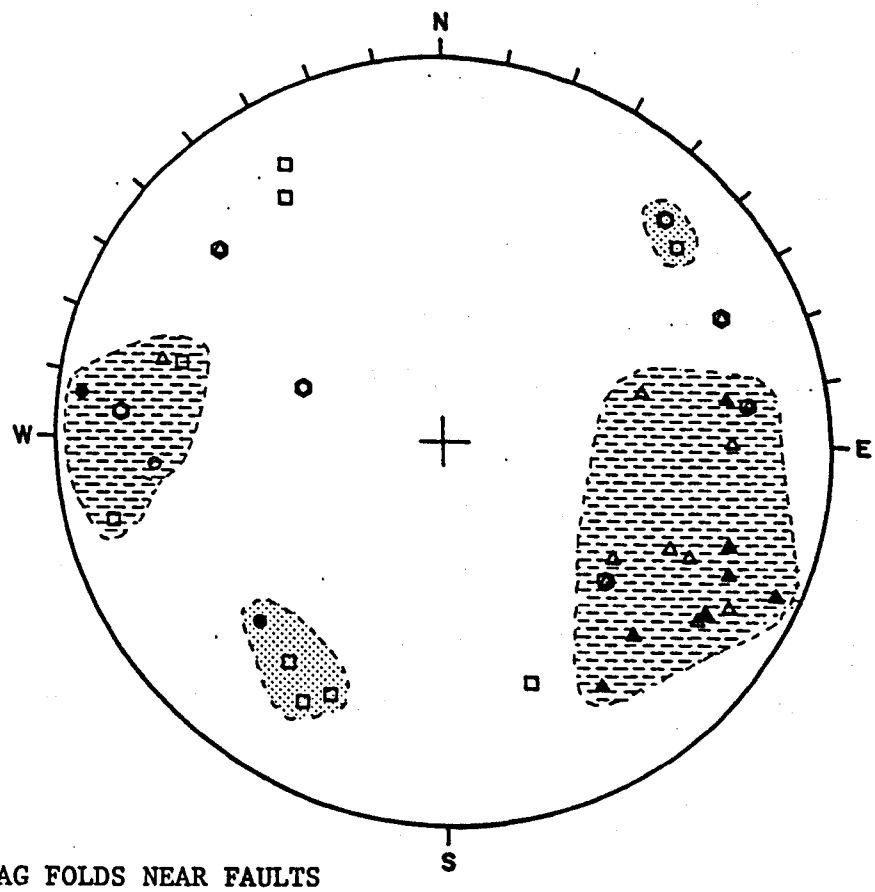

□ DRAG FOLDS NEAR FAULTS

△ FOLDS IN THE ABRIGO FORMATION
○ FOLD AXES RELATED TO INCIPIENT TRANSPOSITION

} OPEN SYMBOL- 'Z' FOLD
SOLID SYMBOL-'S' FOLD

⬡ SUPERIMPOSED ON OTHER SYMBOLS IF ASYMMETRY COULD NOT BE DETERMINED

Figure 58. Selected Minor Fold Axes.

The kinematics of deformation before deposition of the Apache Wash Formation cannot be determined due to the absence of associated structures. The presence of basement clasts in the Mesozoic sandstone unit suggests significant uplift, and probable high-angle faulting. Only one clast of possible basement derivation was observed in the lower member of the Apache Wash Formation. Predominance of upper Paleozoic and volcanic clasts indicates only minor uplift during pre-Apache Wash deformation.

Consistent northeast strike of strata in the Black Mesa area of the southern Plomosa, Little Harquahala and western Harquahala Mountains (Figure 7) reflects the northeast trend of large scale F_1 folds. Northwest-dipping overturned strata indicate a southeast vergence for the folds.

The steep axes of F_2 folds suggest that the folds were formed by drag in a sub-vertical shear zone. Two models are possible to explain the folds: northwest-trending right shear and northeast-trending right shear (Figure 59). The first model would require that the Martin Peak and Needle F_2 folds are separate. This hypothesis eliminates the need for a large vertical F_1 fold limb above the hinge on Martin Peak mentioned in the section on the northeast-dipping normal faults. However, the absence of the fold hinge connecting these two folds cannot be explained using any of the known structures in the area. The second model, with northeast-trending shear zones is

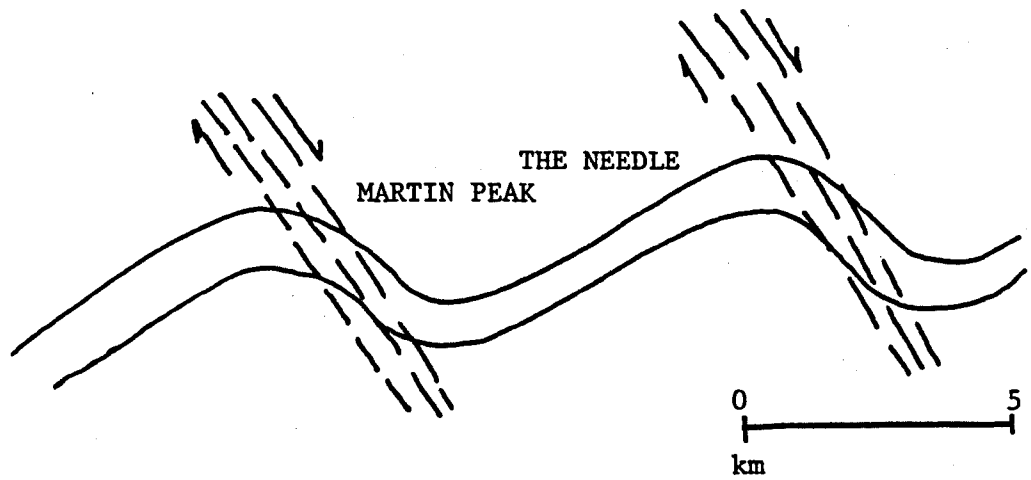

MODEL 1: Northwesterly-trending right-shear zones

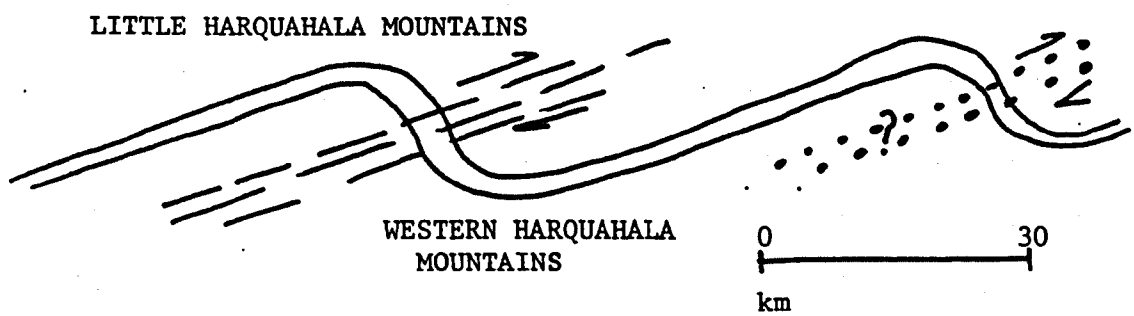

MODEL 2: Northeasterly-trending right-shear zones spaced at wider intervals

Figure 59. Models for F_2 development

preferred and will be used in the remainder of this chapter. In this hypothesis, one large-scale drag fold was formed along a north- to northeast-trending shear zone. The overall effect of right shear across the zone was to juxtapose rocks of the Sore Fingers Assemblage against the sedimentary rocks of the southern Little Harquahala Mountains. Minor faults in this zone are present at the southeast end of the northwest-striking limbs of F_2 folds. This model predicts that Paleozoic rocks to the east of the map area may be deposited on rocks of the Sore Fingers Assemblage.

No kinematic data were collected in the map area to constrain the transport direction on the Hercules thrust. Reconnaissance in other nearby areas has failed to yield conclusive results as well. The distance of transport on the fault is also unknown, but the difference in Mesozoic strata in the upper and lower plates suggests significant horizontal transport.

Interpretation of the Sore Fingers thrust is equally difficult. If the fault does cut across an older north- to northeast-trending shear zone, as proposed in the thrust faults and foliation section, then transport on the fault must have some component across the older fault zone, suggesting a transport direction lying between northeast and south. If the thrust is itself a major structure juxtaposing the rocks of the southern Little Harquahala Mountains against the Sore Fingers Assemblage this argument is not valid. The apparent association of east-southeast- to east-northeast-trending

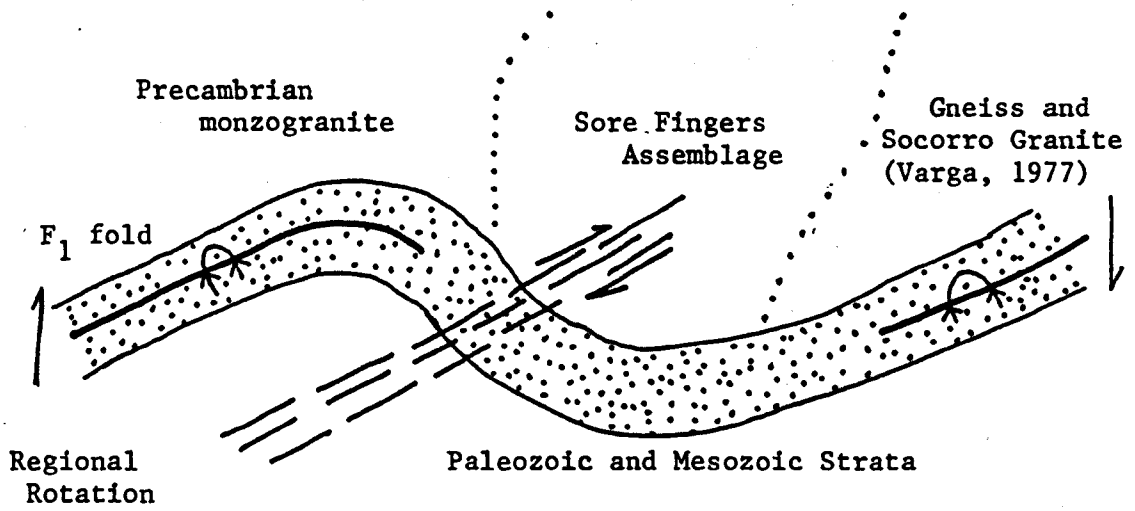

PHASE 1: INITIATION OF F_2 FOLDING

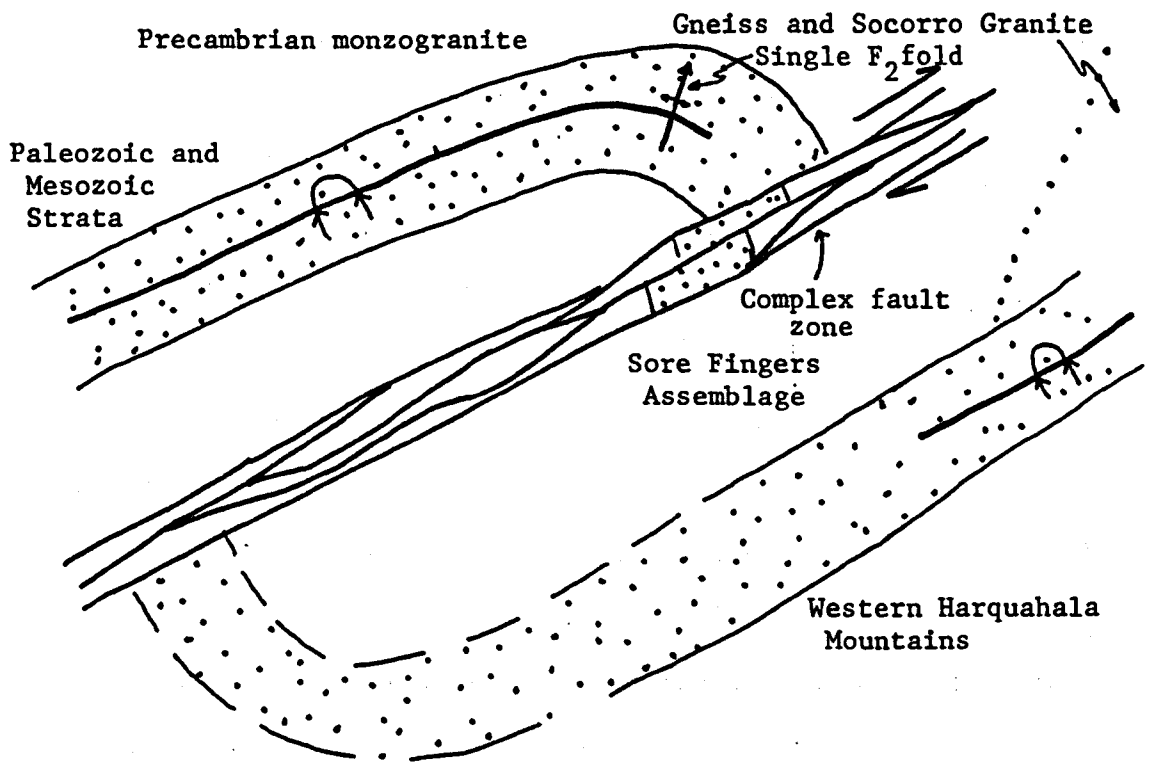

PHASE 2: F_2 FOLD BREACHED BY A LARGE STRIKE-SLIP FAULT ZONE

Figure 60. Evolution of F_2 structures.

fold axes with foliations noted at the beginning of this section suggests northerly transport on faults related to the foliation-forming event.

The southward-dipping reverse faults are the result of minor shortening in a direction perpendicular to the strike of bedding. The variable attitudes and poor exposure of low-angle faults with upper plates transported south makes interpretation difficult. The age and significance of these two sets of structures are problematic.

Northwest-dipping normal faults are associated with north- and north-west-striking tear structures, indicating transport to the north and northwest. On Mixmaster Hill the north-trending brecciated faults post-date the northwest-trending tear faults (Figure 50). The Golden Eagle Fault and Mixmaster Hill Faults thus bound a plate which was translated to the northwest and then to the north. Displacement on this fault system dies out to the northeast, and disappears in the Coconino Sandstone west of the Needle. Stratigraphic separation across the Elbow Hill Fault and across the imbricate faults on Corral Hill and on Split Mountain also indicates normal faulting with northerly transport of the upper plates.

An alternate explanation of these northwest-dipping normal separation faults is that they are thrust faults which have been rotated from flat or southerly dips to their present northwest dip. These faults would correlate with similar minor thrust faults in the western Harquahala Mountains (Keith and others, 1981). Apparent

northwest to north transport direction is more consistent with northerly transport direction indicated for late Cretaceous thrust faults in the western Harquahala Mountains (Reynolds, 1982), than with regional northeast extension indicated by southwest-dipping mid-Tertiary strata in the area (Rehrig and Reynolds, 1980; Rehrig, Shafiqullan and Damon, 1980; Scarborough and Wilt, 1979). A thrust interpretation requires post-thrust northwest tilting of the faults. The northest-trending arch which now forms the Harquahala Mountains (Reynolds, 1980) provides a possible means of achieving this tilting, but independent evidence for extension of the arch into the Little Harquahala Mountains is presently lacking. Also, the present south and southeast dip of the Hercules thrust in the area is not consistent with rotation to the northwest. Flattening of the Mixmaster Hill fault and the Elbow Hill fault to the northwest (cross sections D-D' and C-C' on Figure 6) and the convergence to the northwest of Faults A and B on Corral Hill (cross section G-G' on Figure 6) and Faults C and M on Mixmaster Hill (cross section C-C' on Figure 6) are more consistent with normal fault geometries than with thrust fault geometries. In addition, the association of the highly brecciated north-trending faults with the normal faults, and local brecciation along the faults themselves is more characteristic of Tertiary structures than Mesozoic thrusts. It should be noted that metamorphic grade decreases from the western Harquahala Mountains southwest to the Little Harquahala Mountains. Mylonitic fabric along thrust faults in the western Harquahala Mountains may give way to more brittle fabrics

in the Little Harquahala Mountains. In summary, data from the map area do not conclusively define the kinematics of the northwest-dipping faults. They are interpreted as normal faults based on normal separation observed in the field, geometry of the faults, and brecciation associated with the faults.

Northeastward transport on northeast-dipping low-angle faults is indicated by correlation of structures and stratigraphic markers. The overall effect of this fault system has been to repeat the highly-disrupted F_2 fold three times across the area: on Martin Peak, in the Needle area and on the Northeast Hills block above the East Sore Finger Normal Fault (Figure 61 and 62). Northeast extension in the map area is supported by northwest-trending minor normal faults in rocks of the main Paleozoic outcrop belt (Figure 63).

As previously mentioned, some strike-slip on the Needle fault preceded movement on the Elbow Hill and Breccia faults. Strike-slip on faults of the Needle set is similar to regional patterns of northwest-trending strike- and dip-slip faults. Opposite separation on the Northeast Hills Fault may indicate that it is older than other faults of the set as in the southern Plomosa Mountains (Miller, 1970). Alternatively, the Northeast Hills fault may be a complementary fault in a north-northwest trending right shear system.

Kinematic history of the southern Little Harquahala Mountains includes: 1) northwest-southeast compression (F_1); 2) north-to northeast-trending right shear (F_2); 3) compression (thrust faults); 4) northeast-trending right and left shear (early strike

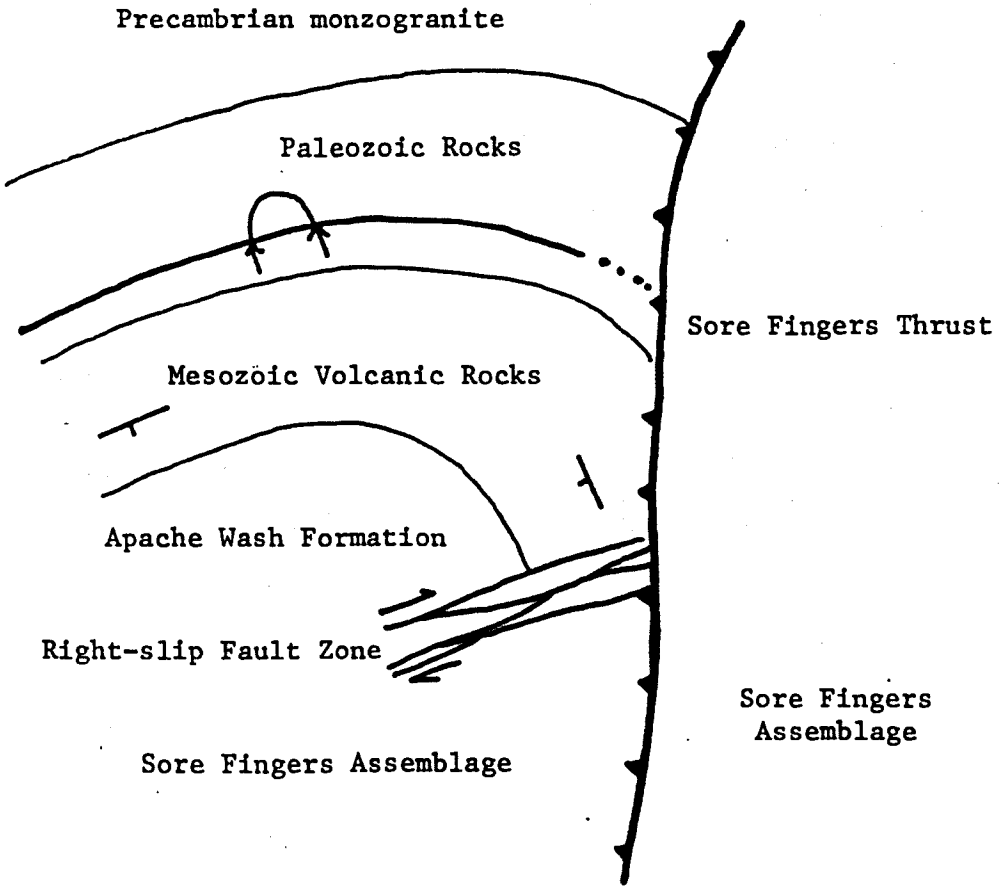

Figure 61. Paleogeologic Map, after Sore Fingers Thrusting

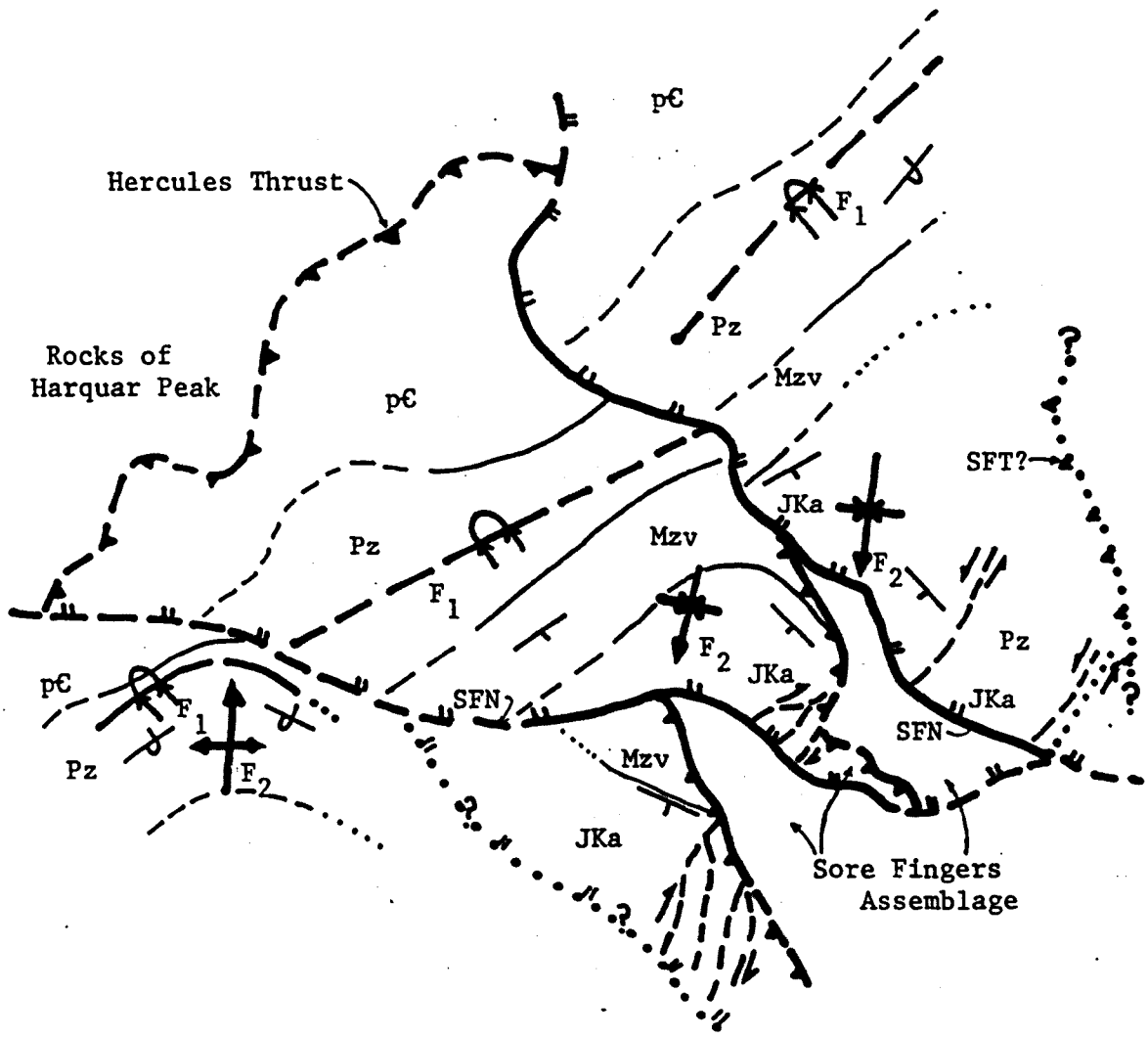

Figure 62. Paleogeologic Map, after northeast-dipping normal faulting

Northwest-dipping normal faults and Needle fault set omitted. Key to abbreviations: F_1--Early fold set; F_2--Refolding axes; SFN--Sore Fingers normal faults; SFT--Sore Fingers thrust; pC--Precambrian rocks; Pz--Paleozoic rocks; Mzv--Mesozoic volcanic rocks; JKa--Apache Wash Formation

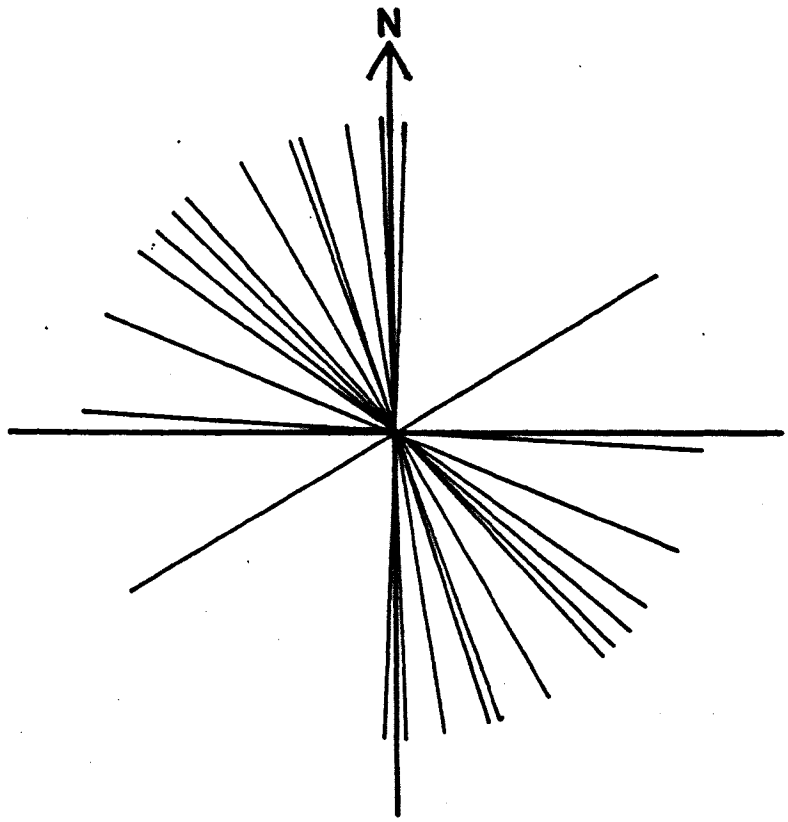

Figure 63. Strike lines of minor normal faults in Paleozoic rocks

slip, Needle fault set); 5) northwest-southeast extension(?) (northwest-dipping normal faults); 6) northeast-southwest extension (northeast-dipping low-angle normal faults, late dip-slip on Needle Fault set).

TECTONICS

In this chapter, observations from the southern Little Harquahala Mountains and known regional relations are integrated to generate a geologic history of the area. Early to middle(?) Proterozoic volcanic and sedimentary rocks were metamorphosed and intruded by granitic plutons between about 1.7 and 1.4 billion years before present. These rocks were uplifted and eroded to provide a basement upon which Paleozoic sediments were deposited in a cratonic platform setting similar to that in central Arizona (Peirce, 1976). Paleozoic stratigraphy was not studied in sufficient detail to correlate with specific sections in southeast Arizona or on the Colorado Plateau. The thinness of the total section, only 1000 meters, indicates the rocks were deposited on an extension of a persistent positive element that crosses Arizona from northeast to southwest (Peirce, 1976). The transition between Paleozoic facies of northern and southern Arizona generally takes place across this element. Similarity of parts of the Little Harquahala Paleozoic section to both the Grand Canyon section and the southeast Arizona section is also consistent with deposition on this positive element. These relations indicate that Paleozoic rocks of the Little Harquahala Mountains probably have not been transported more than about 100 km in a northwest or southeast direction from their original site of deposition relative to the Colorado Plateau.

Early and middle Mesozoic tectonics were dominated by uplift and volcanism. Exposure of crystalline rocks in the source area of the Mesozoic sandstone indicates the onset of Mesozoic tectonism in Arizona. The Mogollon Highland, a northwest-trending uplift in central Arizona, has been recognized as a source area for Triassic and Jurassic strata on the Colorado Plateau (Cooley and Davidson, 1963; Harshbarger, Repenning and Irwin, 1957; Stewart, Poole and Wilson, 1972). This highland probably formed a divide separating depocenters in northern and southern Arizona and was the source area for the Mesozoic sandstone.

Volcanic rocks in the Little Harquahala Mountains are interpreted to be part of the Jurassic magmatic arc in Arizona. Dated volcanic rocks occurring in similar stratigraphic and structural settings in south-central Arizona have ages between 190 and 140 m.y. (compilation by Kluth, 1982). West of the Little Harquahala Mountains, the McCoy Mountains Formation (Pelka, 1973; Harding, 1982) unconformably overlies hypabyssal rhyodacite porphyry which has yielded a plagioclase K-Ar age of 175.8 ± 2.7 m.y. (Pelka, 1973). The porphyry is lithologically similar to the upper volcanic unit in the study area. Based on this date the volcanic rocks of the Little Harquahala Mountains are believed to be Early to Middle Jurassic in age.

Coarse clastic rocks overlie Jurassic volcanic rocks throughout southern Arizona and southeastern California (Bilodeau, 1978; Harding, 1978, 1982; Haxel and others, 1980; Kluth, 1982;

Miller, 1966), indicating that arc activity was followed by a period of uplift and erosion. Complex stratigraphic relations at the base of the Apache Wash Formation in the Little Harquahala Mountains are probably a result of this same event. Sediments in the transition zone between the Mesozoic epiclastic sediments and the Apache Wash Formation become fine-grained to the southeast, and the percentage of Paleozoic limestone clasts in Apache Wash conglomerates increases toward the northeast of present outcrop distribution. However, in order to determine original distribution of facies, the various superimposed folds and faults must be reconstructed. The coarser transitional sediments lie to the northeast after unfolding F_2 folds, indicating the uplifted source of these rocks lay in that direction. Assuming that the present distribution of conglomerate is due to repetition of an originally near continuous conglomerate sheet by northeast-dipping low-angle normal faults as discussed in the Kinematics section, limestone-rich conglomerates lie relatively northwest of volcanic rich conglomerates after reconstruction. This suggests interfingering of sediments derived from Paleozoic rocks to the north and from an arc terrane to the south. Presence of a single fining-upward sequence suggests one uplift event, followed by a period of erosion.

Since the exact age of conglomerates overlying the volcanic rocks in various places in Arizona is poorly constrained, the timing and interrelation of faulting throughout the region is uncertain. Clastic sequences included in the Bisbee Group and Sand Wells

Formation overlie middle to upper Jurassic volcanic and plutonic rocks in south-central Arizona (Haxel and others, 1980; Kluth, 1982). Gross stratigraphic similarity between these sequences and the Apache Wash Formation suggest that these units were deposited in a similar tectonic setting. Bilodeau (1978) has proposed that deposition of the Glance conglomerate was initiated by normal faulting in an extensional environment. The Apache Wash Formation may have been deposited in a similar environment.

Harding (1982) has interpreted the Apache Wash Formation to be a lateral equivalent of some or all of the McCoy Mountains Formation. Paleomagnetic evidence from the McCoy and Dome Rock Mountains can be interpreted to suggest that rocks of the McCoy Mountains Formation were subjected to a Callovian metamorphic event (Harding, Coney and Butler, 1980, 1982). The basin in which the McCoy Mountains Formations was deposited is interpreted to be an intra-arc rhombochasm, (Harding, 1982) formed in a transtensional environment at the intersection of a large-scale intracontinental left-slip transform, the Mojave-Sonora Megashear (Anderson and Silver, 1979) and the Jurassic volcanic arc (Dickinson, 1981). The McCoy Mountains Formation is probably older than the late Jurassic to early Cretaceous age accepted for the initiation of upper Mesozoic clastic deposition in southeast Arizona (Kluth, 1982; Drewes, 1981). Events accompanying termination of arc activity in Arizona and inception of the new arc further to the west apparently include a period of strike-slip and normal faulting which shortly followed the magmatic activity. This

transition may have been diachronous, occuring earlier in the Colorado River region than in southeast Arizona, and causing the timing discrepancy between the two areas. More data are required to clarify the relationship between the various clastic units deposited during this period and to determine their tectonic setting.

The age of the large-scale, southeast vergent recumbent fold is poorly constrained. Varga (1977) presented a model for the western Harquahala Mountains wherein the Socorro Granite intruded to the base of the Paleozoic section in mid-Tertiary time. He proposed that the resulting uplift led to formation of large-scale cascade folds by gravitational transport to the southeast. More recent work (Reynolds, Keith and Coney, 1980; Keith and others, 1981) in the western Harquahala Mountains and mapping described in this report makes this hypothesis untenable. The Bolsa Quartzite is in depositional or fault contact with underlying granitic rocks throughout the area. The Harquahala thrust cuts overturned Paleozoic strata and is intruded by Eocene or older muscovite granite in the Harquahala Mountains (Reynolds, Keith and Coney, 1980; Reynolds, 1982). In the Little Harquahala Mountains, Mesozoic volcanic rocks and the Apache Wash Formation are involved in the folding that overturned the Paleozoic section. The age of folding is thus constrained between Jurassic and early Tertiary.

A band of generally southwest- to south-vergent structures bounds the McCoy Mountains Basin on the north, separating Paleozoic and Mesozoic rocks which can be correlated with strata of the North

American Craton from rocks of the McCoy Mountains Formtion whose only correlation with North American Paleozoic sections is via the allochthonous and possibly younger Apache Wash Formation (Harding, 1982). This belt of deformation is continuous into the Little Harquahala and Harquahala Mountains. The Hercules thrust juxtaposes North American Paleozoic rocks with the Rocks of Harquar Peak, which are herein correlated with the McCoy Mountains Formation; the thrust is thus analogous to the fault zone bounding the McCoy Basin on the north. Large-scale folds are present in Paleozoic rocks above this fault zone in southeast California (Harding, 1982; Krummenacher et al., 1981; Emerson, 1982; Leveque, 1982) suggesting that the early southeast-vergent folds in the western Harquahala Mountains are a result of the same event which culminated in southward thrusting along the northern boundary of the McCoy basin. Right shear on the scale indicated by F_2 folds has not been observed in areas adjacent to the Little Harquahala Mountains, suggesting that the folds are local phenomena. Kinematic indicators from the western Harquahala Mountains (Keith and others, 1981; Reynolds, 1982) indicate transport to the north on the Harquahala thrust which truncates the large-scale, southeast-vergent fold (Reynolds, Keith and Coney, 1980). It is possible that the Harquahala thrust is a younger structure than the Hercules thrust and has a radically different history. Similarity of structural position suggests that the Sore Fingers thrust fault and foliations in the southern Little Harquahala Mountains are related to the Golden Eagle thrust as it is recognized in the western Harquahala

Mountains (Keith and others, 1981). Similar orientation of foliation throughout the map area is consistent with fabric development during or after Hercules thrust development. The cleavage is clearly older than the microdiorite dikes that cut it. These are probably 22 to 28 m.y. old based on correlation with similar dated dikes in the Harquahala Mountains (Shafiqullah and others, 1980).

In summary, superposed Mesozoic thrust events are probably present in the Little Harquahala Mountains area, but data from within the map area do not definitively constrain the relation between the various faults. The timing of F_2 development, after the early southeast-vergent folds and before development of the Sore Fingers thrust, is not consistent with a genetic relationship between F_1 folding and thrusting unless an oblique convergence component was introduced between the two structural events. It thus seems probable that the F_1 fold and Sore Fingers thrust are unrelated. South-dipping reverse faults and low-angle faults with southward transport of upper plates (Figure 56) are difficult to place in a regional picture. Transposition fabrics present along south-dipping reverse faults are similar to other foliations in the area, suggesting that these faults may be minor structures related to the Sore Fingers thrust.

The northwest-dipping normal separation faults are significant structures within the southern Little Harquahala Mountains, but have not been described in other nearby areas. As discussed in the kinematics section, they either represent a deformation unique to the Little Harquahala Mountains, or they may be related to one of the

thrust faults. The northeast-trending Harquahala and Harcuvar Mountains are truncated at a lineament trending northwest along the Eagle Tail, the Little Harquahala, and the Granite Wash Mountains. This feature may be the physiographic expression of a major structural boundary. Local irregularities in this boundary region may be responsible for the unusual orientation of low-angle normal faults in the Little Harquahala Mountains. Thus the faults may be late Mesozoic or Middle Tertiary in age.

Northwest- and north-northwest-trending strike- and dip-slip faults are present in the Plomosa and Dome Rock Mountains (Miller, 1970; Crowl, 1979). In the Quartzite Quadrangle, northwest-trending left separation faults cut Tertiary volcanic units dated at 19.1 and 20.2 m.y. (K-Ar, biotite, Miller and McKee, 1971) and are cut by north-northwest-trending right separation faults. These relations suggest that the northwest-trending Northeast Hills fault may be older than the more northerly-trending Hovatter Road and Needle fault. Right separation between northeast-trending Paleozoic and Mesozoic outcrop belts north of Black Mesa in the southern Plomosa Mountains and the Little Harquahala Mountains is attributed to northwest-trending strike- or oblique-slip faults (Figure 7). The northwest trending oblique-slip faults that are present in the Harquahala Mountains (Reynolds, 1982), may be part of this fault system as well.

Poorly exposed northwest-trending low-angle normal faults are similar in orientation to the Bullard Detachment (Reynolds, 1982) in the northeast Harquahala Mountains and to a detachment fault on the

east side of the Plomosa Mountains (Jemmett, 1966; Richard, unpublished reconnaissance, 1982). The faults in the Little Harquahala Mountains may represent minor intraplate extension related to mid-Tertiary low-angle normal faulting.

Late dip-slip on the Needle fault is interpreted to be minor normal faulting related to the Basin and Range high-angle normal fault event which gave rise to the present physiography.

CONCLUSIONS

In summary, Paleozoic rocks in the Little Harquahala Mountains record shallow marine deposition on a broad positive element separating regions of greater subsidence in northwestern Arizona and southeastern Arizona. Mesozoic rocks record repeated uplift and volcanism related to growth of the Mogollon Highland, magmatism in the Jurassic Arc, and possible strike-slip on the Mojave-Sonora megashear. Late-Mesozoic compression resulted in large-scale southeast-vergent folding and possible thrusting and north-vergent thrusting which resulted in juxtaposition of Paleozoic and Mesozoic rocks deposited on the North American craton with Mesozoic rocks of the McCoy Mountains Formation. Earlier deformational events are obscured by Tertiary(?) northwest-dipping normal faults, northwesterly-trending oblique slip faults, and northeast-dipping low-angle normal faults. Although the general sequence of events is similar to adjacent areas, the Little Harquahala Mountains are characterized by more brittle deformation and a number of apparently unique structures.

REFERENCES

Anderson, T. M., and Silver, C. T., 1979, The role of the Mojave-Sonora Megashear in the tectonic evolution of northern Sonora, T. M. Anderson and J. Roldan-Quitana, eds., Geology of Northern Sonora: Geol. Soc. America Ann. Mtg. Field Trip Guide No. 27, p. 59-68.

Bilodeau, W. L., 1978, The Glance Conglomerate, a lower Cretaceous syntectonic deposit in southeastern Arizona, New Mexico Geological Society Guidebook, 29th Field Conference, p. 209-214.

Bilodeau, W. L. and Keith, Stanley B., 1979, Intercolated volcanics and eolian 'Aztec-Navajo-like' sandstones in southeast Arizona: another clue to the Jurassic-Traissic paleotectonic puzzle of the southwestern U.S., Geol. Soc. America Abstracts with program, Vol. 11, No. 3, p. 70.

Bryant, D. L., 1968, Diagnostic characteristics of the Paleozoic formations of Southeastern Arizona, Southern Arizona Guidebook III, Arizona Geol. Soc., p. 33-47.

Ciancanelli, E. V., 1965, Structural Geology of the western edge of the Granite Wash Mountains, Yuma County, Arizona, M.S. Thesis, University of Arizona, 70 p.

Cooley, M. E. and Davidson, E. W., 1963, The Mogollon Highlands - their influence on Mesozoic-Cenozoic erosion and sedimentation, Arizona Geol. Soc. Digest, Vol. VI, p. 7-36.

Crowl, W. J., 1979, Geology of the Central Dome Rock Mountains, Yuma County, Arizona, M.S. Thesis, University of Arizona, 76 p.

Darton, N. M., et. al., 1924, Geologic map of the State of Arizona, 1:500,000, University of Arizona, Ariz. Bur. Mines and U. S. Geol. Survey.

Davis, G. A., Anderson, J. L., Frost, E. G., Shackelford, T. J., 1980, Ionitization and detachment faulting in the Whipple-Buckskin-Rawhide Mountains terrane, Southeastern California and Western Arizona, Geol. Soc. America, Memoir 153, p. 79-129.

DeSitter, L. V., 1964, Structural Geology, 2nd Ed., McGraw-Hill, New York, 551 p.

Dickinson, W. R., 1981, Plate tectonic evolution of the Southern Cordillera, W. R. Dickinson and W. D. Payne, editors, Relations of Tectonics to Ore Deposits in the Southern Cordillera, Arizona, Geol. Soc. Digest, Vol. XIV, p. 113-136.

Dickinson, W. R. and Suczek, C. A., 1979, Plate Tectonics and Sandstone Compositions, American Assoc. of Petrol. Geol. Bull., V. 63, No. 12, p. 2164-2182.

Drewes, Harold, 1981, Tectonics of Southeast Arizona, U. S. Geol. Survey Professional Paper 1144, 96 p.

Eberly, L. D. and Stanley, T. D., Jr., 1978, Cenozoic stratigraphy and geologic history of southwestern Arizona, Geol. Soc. America, Bull. Vol. 89, p. 921-940.

Emerson, W. S., 1982, Geological development and late Mesozic deformation of the Little Maria Mountains, Riverside County, California, E. G. Frost and D. L. Martin, eds., Mexozoic-Cenozoic Tectonic Evolution of the Colorado River Region, California, Arizona and Nevada, Cordilleran Publishers, San Diego, p. 245-255.

Fisher, R. V., 1961, Proposed classification of volcaniclastic sediments and rocks, Geol. Soc. America Bull., Vol. 72, p. 1409-1414.

Frost, E. G., and Martin, D. L., 1982. Comparison of Mesozoic compressional tectonics with mid-Tertiary detachment faulting in the Colorado River area, California, Arizona and Nevada, in Guidebook, Geologic Excursions in the California Desert, 78th Ann. Meeting, Cordilleran Section, Geol. Soc. America, Anaheim, Ca, p. 113-158.

Grose, L. T., 1959, Structure and petrology of the northeast part of the Soda Mountains, San Bernardino County, California, Geol. Soc. America Bull., Vol. 70, p. 1509-1548.

Harding, L. E., 1978, Petrology and tectonic setting of the Livingston Hills Formation, Yuma County, Arizona, M. S. Thesis, University of Arizona, Tucson, 57 p.

Harding, L. E., 1980, Petrology and tectonic setting of the Livingston Hills Formation, Yuma County, Arizona, Arizona Geol. Soc. Digest, Vol. XII, p. 135-146.

Harding, L. E. 1982, Tectonic significance of the McCoy Mountains Formation, southeastern California and southwestern Arizona, Ph.D. Dissertation, University of Arizona, Tucson, Az.

Harding, L. E., Coney, P. J., and Butler, R. F., 1980, Paleomagnetic evidence for a Jurassic age assignment on a 6 km thick sedimentary terrane in southwestern Arizona and southeastern California, Geol. Soc. America, Abstracts with Program, Vol. 12, p. 109.

Harding, L. E., Coney, P. J. and Butler, R. F., 1982, Stratigraphy, sedimentary petrology, structure and paleomagnetism of the McCoy Mountains - Livingston Hills Formation, southeast California and southwest Arizona, Geol. Soc. America, Abstracts with Programs, Vol. 14, No. 4, p. 170.

Harshbarger, J. W., Repenning, C. A., and Irwin, J. M., 1957, Stratigraphy of the uppermost Triassic and Jurassic rocks of Navajo County, U. S. Geological Survey Professional Paper 291, 74 p.

Haxel, G., Wright, J. E., May, D. J., and Tosdal, R. M., 1980, Reconnaissance geology of the Mesozoic and lower Cenozoic rocks of the southern Papago Indian Reservation, Arizona: a preliminary report, Arizona Geol. Soc. Digest, Vol. XII, p. 17-30.

Jemmett, J. P., 1966, Geology of the Northern Plomosa Mountain Range, Yuma County, Arizona, Ph.D. Thesis, University of Arizona, Tucson, 128 p.

Keith, Stanley B., Reynolds, S. J., Rehrig, W. A., Richard, S. M., 1981, Low-angle tectonic phenomena between Tucson and Salome, Arizona, Arizona Bur. Geol. and Min. Tech., Open File Report 81-2, 114 p.

Kluth, C. F., 1982, The geology and mid-Mesozoic tectonics of the Northern Canelo Hills, Santa Cruz County, Arizona, Ph.D. Dissertation, University of Arizona, Tucson, Az.

Krummenacher, D., et al., 1981, Middle Mesozoic compressional tectonics and tertiary extensional overprint in the Big Maria, Little Maria, Riverside and Arica Mountains and Palen Pass areas

of Riverside County, California, Geol. Soc. America, Abstracts with programs, Vol. 13, p. 492.

Lee, W. T., 1908, Geological reconnaisance of a part of western Arizona with notes on the igneous rocks of Western Arizona by Albert Johannsen, U. S. Geological Survey Bulletin 352, p. 9-80.

Leveque, R. A., 1982, Stratigraphy and structure of the Palen Formation, Palen Mountains, Southeastern California, in E. G. Frost and D. L. Martin (eds.), Mesozoic-Cenozoic tectonic evolution of the Colorado River Region, California, Arizona and Nevada, Cordilleran Publishers, San Diego, Ca., p. 267-274.

Leveque, R. A., 1981, Stratigraphy and structure of the Palen Formation, Palen Mountains, southeastern California, M. S. Thesis, University of Arizona, Tucson, Az., 58 p.

Marshak, R. S., 1979, A reconnaisance of Mesozoic strata in northern Yuma County, southwestern Arizona, M.S. Thesis, University of Arizona, Tucson, Az. 108 p.

McKee, E. D., 1934, The Coconino Sandstone - its history and origin, Carnegie Inst. Wash. Pub. 440, p 77-115.

McKee, E. D., 1938, The environment and history of the Toroweap and Kaibab Formations of northern Arizona and southern Utah, Carnegie Inst. Wash. Pub. 491, 268 p.

McKee, E. D., 1954, Sedimentary basins of Arizona and adjoining areas, Geol. Soc. America Bull., Vol. 62, p. 481-505.

McKee, E. D., 1969, Stratified rocks in the Grand Canyon, in The Colorado River Region and John Wesley Powell, U. S. Geol. Survey Professional Paper 669-B.

McKee, E. D., 1975, The Supai Group Subdivisions and nomenclature, U. S. Geol. Survey Bulletin 1395-J, 11 p.

McKee, E. D., and Gutschick, R. C., 1969, History of the Redwall limestone of Northern Arizona, Geol. Soc. America, Memoir 114, 71p.

Miller, E. L., and Cameron, C. S., 1982, Late precambrian to late Cretaceous evolution of the southwestern Mojave Desert, California, in J. D. Cooper, B. W. Troxel, L. A. Wright, eds., Guidebook and Volume: Geology of selected areas in the San Bernardino Mountains, Western Mojave Desert, and Southern Great Basin, California, Death Valley Publishing Company, p. 21-34.

Miller, F. K., 1966, Structure and petrology of the southern half of the Plumosa Mountains, Yuma County, Arizona, Ph.D. Dissertation, Stanford University, Stanford, Ca., 107p.

Miller, F. K., 1970, Geologic Map of the Quartzite Quadrangle, Yuma County, Arizona, U.S . Geol. Survey, Geologic Quadrangle Map, GQ 891, 1:62,500.

Miller, F. K., and McKee, E. M., 1971, Thrust and Strike slip faulting in the Plomosa Mountains, Southwestern Arizona, Geol. Soc. America Bull., Vol. 82, p. 717-722.

Pelka, G. J., 1973, Geology of the McCoy and Palen Mountains, Southeastern California, Ph.D. dissertation, Universty of California, Santa Barbara, 162 p.

Pierce, W., 1976, Paleozoic tectonics of Arizona, Arizona Geol. Soc. Digest, Vol. 10, p. 37-58.

Ragan, D. M., 1973, Structural Geology, an Introduction to geometrical techniques, 2nd Edition, John Wiley & Sons, New York, 208 p.

Ramsay, J. G., 1976, Folding and Fracturing of Rocks, McGraw Hill Book Company, New York, 568 p.

Ransome, F. L., 1904, The Geology of Ore Deposits Bisbee Quadrangle, Arizona, U. S. Geol. Survey Professional Paper 21, 168 p.

Rehrig, W. A., and Reynolds, S. J., 1980, Geologic and geochronologic reconnaissance of a northwest-trending zone of metamorphic core complexes on southern and western Arizona, Geol. Soc. America, Memoir 153, p. 131-157.

Rehrig, W. A., Shafiqullah, M., and Damon, P. E., 1980, Geochronology, geology and listric normal faulting of the Vulture Mountains, Maricopa County, Arizona, Arizona Geol. Soc. Digest, Vol. XII, p. 89-110.

Reynolds, S. J., 1980, Geologic framework of west-central Arizona, Arizona Geol. Soc. Digest, Vol. XII, p. 1-16.

Reynolds, S. J., 1982, Multiple Deformation in the Harcuvar and Harquahala Mountains, West Central Arizona, in Frost, Eric and Martin, D. M., eds., Mesozoic-Cenozoic tectonic evolution of the Colorado River Region, California, Arizona and Nevada; Cordilleran Publishers, San Diego, p. 137-142.

Reynolds, S. J., Keith, S. B., and Coney, P. J., 1980, Stacked overthrusts of Precambrian crystalline basement and inverted Paleozoic sections emplaced over Mesozoic strata, West Central Arizona, Arizona Geol. Soc. Digest, Vol. XII, p. 45-52.

Robison, B. A., 1980, Description and analysis of Mesozoic red beds, western Arizona and Southeastern California, Arizona Geol. Soc. Digest, Vol. XII, p. 147-154.

Scarborough, R. and Wilt, J. C., 1979, A study of uranium favorability of Cenozoic sedmentary rocks, Basin and Range Province, Arizona, part I, general geology and chronology of pre-late Miocene Cenozoic sedimentary rodks, Arizona Bur. Geol. Min. Tech. Open File Report 79-1, or U. S. Geol. Survey Open File Report OFR 79-1419, 101 p.

Shifiqullah, M., and others, 1980, K-Ar geochronology and geologic history of southwestern Arizona and adjacent areas, Arizona Geol. Soc. Digest, Vol. XII, p. 201-259.

Stewart, J., Poole, F. G., and Wilson, R. F., 1972, Stratigraphy and origin of the Triassic Moenkopi Formation and related strata in the Colorado Plateau Region, U. S. Geol. Survey Professional Paper 690, 335 p.

Streickeisen, A. L., 1973, Plutonic rocks: Classification and nomenclature recommended by the IUGS Subcommission on the systematics of igneous rocks, Geotimes, Vol. 18, No. 10, p. 26-30.

Varga, R. J., 1977, Geology of the Socorro Peak area, Western Harquahala Mountains, Arizona Bur. Geol. Min. Tech. Circular 20, 20 p.

Wilson, E. D., 1960, Geologic map of Yuma County, Arizona, Arizona Bureau of Mines, 1:375,000.

6 maps

COLUMN I

APACHE WASH FORMATION

JKau—Upper Member: Gray and medium gray-green medium to medium thin-bedded qtz. rich sandstone with quartzite and volcanic rock pebbles; interbedded with thin light gray-green silty or muddy partings: distinct reddish stain common on weathered surfaces.
Interbedded sandstone, siltstone and shale; conglomeratic at base, thin pebble conglomerates occur locally throughout; forms fining upward sequence. Sandstone weathers medium to dark brown, is gray on fresh surfaces; fine to coarse-grained, poorly sorted, medium- to thick-bedded; beds massive or vaguely plane laminated; low-angle cross bedding present, but not common. Petrology: mono- and polycrytsalline quartz, feldspar (plagioclase and albitized potassium feldspar), rock fragments (mostly volcanic) and chert; cement is diagenetic phyllosilicates, locally with abundant calcite replacement. Siltstone and silty shale are light brown or gray weathering, medium to dark gray on fresh surfaces, commonly micaceous; poorly preserved shells present locally in siltstone. Conglomeratic beds mostly coarse sand and grit with clasts up to 15 cm in diameter of vitreous, tan quartzite, gray limestone, volcanic rocks and rarely, intrusive rocks. Limestone conglomerate lenses similar to base of lower member in the Limestone Hills occur in N. center Sec. 29, T.4 N., R.12W. and in N center Sec. 30, T.4N., R.12W.

Lower Member absent

VOLCANICLATIC SEDIMENTS

Jvsh—Shale Member: White weathering silty calcareous shale and siltstone interbedded with thin-bedded brown porcelaneous dolomite; gradational interbedding with overlying and underlying sandstone.

Jvss—Sandstone Member: Gray drab medium coarse-grained volcaniclastic sandstone. Composed of altered volcanic rock fragments and sericitized feldspar with disseminated 1-2 mm quartz grains and tiny opaque grains; chloritized biotite flakes are present; alteration and diagenesis make determination of original grain size and shape difficult. The sandstone is generally massive, featureless and unsorted. Pebble conglomerate lenses occur with decreasing abundance up section; bedding is visible through uncommon reworked quartz-rich sandstone beds, magnetite-rich lamina and grain size or compositional variations. Cross bedding is present in some magnetite rich beds. Secondary calcite is locally abundant.

Jvsc—Agglomerate-conglomerate Member: Medium- to coarse-grained lithic sandstone with abundant angular volcanic clasts up to 30 cm in diameter; scattered round to sub-round tan, vitreous quartzite up to 10 cm in diameter and rare Paleozoic limestone clasts. Volcanic clasts include light gray aphanitic felsite, quartz-feldspar porphyries identical to the upper volcanic unit, and uncommon maroon porphyritic felsites similar to flows in the lower volcanic unit. Conglomerates are massive, chaotic, matrix supported; bedding is rarely visible. Matrix is similar to clasts in appearance; secondary calcite is common.

UPPER VOLCANIC UNIT

Jvu—Massive homogeneous porphyry, tan-gray to dark brown weathering, medium gray to greenish gray on fresh surfaces. Phenocrysts: altered subhedral to euhedral 2-3 mm plagioclase and albitized(?) potassium feldspar, 2-3 mm rounded to subhedral quartz and 2 mm chloritized hornblende or biotite. Groundmass: very fine-grained silicious with dissiminated tiny (5 mm) opaque grains.

LOWER VOLCANIC UNIT

Jvl—Red beds are commonly interfingered at and near the base; rest of the unit is complexly interfingered flows or welded tuff, agglomerate, volcanic conglomerate and massive and laminated tuff.
Flows or welded tuff: subhedral to euhedral plagioclase feldspar phenocrysts 1-3 mm in diameter, and tiny opaque grains in a medium dark gray-maroon or purple matrix. Weak foliation defined by quartz stringers or flow banding is common. Thin secondary quartz and red alteration veinlets common.
Massive tuffs: dark gray-green fine- to very fine-grained sand composed of altered feldspar and volcanic rock fragments with dissiminated round quartz grains up to 3 mm in diameter; there is no visible bedding.
Laminated tuff: dark gray-green to dark maroon-gray on fresh surfaces, well-bedded with banded or laminated appearance; bands formed by grain size and compositional variation; coarser layers seem more feldspathic with local subhedral feldspar phenocrysts. Well exposed on south side of valley east of Needle.
Agglomerate and volcanic conglomerate: maroon, medium to dark gray-green and gray-purple conglomerate; clasts angular volcanic rock fragments-flows, tuffs, and various obscure aphanitic lithologies-clasts up to 40 cm in diameter. Massive chaotic texture; no evidence of aqueous transport.
Red beds: In NW Sec. 31 T.4N., R.12W. brick red very fine- to coarse-grained feldspathic-lithic sandstone, grit and pebbly conglomerate; indistinct bedding-internally massive or laminated; low-angle cross beds uncommon; clasts in grit or pebble conglomerates are angular volcanic rock fragments of aphanitic lower volcanic unit lithologies up to 5 cm in diameter. In the Needle and Mixmaster Hill area conglomeratic red beds, chaotic maroon mudstone, feldspathic-lithic sandstone and conglomerate. Southwest of Needle, conglomerate contains limestone clasts up to .5 m in diameter, also volcanic rock, quartzite and uncommon intrusive rock clasts; igneous clasts rounded, up to 20 cm in diameter, coarse crystalline to porphyritic granitoid. On Mixmaster Hill, mixed lithology conglomerates are interfingered with conglomerates whose clasts are almost exclusively lower volcanic unit lithologies. Limestone slide blocks or tectonic slivers are present south of the Needle.

MESOZOIC SANDSTONE

Mzss—Southeast of Mixmaster Hill: medium-grained well indurated quartzite interbedded with maroon and red-brown siltstone. In Needle area: sandstone and conglomerate with maroon siltstone partings. Sandstone is buff-gray to light gray, fine- to very coarse-grained, laminated, locally with low-angle lenticular cross sets. Magnetite-rich lamina are present. Conglomerates contain subrounded to well-rounded clasts up to 15 cm in diameter; is clast supported or sand dominated; afew lenses of limestone conglomerate are present. White crystalline limestone beds up to 30 cm thick are interbedded locally. Microdiorite dikes or basalt flows are present on E. Needle ridge and SE Corral Hill. Small porphyritic latite bodies intrude the sandstone southeast of the Needle and Mixmaster Hill.

Needle Domain

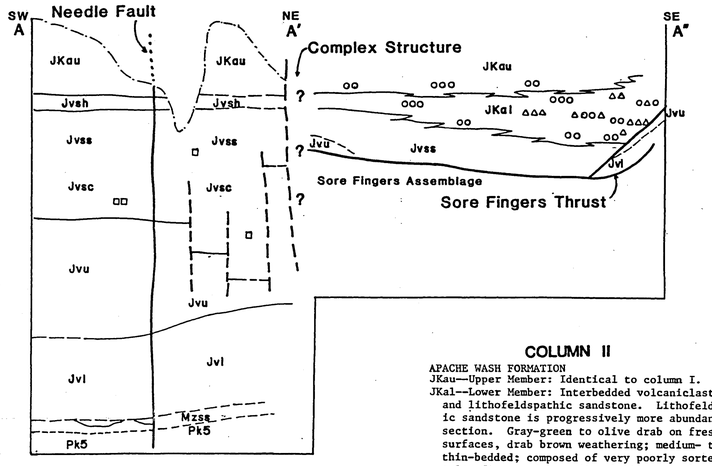

Limestone Hills Domain

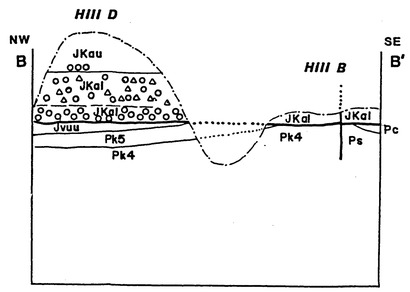

Sore Fingers West Domain

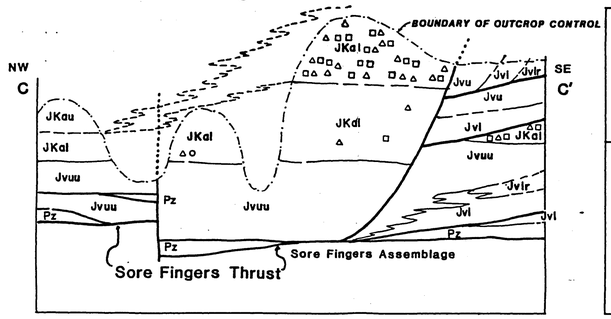

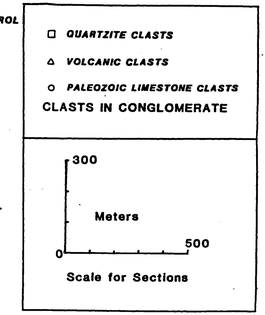

COLUMN II

APACHE WASH FORMATION

JKau—Upper Member: Identical to column I.

JKal—Lower Member: Interbedded volcaniclastic and lithofeldspathic sandstone. Lithofeldspathic sandstone is progressively more abundant upsection. Gray-green to olive drab on fresh surfaces, drab brown weathering; medium- to thin-bedded; composed of very poorly sorted angular fine sand to grit; clasts are volcanic rock fragments and feldspar with minor quartz. Minor limestone, quartzite and volcanic clast conglomerate present, becomes more abundant to the south.
Gradational contact at the base: massive volcaniclastic sandstone grades upsection into poorly to moderately well-bedded volcaniclastic sandstone, and detrital quartz becomes a more prominent component of the sand.

VOLCANICLASTIC SEDIMENTS

Jvss—Sandstone Member: identical to column I

COLUMN III

APACHE WASH FORMATION

JKau—Upper Member: Medium- to coarse-grained lithofeldspathic sandstone as described in col. I. Lower contact abrubt.

JKal—Lower Member: Medium- to thin-bedded volcaniclastic sandstones as described in col. B. Spotty outcrops of volcaniclastic sandstone and mixed clast conglomerate occur in alluvium of strike with massive conglomerate on Limestone Hill D. Mixed clast conglomerate: upper Paleozoic and volcanic clast conglomerate interbedded with volcaniclastic sandstone and sedimentary-clast conglomerate and volcanic-clast conglomerate. Paleozoic-clast conglomerate: clasts of Supai, Coconino and Kaibab formation up to 1 m in diameter; matrix is quartz rich calcareous sandstone and siltstone; rare thin sandy limestone beds, one of which contains algal structures. Slide blocks of Kaibab Limestone up to 20 m long are present near the base of the conglomerate in several places

Sheared Unconformity

VOLCANIC(?) ROCKS

Jvuu—Upper volcanic unit or volcaniclastic sediments: a thin, highly altered lense of volcanic rocks is present below the conglomerate on the southwest of Hill D.

PALEOZOIC ROCKS

Described on figure 9.

COLUMN IV

APACHE WASH FORMATION

JKal—Lower Member: interbedded pebble conglomerate sandstone and siltstone; thin- to medium-bedded. Quartzite, Paleozoic limestone and volcanic rock pebbles are present in conglomerate. Sandstone is same as that in underlying units. Siltstone is dense, maroon or olive drab in color. Grades down into massive conglomerate: clasts subangular, laminated vitreous tan quartzite, and volcanic clasts up to 30 cm in diameter; matrix is volcaniclastic sandstone. Volcanic clasts are obscure because they are nearly identical in appearance to the matrix.
Underlain by olive drab volcaniclastic sandstone as described in col. B. Bedded volcaniclastic sandstone is in gradational contact with underlying massive epiclastic or volcanic rock. Unit is conglomeratic at base in southern fault bound exposures.

VOLCANIC AND VOLCANICLASTIC ROCKS

Jvuu—Volcaniclastic sediments and/or upper volcanic unit, as described in column I. A quartz sandstone marker bed is present at the northern end of the outcrop belt.

LOWER VOLCANIC UNIT

Jvl—lower volcanic unit, as described in column I. Includes Jvlr—red beds, as described in column I.

PALEOZOIC ROCKS

SORE FINGERS THRUST

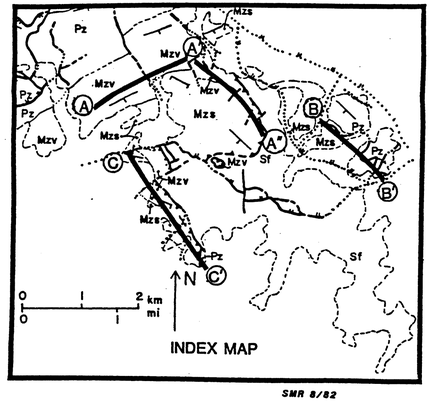

SMR 8/82

FIGURE 17. SCHEMATIC STRUCTURAL-STRATIGRAPHIC SECTIONS OF MESOZOIC ROCKS, SOUTHERN LITTLE HARQUAHALA MOUNTAINS

Figure 17 S. Richard, M.S. Thesis, 1983

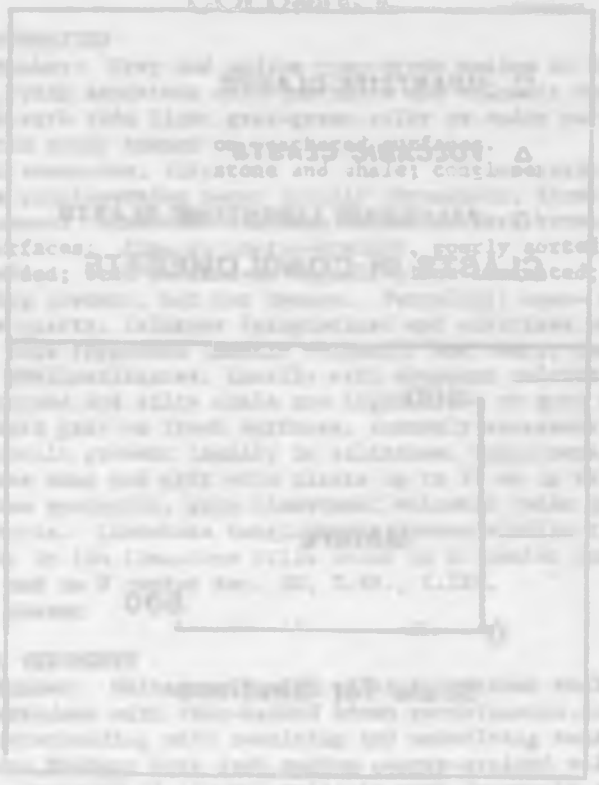

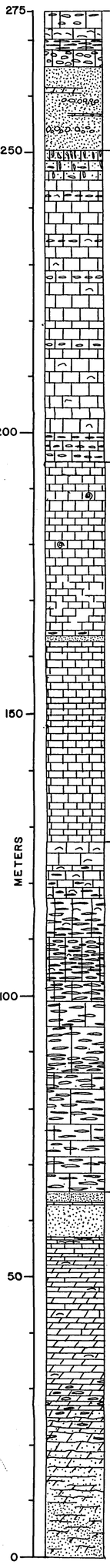

MESOZOIC SANDSTONE--Sandstone, grit and conglomerate with interbedded siltstone

KAIBAB LIMESTONE

Unit 5--Massive Limestone with local cherty zones; very light pink-grey limestone; fossiliferous pink-grey to white limestone containing brachiopods, echnoid spines and gastropods; very thin-bedded light pink-grey limestone interbedded with very thin chert beds; light pink-grey limestone with globy nodular chert.

Tan, medium tan and grey medium- to fine-grained sandstone with local conglomerate lenses and sandy dolomite beds. Conglomerate has pink-grey calcareous sandy matrix, with clasts of pink limestone, sandstone and sandy limestone; poorly bedded; grain size .1 to 40 cm. Sandstone is poorly sorted with texture inversion; it resembles the sand at the top of unit 1.

Unit 4--Silty and sandy grey limestone beds with ropy chert nodules, 1-3 cm in diameter and up to 20 cm long, both in and across bedding. Thicker tubes have hollow or carbonate cores; local sandstone beds, poorly sorted with texture inversion. These are interbedded with light grey limestone.

Medium grey to light pink-grey fine- to medium-grained limestone, medium- to thick-bedded, interbedded with cherty beds. Chert occurs in some beds as fragmental inarticulate silica masses up to 3 cm long which may be relict fossils; also nodular chert. Fossils include Chaetetes coral, brachiopods and gastropods.

Thick bedded to massive light grey limestone with 10 to 20 cm chert beds

Unit 3--In Limestone Hills the top is very fine-grained micrite, well bedded with some chert lense horizons. On the Needle and Mixmaster Hill the top is tan to yellow ocher and light grey limestone with some chert lenses and local calcareous siltstone.

Medium bedded medium to dark grey limestone; occasional poorly preserved large gastropods and fusulinids

Light and dark grey limestone, bedding is indistinct; beds 20 cm to 1 meter thick. A possible solution collapse breccia is present on Limestone Hill D.

Cherty light grey fine grained limestone

Tan sandstone, poorly sorted, texture inversion

Medium bedded medium to dark grey limestone; occasional poorly preserved large gastropods and fusilinids.

Unit 2--Medium- to thick-bedded light grey limestone in beds .3 to 1 m thick; well bedded; even beds. Lumpy chert stringers are present and become less common towards the top of the unit. Large productid brachiopods are common. Rounded calcite lumps 1 to 10 mm in diameter, which may be grapestones or birdseye structures, are a diagnostic feature.

Resistant massive cherty limestone, containing up to 50% chert. The limestone is medium grey crinoidal grainstone.

Resistant cherty and massive medium grey limestone, crinoid hash abundant, quartz sand locally present

In the Limestone Hills a conglomerate or breccia is locally present at the base

Unit 1-- Limestone Hills

Tan fine-grained sandstone
30 cm vitreous quartzite like Coconino
Tan fine-grained sandstone
Grey, dark grey and tan laminated limest.
Tan fine grained sandstone, thin bedded to laminated, non-resistant, some med. bedded massive sandstone
Tan, laminated limestone with siliceous stringers; thin- to medium-bedded; algal?

Mixmaster Hill

Tan sandstone interbedded with laminated or very thin bedded light grey to white and dark grey coarse grained limestone (zebra rock limestone)

Medium grey dolomite and dolomitic limestone, bedding well developed, 5 to 50 cm beds
Light medium grey on fresh surface; fine to very fine grained. Poorly preserved fossils abundant: crinoid columnals, echnoid spines, afew brachiopods. Crinoids are large, up to 1.5 cm in diameter. Calcite globs similar to those at the top of Unit 2 are present

Tan-grey dolomitic limestone, poorly bedded, unfossiliferous, cherty or slightly slightly silty with chert nodules and 1 to 2 cm calcite globs.

Dolomite is less silty up section.

Silty and sandy dolomite, brown and grey; sand locally silicified to look like chert

Dolomitic sandstone; tan fresh, dark brown to black desert varnish contrasts markedly with underlying Coconino Sandstone.

COCONINO SANDSTONE--very thin bedded white quartzitic sandstone

Figure 14. Detailed Stratigraphic Column of the Kaibab Limestone

Thicknesses approximate

Figure 14, S. Richard, M.S. Thesis, 1983

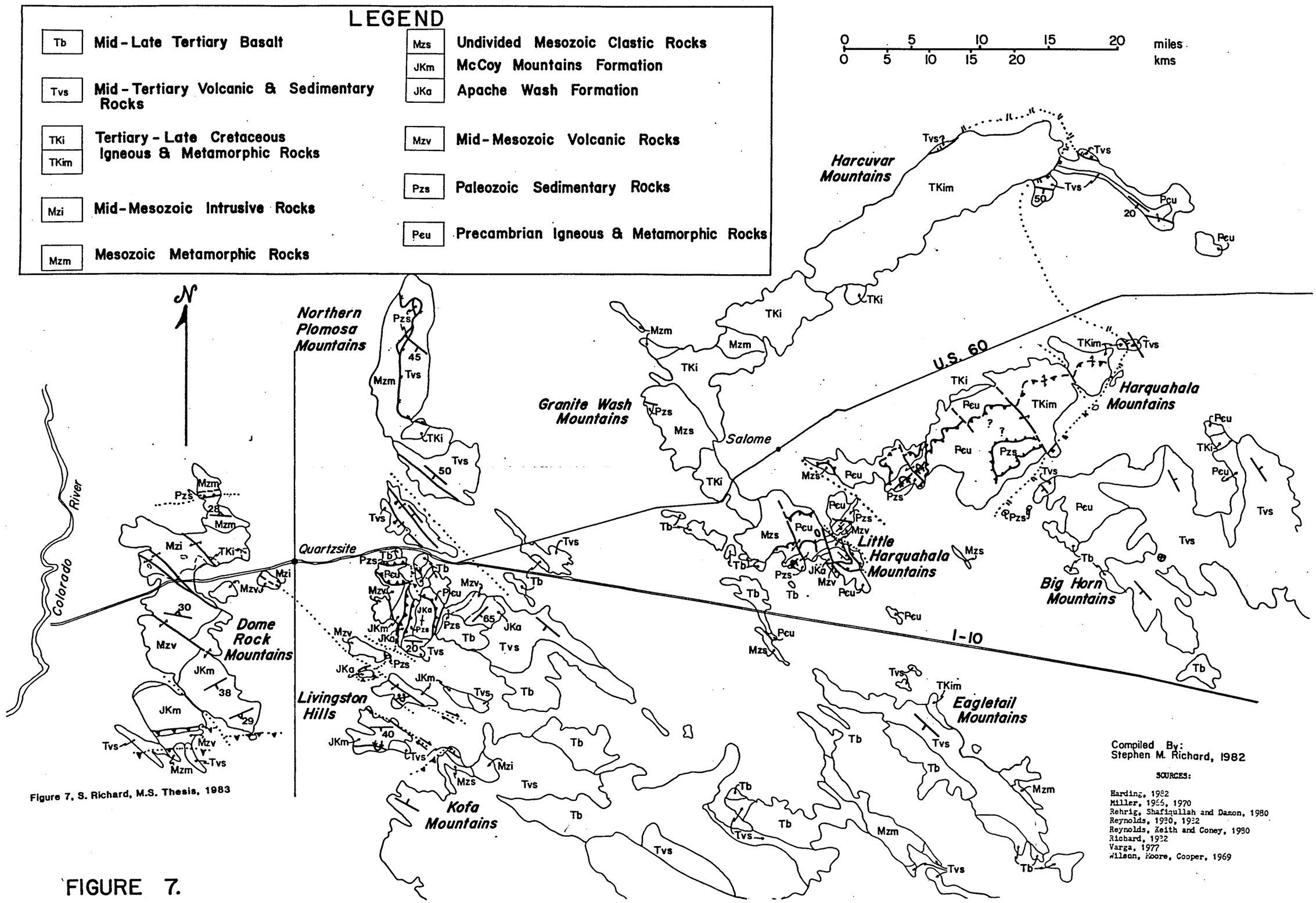

Figure 7, S. Richard, M.S. Thesis, 1983

FIGURE 7.

GENERALIZED GEOLOGIC MAP OF WEST CENTRAL ARIZONA

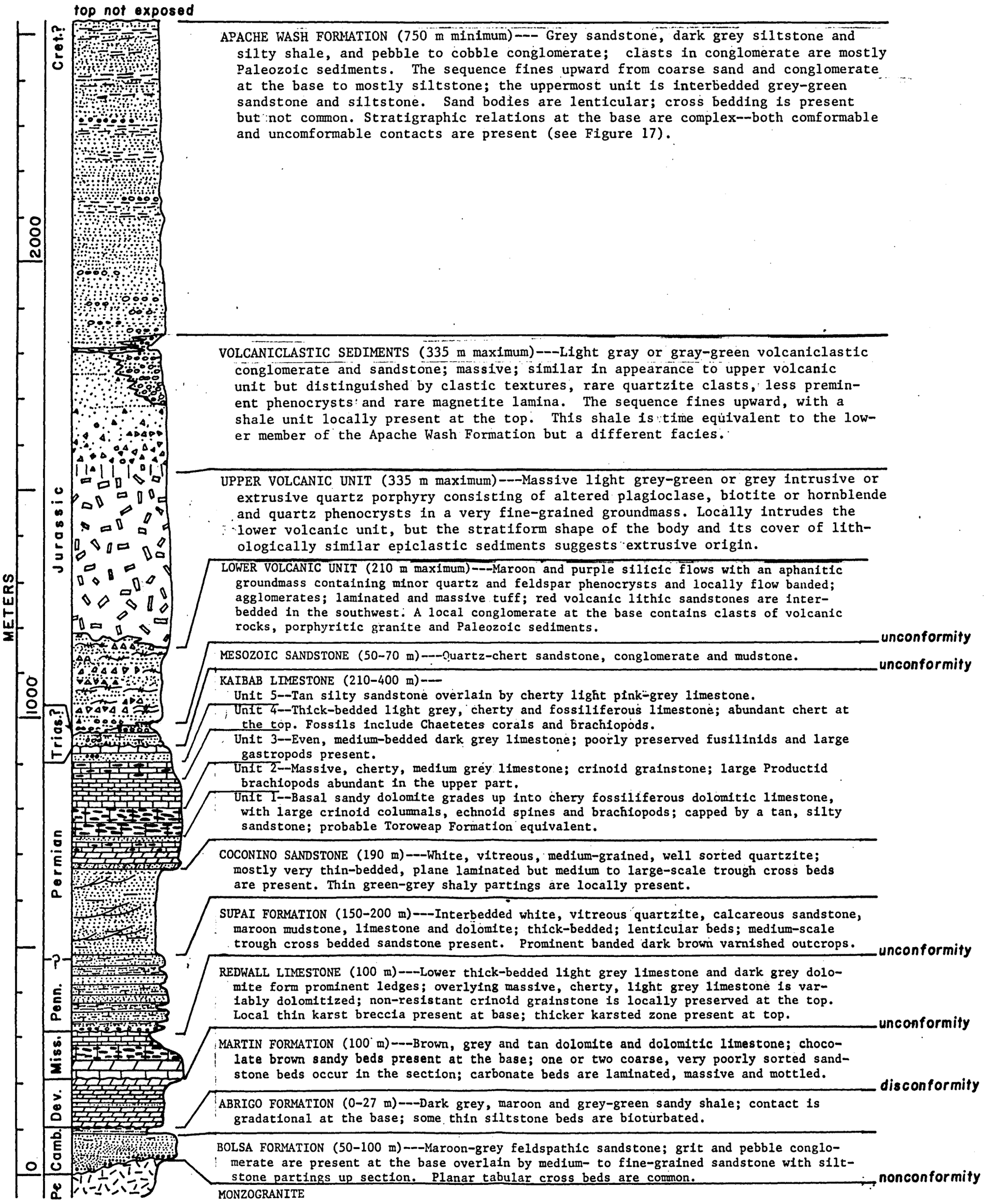

FIGURE 9. STRATIGRAPHIC COLUMN SOUTHERN LITTLE HARQUAHALA MOUNTAINS

Figure 9, S. Richard, M.S. Thesis, 1983

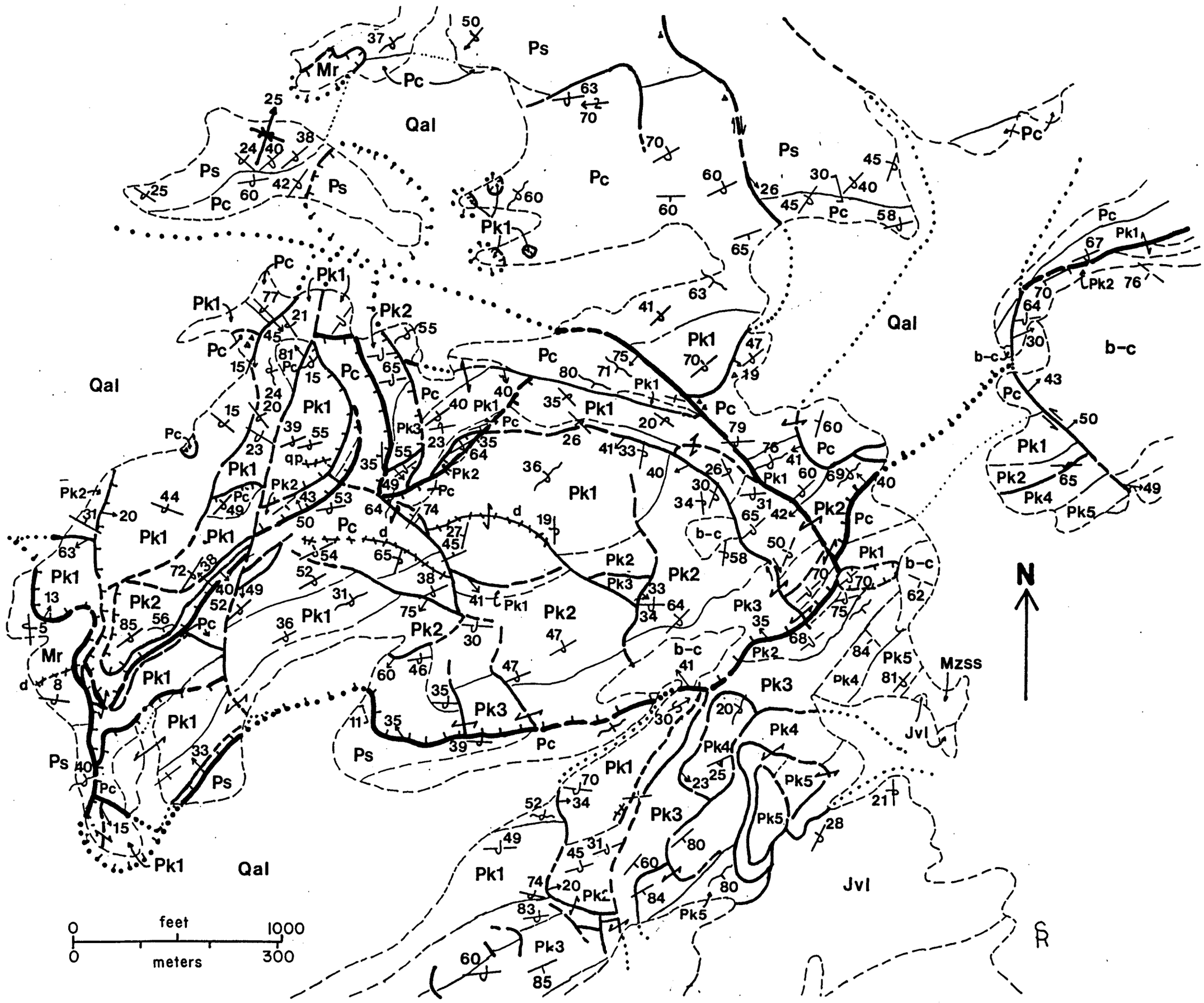

Figure 50. Detailed Geologic Map of Mixmaster Hill

For Explanation See Figure 5

Figure 50, S. Richard, M.S. Thesis, 1983

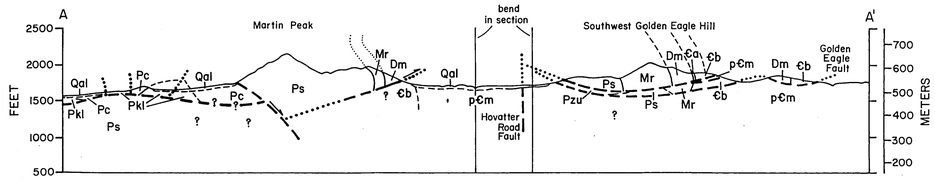

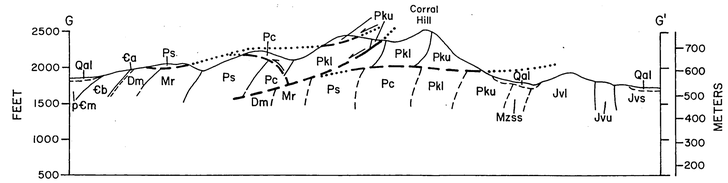

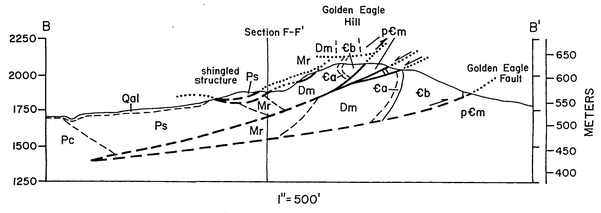

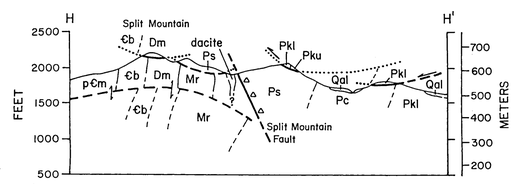

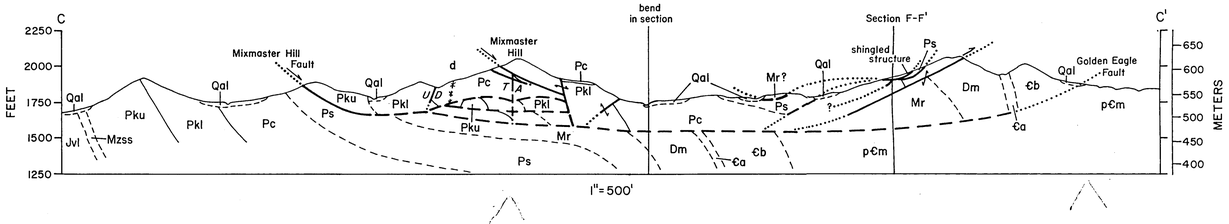

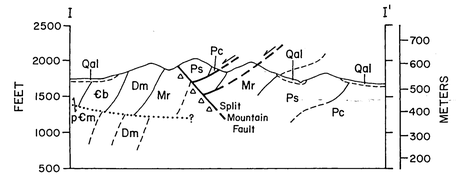

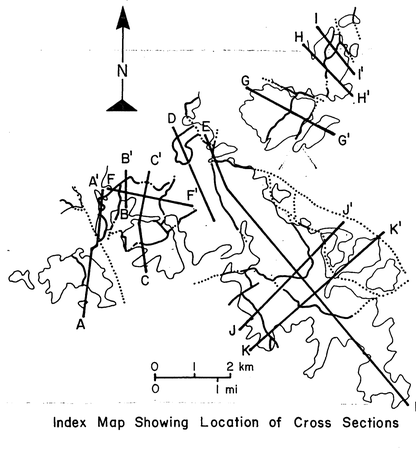

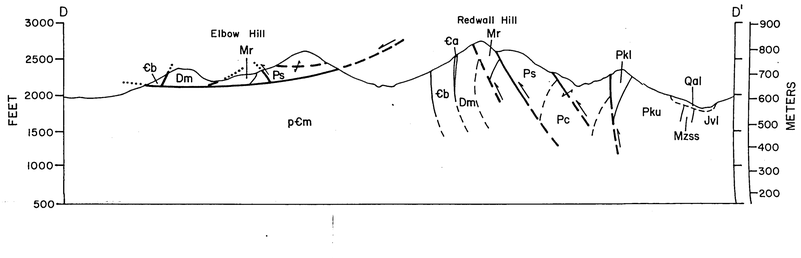

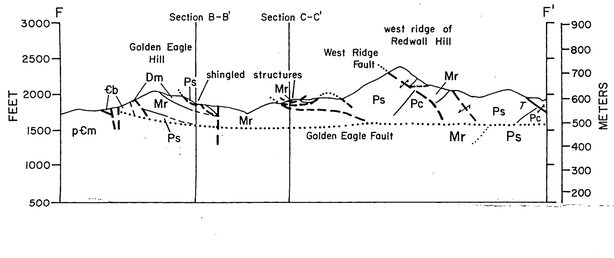

Index Map Showing Location of Cross Sections

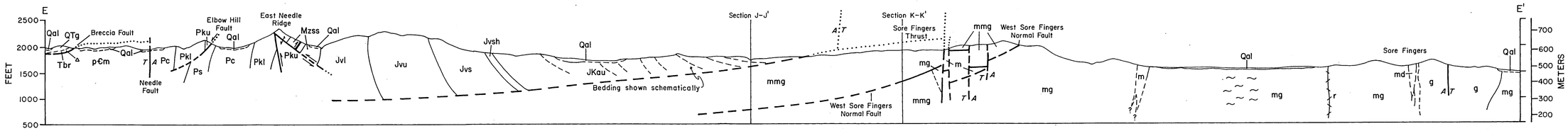

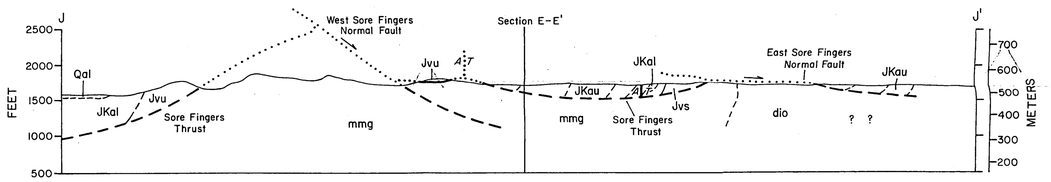

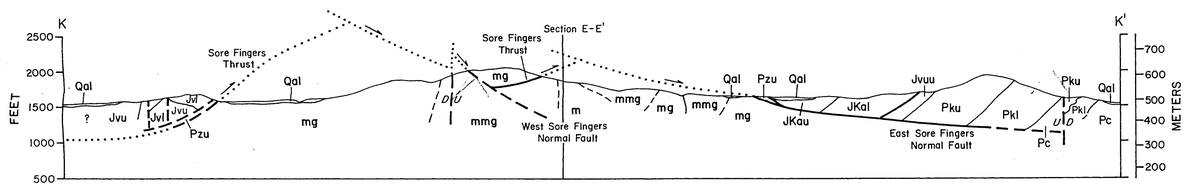

Cross Sections of the Southern Little Harquahala Mountains, La Paz County, Arizona

Scale 1" = 1000', unless noted otherwise

Figure 6, S. Richard, M.S. Thesis, 1983

GEOLOGIC MAP OF THE SOUTHERN LITTLE HARQUAHALA MOUNTAINS LA PAZ COUNTY, ARIZONA

By Stephen M. Richard 1982

Scale 1:12 000

0 1 mile

0 1 kilometer

contour interval 20 and 40 feet

Topographic base by U.S. Geological Survey

Geology mapped 1981

EXPLANATION

MAP UNITS

QUATERNARY — Qal — ALLUVIUM

UNCONFORMITY

QUATERNARY OR TERTIARY — Qoal — OLDER ALLUVIUM

UNCONFORMITY

TERTIARY
- Ts — CONGLOMERATE, SANDSTONE, SILTSTONE

UNCONFORMITY
- Tbr — BRECCIA

UNCONFORMITY

CRETACEOUS OR JURASSIC

ROCKS OF HARQUAR PEAK
- Mzhs — Sandstone, Siltstone, and Conglomerate
- Mzhv — Volcanic Rocks

APACHE WASH FORMATION
- JKa: JKau — Upper Member
- JKa: JKal — Lower Member

JURASSIC(?)

VOLCANICLASTIC SEDIMENTS
- Jvsh — Shale Member
- Jvs — Sandstone and Conglomerate Member
- Jvuu
- Jvu — UPPER VOLCANIC UNIT
- Jvl — LOWER VOLCANIC UNIT

JURASSIC OR TRIASSIC — Mzss — SANDSTONE AND CONGLOMERATE

DISCONFORMITY(?)

PALEOZOIC (?) — bc — BRECCIA-CONGLOMERATE

PALEOZOIC — Pzu — UNDIVIDED PALEOZOIC ROCKS

PERMIAN

KAIBAB FORMATION
- Pk: Pku — Units 3,4, and 5
- Pk: Pkl — Units 1 and 2
- Pc — COCONINO SANDSTONE

PENNSYLVANIAN
- Ps — SUPAI FORMATION

DISCONFORMITY

MISSISSIPPIAN — Mr — REDWALL LIMESTONE

DISCONFORMITY

DEVONIAN — Dm — MARTIN FORMATION

DISCONFORMITY

CAMBRIAN
- €a — ABRIGO FORMATION
- €b — BOLSA QUARTZITE

NONCONFORMITY

PRECAMBRIAN
- p€m — MONZOGRANITE
- p€u — METAMORPHIC ROCKS

MESOZOIC OR PRECAMBRIAN

SORE FINGERS ASSEMBLAGE
- mg — PORPHYRITIC MONZOGRANITE
- mmg — META-MONZOGRANITE
- mu — METAMORPHIC ROCKS AND ALASKITE
- gr — GRANITE
- di — DIORITE
- gd — GRANODIORITE

DIKES
- md — MICRODIORITE
- r — RHYOLITE
- d — DACITE
- a — ANDESITE PORPHYRY
- qp — RHYODACITE PORPHYRY
- ap — APLITE-PEGMATITE
- QUARTZ AND QUARTZ-CALCITE VEINS
- STRONG ALTERATION

SYMBOLS

CONTACTS–Dashed where approximately located, dotted where concealed; teeth on upper plate of low-angle faults

- Depositional
- U / D — High-angle Fault; U on upthrown side, D on downthrown side; Arrows indicate relative direction of lateral movement
- Low-angle Normal Fault
- Thrust Fault

STRIKE AND DIP OF BEDS

horizontal · inclined · vertical · overturned · approximate · variable · inclined in Breccia-Conglomerate

STRIKE AND DIP OF JOINTS

inclined · vertical · approximate · variable

STRIKE AND DIP OF CLEAVAGE

inclined · vertical · approximate · variable

STRIKE AND DIP OF FOLIATION

inclined · vertical · approximate · variable

FOLDS

axial trace of Syncline, Anticline, Overturned Syncline, showing plunge

FIGURE 5, S. RICHARD, GEOSCIENCES, M.S. THESIS, 1983